AN ABSTRACT OF THE THESIS OF

Chris Goldfinger for the degree of Master of Science in Geology presented on May 31, 1990.

Title: Evolution of the Corvallis Fault and Implications for the Oregon Coast Range

Abstract approved: Redacted for privacy

The Corvallis fault is a 50 km long northeast-trending structure, part of which defines the boundary between the central Willamette Valley and the east-central Coast Range of Oregon. Previously the fault had been mapped as either a high-angle reverse or normal fault, with the east block down. New gravity data suggest that the main structure is a low-angle thrust, with early Eocene Siletz River Volcanics thrust southeastward over middle to late Eocene Tyee and Spencer sandstones. The thrust geometry is similar to that of the Laramide thrusts of the Rocky Mountain foreland. Gravity modeling produces a best-fit geometry with the thrust-plane dipping approximately 10° northwest. The surface geology is consistent with a fault-propagation fold geometry. Consistent dips averaging 20° in the hanging wall block suggest a ramp dipping at the same angle, somewhat steeper than the dip indicated by gravity modeling. Vertical separation is about 6.7 km, and if the ramp dip is the same as bedding dips in the Siletz River Volcanics, horizontal displacement is 13-15 km, assuming no other thrust

faults repeat the Siletz River stratigraphy.

The Corvallis thrust was active during the late Eocene, and was the eastern boundary of a tectonic highland in the Eocene forearc. The highland was a local source of material for the upper Yamhill and lower Spencer Formations, deposited in a partially restricted shallow shelf to neritic setting. Other late Eocene tectonic and volcanic highlands formed an archipelago in the position of the present Coast Range. In the middle Oligocene, the fault was intruded by gabbroic dikes during an intrusive episode that emplaced massive sheets of gabbro throughout the central Coast Range. A younger normal fault paralleling the original Corvallis thrust is interpreted to be the result of gravitational collapse of the tip of the thrust sheet, and has truncated the older structure. Numerous left offsets of the main fault trace along northwest-trending left-lateral faults are interpreted to be the result of clockwise rotations of western Oregon documented by paleomagnetics. Later reactivation of the Corvallis fault as a left-lateral strike-slip fault, indicated by horizontal slickenlines, is consistent with the present north-south compression in Oregon. The Corvallis fault may have continued minor intermittent activity into the late Quaternary.

Evolution of the Corvallis Fault and Implications for the Oregon Coast Range

By

Chris Goldfinger

A THESIS

submitted to

Oregon State University

in partial fulfillment of
the requirements for the
degree of

Master of Science

Completed May 31, 1990

Commencement June 1991

APPROVED:

Redacted for privacy

Professor of Geology in charge of major

Redacted for privacy

Head of Department of Geosciences

Redacted for privacy

Dean of Graduate School

Date thesis is presented May 31,1990

Acknowledgements

I would like to thank Bob Lawrence for suggesting this study, which became more involved than I would have imagined, and for many fruitful discussions of the problems remaining in western Oregon. Also I thank Bob Yeats, Bob Lillie, Alan Niem, Gordon Ness, Dick Couch, Ken Werner, Erik Graven and Mike Parker for their ideas and helpful discussions. Ray Wells, Parke Snavely and Rick Blakely of the U.S.G.S. shared their views on the geology of the northwest. Thanks also to Gordon Ness and Jeb Bowers of CONMAR (OSU School of Oceanography) who went above and beyond in their help with gravity surveying and the loan of the gravity meter, and to Kelly Basquez, Dave Seaver, and Scott Urban who helped enormously with the gravity field work. For their financial support, thanks go to AMOCO Production Company, and ARCO Oil and Gas. And special thanks to my wife Suzanne, who survived being a geo-widow, and helped in hundreds of ways.

TABLE OF CONTENTS

LIST OF FIGURES

LIST OF PLATES

EVOLUTION OF THE CORVALLIS FAULT AND IMPLICATIONS FOR THE OREGON COAST RANGE

INTRODUCTION

The convergent margin of the Pacific Northwest has been an active subduction zone since the Mesozoic. Plate interactions during the Tertiary have shaped the structure and physiography of western Oregon, but many basic structural relationships remain poorly known. The Cascadia convergent margin is the present site of underthrusting of the Juan de Fuca plate beneath North America (Duncan and Kulm, 1989). The arc-subduction complex comprises an accretionary wedge, several forearc basins on the continental shelf, the Coast Ranges, the Puget-Willamette forearc basin, and the Cascade volcanic arc. Much of western Oregon and Washington are underlain by a marine basaltic terrane known as Siletzia, which may be an accreted seamount terrane, or may be the product of rifting of the North American margin in the early Tertiary.

One of the many remaining problems in the regional geology of the Pacific Northwest is the nature and origin of the Oregon and Washington Coast Ranges, the adjacent Puget-Willamette lowland, and the boundary structures between the two provinces. This paper examines the Corvallis fault, the only known location in the region where the Coast Range-forearc basin structural boundary is exposed.

The Corvallis fault trends northeastward from within the central Oregon

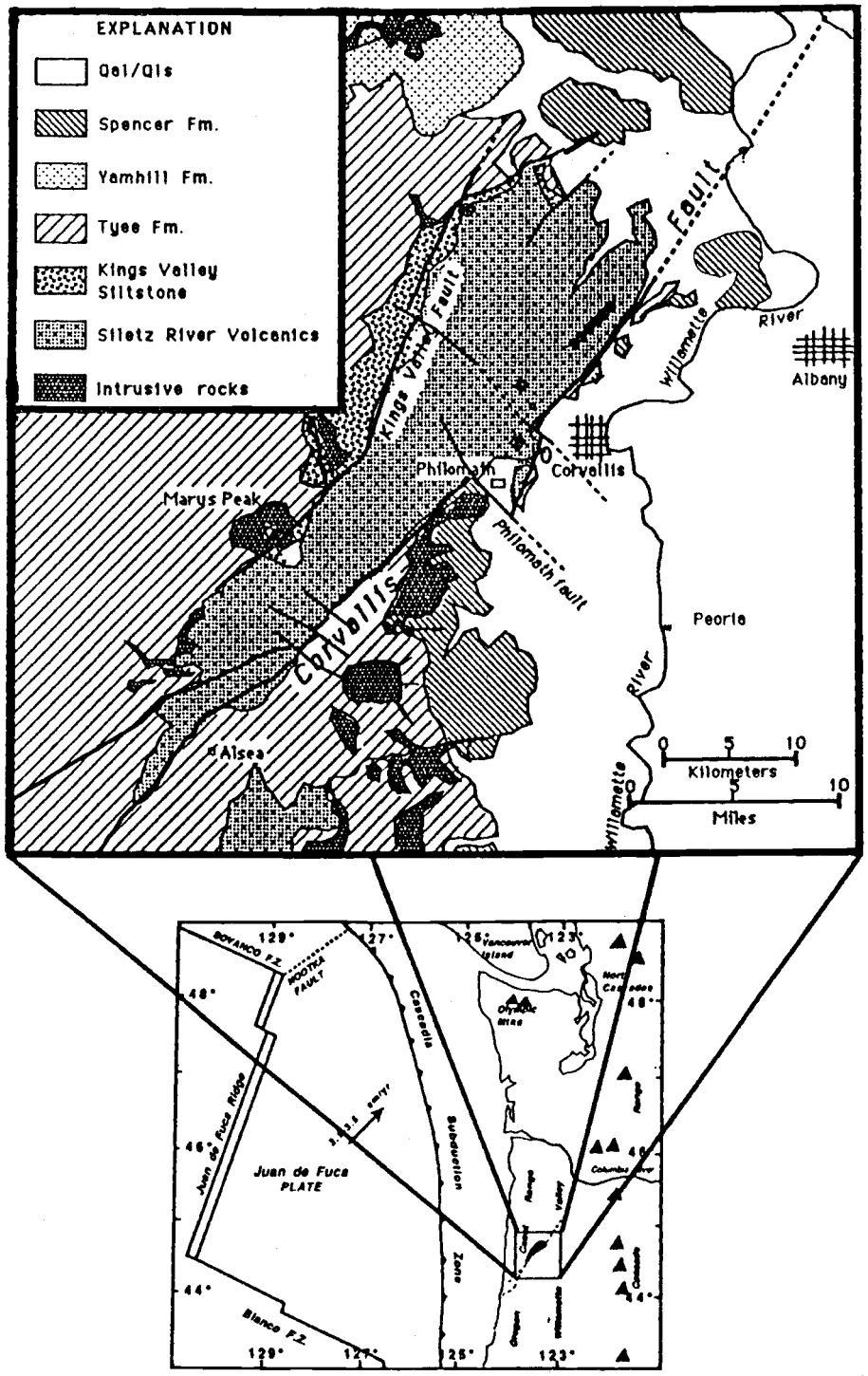

Figure 1. Plate configuration of the Pacific Northwest. Blowup of the general geology of east-central Coast Range includes the study area. After Wells and Peck, 1961, Lawrence and others, 1980, Riddihough, 1984 and present study.

Coast Range to the western Willamette Valley, where it is covered by

Oligocene and younger strata northeast of Corvallis (Fig. 1). With a known length of 50 km, the Corvallis fault is the longest known fault in western Oregon. This study was designed to investigate the Corvallis fault and associated structures in order to define its structural style, timing of motion, horizontal and vertical separation or offset, and its relationship to the tectonics of western Oregon.

Although easy access to the fault is available through the network of logging roads in the Coast Range, and even by city streets where the fault passes through the city of Corvallis, field work is hindered by the limited, vegetated, and heavily weathered outcrops in the wet climate of western Oregon. To mitigate the disadvantages of limited exposure, the study was designed to integrate existing gravity, magnetic, seismic, remote sensing, and well data with new mapping and collection of detailed new gravity and magnetic data to provide a more detailed evaluation of the nature of the Corvallis fault.

Field work was begun in the summer of 1988, with the bulk of the mapping being completed that summer. Mapping, gravity surveying, and field checking of initial results continued intermittently through April, 1990. Although the Corvallis fault is a structure that was initially active in the Eocene, current interest in seismic hazards in Oregon, and the proximity of the structure to a population center, prompted an effort to determine if the fault has been an active structure in the late Quaternary.

Previous Work

Ira S. Allison, Emeritus professor of geology at Oregon State University was the first author to mention the structure later named the Corvallis fault by

Vokes and others (1954). In his 1953 paper and accompanying map Geology of the Albany Quadrangle, Oregon, Allison mapped the northern part of the fault, using the juxtaposition of the Siletz River Volcanics and vertical Eocene sedimentary beds, and he concluded that the structure was probably a northwest-dipping, high-angle reverse fault. He also made note of a "peculiar relation" about a mile north of Lewisburg on highway 99W, the old Pacific Highway: "...a remnant of basalt rests on the beveled edges of nearly vertical beds of tuffaceous shales. The contact slopes southwestward at a low-angle and might be considered to be a warped thrust plane." Allison did not pursue this relation further, perhaps because nothing like it was found elsewhere in the field. As will be discussed in later sections, this outcrop (now extensively weathered) may have been one of only two places where the primary structure of the Corvallis fault is exposed.

Allison (1953) also made an observation concerning the late Eocene Spencer Formation which was not confirmed until this study, 36 years later. He mapped local basaltic breccias and conglomerates within the Spencer in the Dallas quadrangle and several other locations. The nature of these deposits suggested a local source, yet none was located nearby. He conjectured that basaltic deposits were emplaced by submarine sliding from Siletz River Volcanics highlands to the west, on the basis of contemporaneous deformation structures in the Spencer Formation. This study also supports this idea, and establishes that the Corvallis fault was the eastern boundary of such a highland. The uplifted block shed both basaltic debris and the erosion products of the micaceous Tyee Formation into a late Eocene Spencer seaway to the east.

Vokes and others (1954) mapped the Corvallis fault, from its northern

limit where Allison had worked, southwest to the eastern slopes of Marys Peak in the Coast Range. They also interpreted the fault to be a high-angle reverse fault, and mapped substantial folds in Spencer and Tyee strata, dying out to the east. Their reconnaissance mapping was excellent, but missed several important relations, leading to misinterpretations of the location and vertical separation on the fault that have persisted until the 1980's. Baldwin (1955) mapped the Marys Peak and Alsea quadrangles, extending the Corvallis fault to its known southwesterly limit, about 7 km southwest of the town of Alsea. Baldwin considered the Corvallis fault to be a steeply east-dipping normal fault. Wells and Peck (1961) included the previous mapping in their very detailed map of western Oregon, which is still the best available regional reference. No new work on the Corvallis fault was done until the late 1970's, when Lawrence (1977) published a small field trip guide to the geology of the Corvallis area, in which several aspects of the fault zone and one exposure (now covered) were described. Bela (1979) published new geologic maps of Benton County as part of an evaluation of the geologic hazards of the area. These maps were compilations of previous work, but incorporated much new data, including the approximate limits of three levels of Pleistocene to Holocene terrace deposits, air photo lineations suggesting numerous northwest trending faults in the Siletz River Volcanics, and a cross-section that alluded to the presence of the Philomath fault. Lawrence and others (1980) later published a revised map of a portion of the fault which corrected the error of Vokes and others (1954), inferred the existence of the Philomath fault, and mapped several other northwest trending faults in the area. Most recently, Baker (1988) briefly discussed the Corvallis fault in connection with her study on the stratigraphy of the Spencer Formation.

STRATIGRAPHY

Siletz River Volcanics

The oldest exposed rocks in the Oregon Coast Range are pillow and massive basalts, basalt breccias, and interbedded basaltic sedimentary rocks of late Paleocene to middle Eocene age (Baldwin, 1981; Snavely and others, 1968). K-Ar and Ar^{40}-Ar^{39} ages range from 48-62 Ma, with the oldest rocks exposed at the northern and southern limits of the outcrop area, and the youngest in the middle near the Columbia River (Duncan, 1982). Referred to as the Siletz River Volcanics (SRV) in the central Oregon Coast Range, correlative rocks are exposed in the northern Coast Range (Snavely and others, 1970; Wells and others, 1983), and in the southern Coast Range, as the basalts of the Roseburg Formation (Baldwin, 1974; Snavely and others, 1968). Correlative rocks of the Metchosin Volcanics crop out on southern Vancouver Island (Duncan, 1982; Snavely and others, 1968), and in western Washington as the Crescent Formation basalts (Snavely and others, 1958; Tabor and Cady, 1978) (Figure 2).

Snavely and others (1968) distinguished two major units within the Siletz River Volcanics. The lower unit is composed of submarine tholeiitic fine-grained and amygdaloidal pillow basalt and breccia. It is primarily this lower unit that is exposed in the study area. The upper unit of the Siletz River Volcanics is a submarine and subaerial unit of alkalic basalt of earliest middle Eocene age. The upper unit thickens locally, but is of far less volumetric extent than the lower unit (Snavely and others, 1968). The same stratigraphy has been recognized in the Crescent Formation basalts of western Washington and the Olympic Peninsula (Cady, 1975). The lowest exposures of these units have major and trace element affinities to both mid-ocean ridge

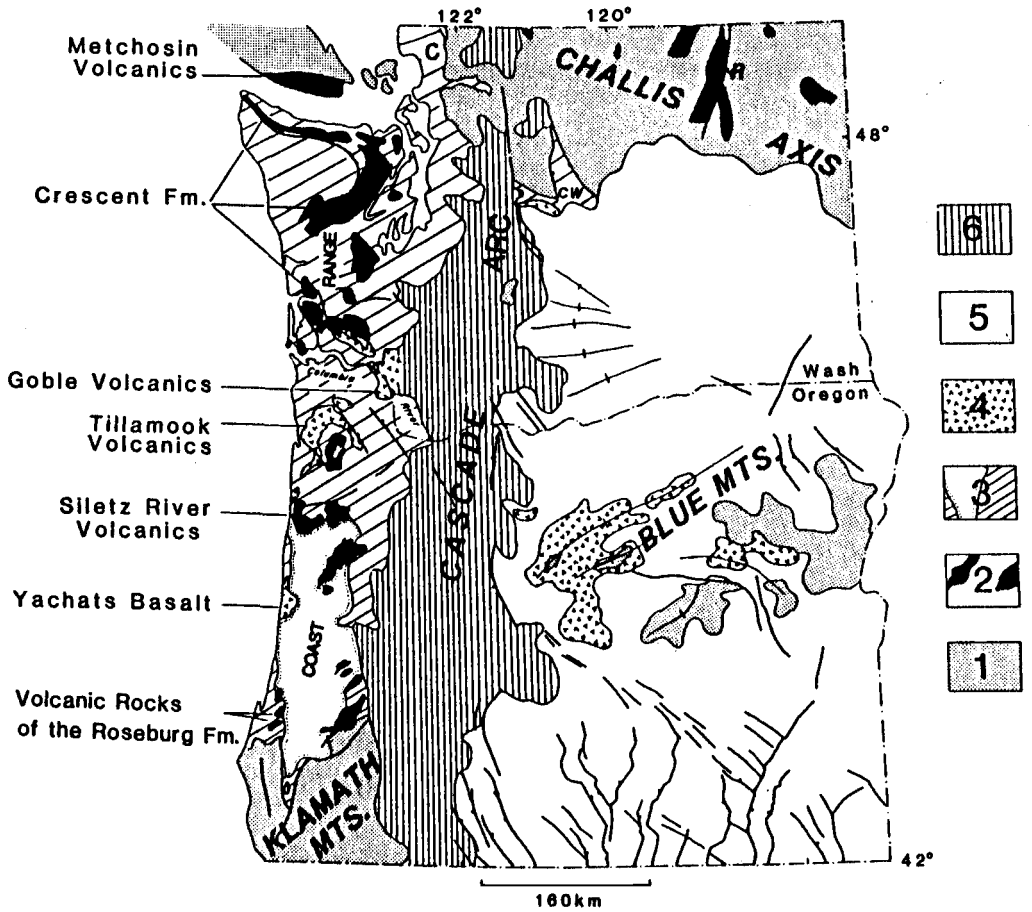

Figure 2. Geologic and tectonic map modified after King and Beikman (1974) and Wells and others, 1984; 1= pre-Tertiary rocks; 2= Paleocene to middle Eocene volcanic rocks, including oceanic basalt of Coast Range basement and of Challis arc; 3= mostly marine Tertiary sedimentary rocks, as mapped includes Quaternary in Puget Sound area; outline of Tyee Formation stippled; 4= Eocene and early Oligocene volcanic rocks, includes basaltic rocks of the Coast Range and andesitic Clarno Formation in central Oregon; 5= Mostly Oligocene and Miocene volcanic rocks of the Columbia Plateau and Oregon Basin and Range; 6= Tertiary and Quaternary volcanic rocks of the Cascade Range; C, CW, and R = Chuckanut, Chiwaukum, and Republic grabens; heavy lines are faults, ball on downthrown side; fine lines with crossbars are fold axes.

basalts and intraplate hot-spot generated seamounts (Duncan, 1982; Snavely, 1987), and may have been generated at a ridge centered hotspot (Duncan, 1982). Interbedded with the pillow basalts are occasional basaltic clastic interbeds that are variable in thickness from 0.5 m to 60 meters (Baldwin, 1947; 1964), and are of limited areal extent. In the Crescent Formation, lower unit basalts are interbedded with red pelagic limestones (Tabor and Cady, 1978).

The western limit of the Siletz River Volcanics in Oregon lies beneath the mid-continental shelf, where the unit may be truncated by the Fulmar fault, a probable north-south trending dextral fault inferred from exploratory well and seismic reflection data (Snavely, 1987; Snavely and Wagner, 1982). The eastern limit is unknown. Seismic reflection data show the Siletz River Volcanics to be present in the subsurface as far as the eastern Willamette Valley, and no evidence of a suture between the SRV and continental rocks beneath the valley has been observed. The eastern limit thus most likely lies beneath the Cascades or farther to the east.

Thickness of the Siletz River Volcanics is not well known. Geophysical studies suggest a thickness of 8-18 km (Dehlinger and others, 1968; Couch and Braman, 1979; Keach and others, 1989). Thickness of the correlative Crescent basalts in the Olympics is similar to that inferred for the Siletz River Volcanics, and ranges from 5-15 km in a completely exposed section, albeit complicated by thrust faults (Tabor and Cady, 1978). In the study area, a thickness of about 4.5 km of SRV is exposed between the Corvallis and Kings Valley faults, based on an average dip of 20° in the northern half of the exposed block, and assuming no other significant faulting.

Kings Valley Siltstone

Overlying and locally interfingering with the Siletz River Volcanics in the east-central Oregon Coast Range is the Kings Valley Siltstone, named for the community and valley about 13 km northwest of Corvallis. This unit consists of up to 1000 m of thin-bedded brown to grey tuffaceous marine siltstones and shales, with thin lenses of basaltic sandstone and a few thin white tuff layers. The Kings Valley Siltstone has been considered to represent a late stage of submarine volcanic activity, combined with a terrigenous component derived from the east (Penoyer and Niem, 1975; Vokes and others, 1954). The Kings Valley Siltstone has been mapped as overlying or interfingering with the upper Siletz River Volcanics in a belt trending northeast-southwest from the northern end of Kings Valley in the north to a few km southwest of Marys Peak in the south. (Figure 1)

Tyee Formation

Thick rhythmically bedded turbidites of the Tyee Formation overlie the Kings Valley Siltstone in the study area, and directly overlie the Siletz River Volcanics elsewhere in the Coast Range (Vokes and others, 1954; Baldwin, 1947, 1974). (Figure 3)

Tyee turbidites are the most widespread unit cropping out in the central and southern Coast Range. The Tyee contains microfossils of the Ulatisian Stage of Mallory (1959) which is middle Eocene (Molenaar, 1985). Microfossils indicate middle bathyal depths for the northern exposures (D.R. Mckeel *in* Heller and Dickinson, 1985).

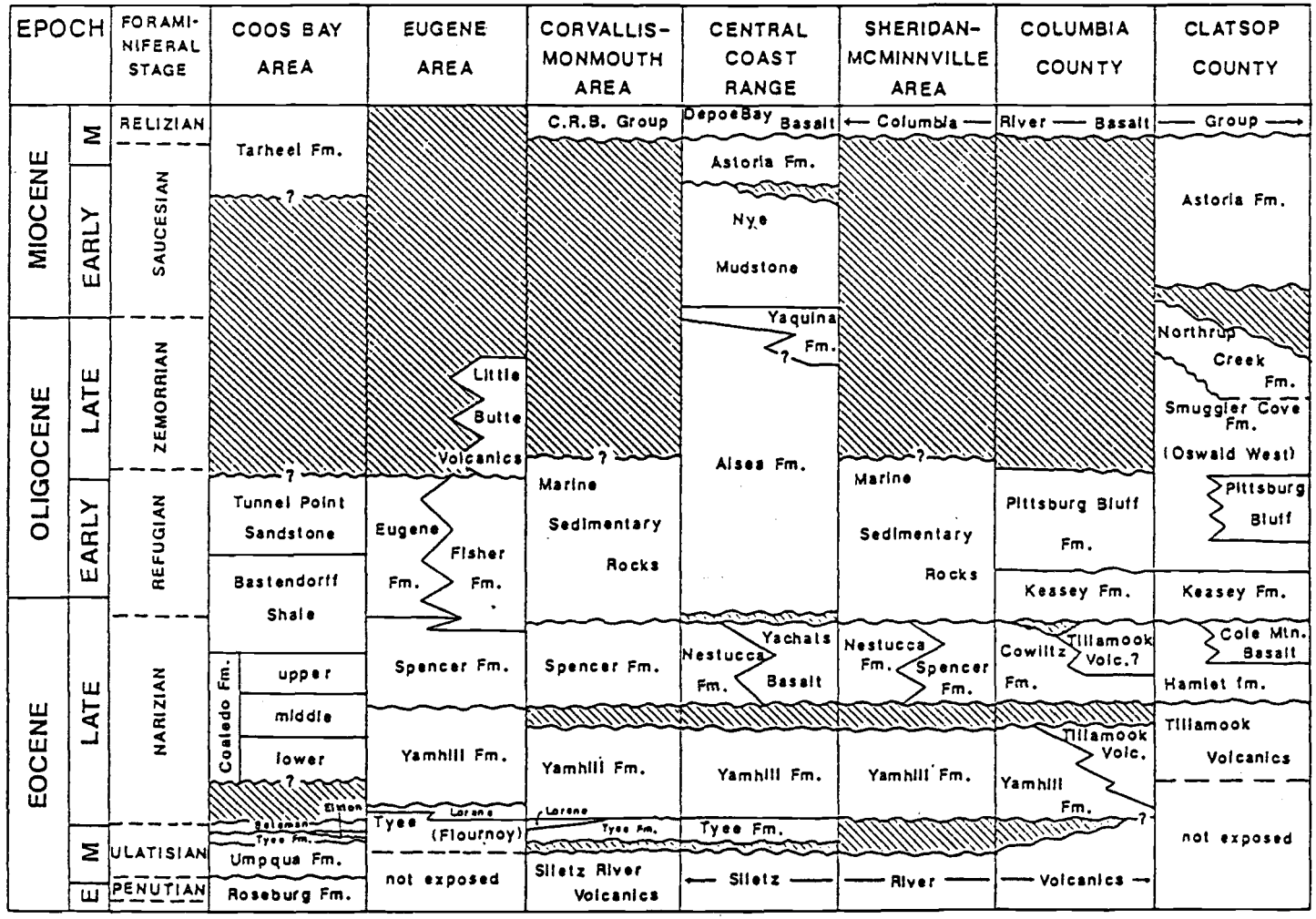

Figure 3. Stratigraphic columns in western Oregon. From Baker, 1988.

The Tyee turbidites are characterized by thick sequences of repetitive graded arkosic, micaceous sandstone with interbedded siltstone and mudstone, with no known stratigraphic marker horizons in the section. Thickness of the Tyee is highly variable, and can only be estimated in most locations, as much of the upper Tyee section has been eroded, and repetition or omission by faulting is difficult to recognize. Snavely and others (1964) estimated a total thickness of about 3000 m in the axis of the Tyee basin, thinning locally where the turbidites lap onto the flanks of Siletz River seamounts. Baldwin (1961) mapped a complete section in the Elkton-Drain area and estimated its thickness to be 2400 m. A similar thickness was estimated for the Tyee near Marys Peak by Baldwin (1955), and in the present study. East of the study area, thickness decreases sharply in the subsurface of the Willamette Valley, to 320 m in the Gulf Oil T.J. Porter #1 well (Bruer and others, 1984), 51 m in the Exxon Miller #1, and a minimum of 92 m in the Mobil Ira Baker #1 (Graven, in prep; Yeats and others, in prep.). Graded units have well developed basal sole markings, generally flute and groove casts. Analysis of more than 500 such casts in the Tyee indicate northward transport from a source area near the Klamath Mountains (uncorrected for subsequent rotation) (Snavely and others, 1964; Chan and Dott, 1983; Heller and Dickinson, 1985).

More recent paleomagnetic work has shown that Eocene rocks of the Oregon Coast Range, including the Tyee, have rotated 50°-70° clockwise (Beck and Plumley, 1980; Globerman and others, 1982; Magill and others, 1982; Simpson and Cox, 1977). On the basis of mineralogy, current directions, and observed east-west facies boundaries within the Tyee, Snavely and others (1964) concluded that the source of the Tyee sands was

the Klamath Mountains of southern Oregon and northern California. Facies relationships within the Tyee were observed by Snavely and others (1964), Lovell (1969), and Bird (1967). These investigators noted an increase in grain size, sand content, and shallow water sedimentary structures to the south, leading them to conclude that the source of the Tyee turbidites was in the Klamaths. Additionally, Lovell (1969) observed that the shift from deep water turbidite facies to shallow water cross-bedded facies occurred along a fairly narrow northeast-trending belt in the area between Florence and Eugene. He suggested this to be the shelf edge during Tyee deposition. Heller and others (1985) have examined the mineralogy and isotopic provenance in detail, and concluded that the major source of material for the Tyee was the Idaho batholith, now far to the east.

Yamhill Formation

The Yamhill Formation is distinguished from the underlying Tyee Formation in the central Coast Range by its greater mudstone and siltstone content, and lack of turbidite sandstones (Baldwin and others, 1955; McWilliams, 1973). The type section of the Yamhill located along Mill Creek contains a Narizian foram assemblage (Brownfield, 1982), and late Ulatisian to Narizian microfossils are found in Yamhill of the northern Willamette Valley (McKeel, 1984; Yeats and others, in prep.).

The Yamhill consists mainly of weakly stratified dark gray siltstones and mudstones with minor arkosic and basaltic sandy interbeds of a few centimeters to a few meters thickness (Baldwin,1964; Baldwin and others, 1955; Wells and others, 1983). Locally, thick sandstone units have been recognized within the Yamhill. The most prominent of these is the Miller sand

(Bruer and others, 1984), which is found immediately east of the study area in the subsurface. The Miller sand member lies in an elongate northeast trending trough parallel to, and centered about 10 km east of the Corvallis fault, reaching its greatest thickness immediately east of the study area in the subsurface (Baker, 1988; Bruer and others, 1984).

The Yamhill Formation has been correlated with the Elkton Formation of the south central coast, and with the Lorane Siltstone of the Eugene area (Vokes and others, 1954; Bird, 1967; Snavely and others, 1969; Baldwin, 1974). Foram ages from the Elkton and Lorane indicate a middle to early late Eocene age, late Ulatisian or early Narizian. (Rau *in* Baldwin,1961; Stewart *in* Vokes and others, 1951; Stewart, 1957).

The thickness of the Yamhill Formation varies throughout its outcrop area. North of the study area, estimates of 1200 and1500 m have been made for the type section at Mill Creek and the Yamhill Valley respectively (Baldwin and others, 1955). To the west, thickness of the Yamhill strata has been estimated at 600 m (Snavely and others, 1969; Vokes and others,1949). In the subsurface east of the study area, thickness of the Yamhill is 1020 m in the Porter well, including the 570 m thick Miller sand.

Depositional relationships with the Tyee are generally conformable and gradational, although locally in areas of probable volcanic centers the Yamhill lies above an angular conformity with either the Tyee or the Siletz River Volcanics (Baldwin and others, 1955). The unconformities are probably the result of onlapping local volcanic highs, while in deeper water the Tyee grades upward into the Yamhill (Baldwin, 1964; Baldwin and others, 1955; Snavely and others, 1969). Non-deposition or erosion of Yamhill strata can also be attributed to an episode of uplift and folding during a compressional

event in the east-central Coast Range (McWilliams, 1973 and this paper). The Yamhill Formation does not crop out in the study area, its stratigraphic position being occupied by an angular unconformity between the Tyee Formation and the late Eocene Spencer Formation.

The Yamhill Formation grades eastward and southward into a volcanic-rich facies called the Cascade volcanic facies by Bruer and others (1984), and the Yamhill volcanic facies by Baker (1988). This sequence of tuffs, welded tuffs, basalts, and tuffaceous sandstones records the onset of Cascade volcanism during the early late Eocene at about 45 Ma (Baker, 1988; Graven, in prep.).

Spencer Formation

Within the study area, the Spencer Formation overlies the Tyee Formation with a gentle to sharp angular unconformity of up to 45°. Microfossils in the Spencer are upper Narizian, or late Eocene in age (Baker, 1988). The Spencer has been informally divided into a lower sand rich member, and an upper mudstone and siltstone member (Baker, 1988; Thoms and others, 1983). The lower member consists primarily of tuffaceous and arkosic micaceous sandstone, siltstone, and minor coal, grading eastward into tuffaceous sandstones and volcanoclastics related to Cascade volcanism (Al Azzaby, 1980; Baker, 1988). The majority of the outcrops in the study area are of the lower sandy member of the Spencer, with some cross-stratification and abundant megafossils. The upper member is composed of siltstone, mudstone, and lesser sandstone, also grading southeastward into increasingly volcanic facies (Baker, 1988; Yeats and others, in prep.).

A limited, but important facies of the Spencer was observed in the

field adjacent to the Corvallis fault at 6 locations (Plate 1). This facies consists of tuffaceous, basaltic shallow marine sandstone and conglomerate in a chaotic high-energy assemblage. Rounded clasts of Siletz River Volcanics dominate the fault zone facies, and grain size ranges from coarse sand to clasts of 1-2 m in diameter. Marine megafossils are abundant, with shallow water and intertidal forms predominant (Ellen J. Moore, personal communication, 1989). The fault zone facies interfingers eastward and channels into more typical shallow marine arkosic micaceous Spencer sandstones in several locations, and is thus considered to be an east-facing strandline facies of the Spencer Formation.

The Spencer Formation correlates with the Cowlitz Formation of the northern Oregon Coast Range, and the Coaledo Formation in the Coos Bay area of the southern Oregon coast (Baldwin, 1974; Dott, 1966; Niem and Niem 1984). Both the Coaledo and the Cowlitz are interpreted as shallow shelf to coastal swamp sequences (Dott, 1966; Niem and others,1985). The Coaledo is composed of upper and lower sand-rich units of deltaic feldspathic coal-bearing lithic arenites, with an intervening deep marine mudstone member. The Cowlitz Formation of the northern Coast Range has been interpreted as a wave dominated shallow shelf to strandline coastal delta and lagoon deposit (Berkman, 1990; Niem and Niem 1985). The Cowlitz stratigraphy is confused by nomenclature problems (Rarey, 1986; Berkman, 1990), but consists of one or more sand rich units and one or more mudstone units similar to the Spencer and Coaledo Formations. The Clark and Wilson sand member of the Cowlitz is the producing reservoir in the Mist gas field of northwestern Oregon.

The depositional environment of the Spencer Formation is thought to

have been primarily a storm-dominated shallow shelf environment, the sandy lower member being commonly cross-stratified and with hummocky sequences identified within the section (Baker, 1988). Al-Azzaby (1980) and Thoms and others (1983) inferred the lower unit to have been deposited in middle shelf to strandline depths. The upper siltstone unit may have been deposited in somewhat deeper water (McKeel, 1984, 1985; Schlicker, 1962; Thoms and others, 1983).

The primary source for the Spencer is thought to be the Cascade arc, with a secondary distant plutonic component (Baker, 1988), and a local component from uplifted Tyee and SRV strata to the west (this paper).

Oligocene through Holocene Stratigraphy

No known outcrops of Oligocene through Pliocene strata occur in the study area, in which Pleistocene and Holocene deposits lie unconformably on Eocene Spencer, Tyee or Siletz River Volcanics. Immediately to the north and south of the study area, and in the subsurface to the east, Spencer sandstone is overlain by shallow water tuffaceous sandstone and siltstone of the early and middle Oligocene Eugene Formation or the non-marine late Miocene or Pliocene Monroe or "Corvallis Clay" (formerly referred to as the Calapooya clay) (CH2M Hill, 1987; Roberts and Whitehead, 1984). In the few outcrops near the study area, probable shallowly dipping Eugene strata lie above an angular unconformity with moderately dipping Spencer Formation sandstones. The Eugene Formation interfingers to the east and south with the shallow water to non-marine volcanoclastic and basaltic flow rocks of the Fisher Formation and the Little Butte Volcanics (Baker,1988; Beaulieu, 1971; Bruer and others, 1984; Yeats and others, in prep.). To the

north, the Eugene Formation probably passes laterally into the shallow marine to deltaic Pittsburg Bluff Formation and Keasey Formation (Beaulieu, 1971).

A significant Miocene event was the deposition of the middle Miocene Columbia River Basalt Group in the Columbia basin and also in the northern Willamette Valley. Isolated mid-Miocene basalts along the coast, previously considered to be of local origin, are identical in composition to flows of the Columbia River Basalt (Snavely, 1973; Beeson and others, 1979). Beeson (1979) proposed that emplacement of these coastal units was accomplished by flows passing through lows in a Miocene coastal plain or low coastal hills. If any remnants of these flows remain in the present Coast Range, they have yet to be found (Beeson,1985; Beeson and Tolan, 1989).

The Quaternary stratigraphy of the valley consists of fluvial, lacustrine, and glaciofluvial deposits. In the field area, Pleistocene Leffler and Lacomb gravels of Allison (1953) are found in high terraces standing at elevations of 30 to 100 m above the valley floor, and the younger Linn gravels (Rowland Formation of Balster and Parsons, 1969) are found at or below the present valley floor. The surface of the valley floor is composed primarily of the Willamette Formation (Balster and Parsons, 1969; McDowell and Roberts, 1987) (Willamette silt of Allison, 1953). The Willamette Formation is a late Pleistocene deposit of thin bedded silts that includes clasts, and probable ice-rafted erratics thought to be the result of the catastrophic Missoula floods (Allison,1953; Bretz, 1969; Glenn, 1965).

Intrusive Rocks

Gabbroic and basaltic intrusive rocks are widespread in the study area and in the central and northern Oregon Coast Range (Snavely and Wagner, 1961; Niem and Niem, 1985), but are generally absent in the southern Coast Range (Baldwin 1961; Niem and Niem, 1989). Sills, dikes, and sill-like bodies or laccoliths are common in the study area (Plate 1). The best known of these is the Marys Peak sill in the southwestern part of the map area. This 390 m thick sill intrudes the Tyee Formation near the Tyee-Kings Valley Siltstone contact, and its resistance to erosion is responsible for the high elevation of Marys Peak, the highest point in the Oregon Coast Range. The Marys Peak sill appears to be typical of the larger intrusive bodies that underlie many of the upland surfaces of the central Coast Range. The sill is a highly differentiated Ti rich body mostly of granophyric gabbro and granophyric diorite, with a downward increase in magnetite, olivine, augite and calcic plagioclase. Aplite dikes are abundant near the upper chilled contact (Roberts, 1953). The Marys Peak sill has been dated at 29.7 $\pm$ 1.2 Ma, or middle Oligocene (P.D. Snavely Jr., *in* Clark, 1969). Within the field area, other large intrusive bodies of similar lithology are found in a hill immediately south of Philomath, called Dike Hill in this report (Plate 1), and at Bald Hill, Dimple Hill, Vineyard Mountain, Coffin Butte, Logsden Ridge, and Witham Hill (Plate 1). The Dike Hill body is the best exposed of these, and intrudes Spencer Formation on the east side, and Tyee Formation on the west. Minimum thickness of this intrusion is about 360 m.

These rocks, although undated, are considered to be of similar age to the Marys Peak sill based on lithology, similar intrusive relationships, dating of other similar rocks in the central Coast Range (Snavely and others, 1980;

Snavely and Wagner,1961), and on paleomagnetics. The Marys Peak sill is normally polarized (Clark, 1969), as are all the other intrusives field checked in this study, circumstantially supporting the assertion of Snavely and Wagner (1961) that the mid-Oligocene intrusive episode was of short duration.

The distribution of intrusions in the central Coast Range generally consists of large sills in the upland areas, and elongate dikes oriented E-W to WNW-ESE. In the vicinity of the Corvallis fault, this pattern also includes NE trending dikes that intrude the Corvallis fault zone, and sub-parallel NE trending sills that occupy the fold hinges of Spencer and Tyee strata. Many of the larger intrusions are found near the Tyee-Spencer contact. A dike has also intruded the WNW trending Philomath fault, but intrusions were not observed in the other numerous NW trending faults mapped or inferred in this study.

TECTONIC SETTING

The convergent margin of western North America has been dominated by the interactions of the Pacific plate, the Farallon plate and the North American plate throughout the Tertiary. Most of the Farallon plate has been subducted beneath North America, leaving the small Juan de Fuca and Gorda plates actively subducting today.

The relatively uniform geochemistry of the Siletz River Volcanics and its correlatives strongly suggests that a broadly coeval terrane extends from north of the Klamath Mountains to the southern tip of Vancouver Island (Duncan, 1982; Wells and Heller, 1988). There is little agreement, however, on the mode of formation of this terrane and of its subsequent attachment to the North American continent.

Accretion of the Siletz River Terrane

Duncan (1982) proposed that the age distribution of the Siletz River basalts (oldest north and south, youngest near the Columbia River) is the result of formation of oceanic crust and seamounts on a hotspot centered on the Kula-Farallon spreading ridge. Geochemical evidence supports this hypothesis, the basalts having both ridge and hotspot affinities (Globerman and Babcock, 1980; Snavely and others, 1968). Although uncertainties as to the spreading history and transform offsets of the now subducted Farallon plate make a precise reconstruction impossible, one such reconstruction by Duncan (1982) is shown in figure 4.

Based on the assumption of symmetrical spreading rates, his reconstruction shows that the Yellowstone hotspot could have been

in about the right position to generate the age-progressive seamount chain. A constraint on accretion models is the proximity of some of the Crescent and Roseburg basalts to the continent, indicated by the interbedding of continentally derived conglomerates with the basalts (Cady, 1975; Niem and Niem, 1989). Plate reconstructions (eg. fig 4) show the Yellowstone hotspot just offshore in the latest Paleocene, suggesting that formation of the

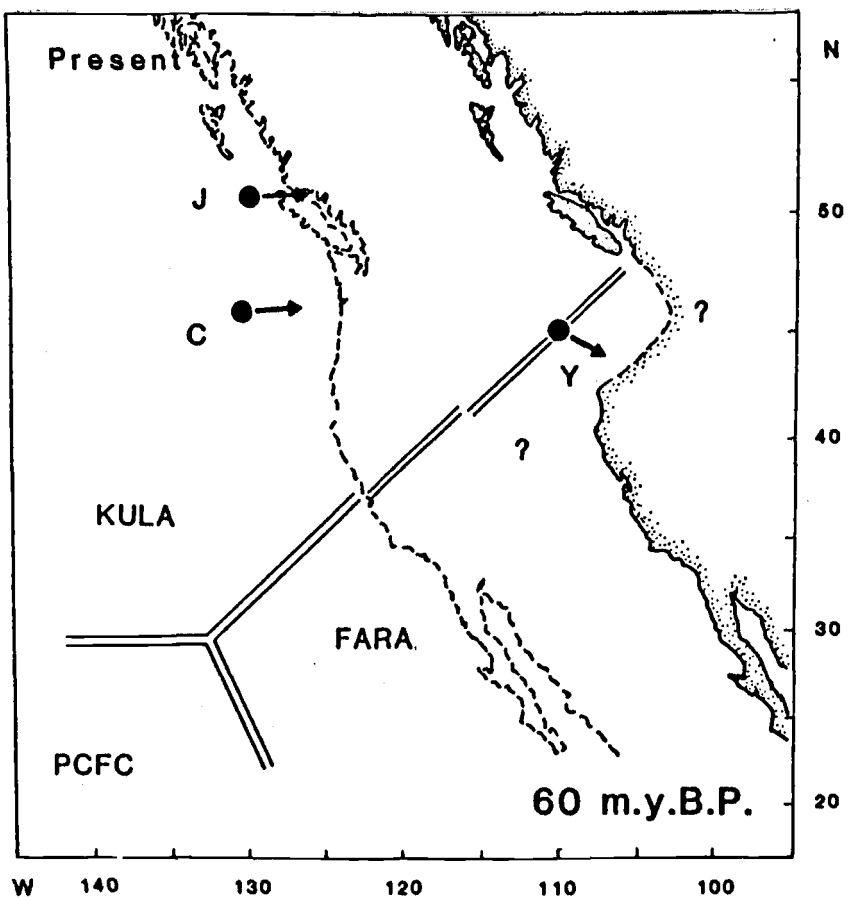

Figure 4. Plate reconstruction at 60 ma showing possible configuration of spreading ridges and hotspots; Y = Yellowstone hotspot, J = J.Tuzo Wilson hotspot, C = Cobb hotspot. Solid arrows show direction of volcano propagation. From Duncan, 1982.

seamounts, accretion, and onlap of continental turbidites all occurred in a relatively short time span.

Wells and others (1984) point out several difficulties with Duncan's model. First, the rapid northeast motion of both the Kula and Farallon plates would produce two northeast-trending seamount chains, which is more difficult to reconcile with the pattern of post-accretion rotations discussed below. Also, the age range of the basalts sampled by Duncan seems to require the hotspot to be some 600 km offshore, to allow enough time for the youngest islands to form before the continent overrode the hotspot. This seems to be inconsistent with the interbedding of basalt with continentally derived conglomerate (Cady,1975; Niem and Niem, 1989).

An alternate origin for the Coast Range basalts has been proposed by Wells and others (1984), Moore (1984), Moore and others (1984), and Snavely (1987). In their model, the terrane was formed in situ by the rifting of the western margin of North America (fig 5). A major element in this hypothesis is the rifting and northward transport of exotic terranes during late Cretaceous and early Tertiary time. Paleomagnetic data from basalt interbedded in the accretionary Prince William and Chugach terranes indicate a paleolatitude of 40.3° ± 6.2° at the time of formation, similar th the paleolatitude of Siletzia (Plumley and others, 1983). It is possible that these terranes were rifted away from the continent adjacent to Oregon and Washington as the North American continent overrode the Yellowstone hotspot. This model is analogous to the rifting of Baja California away from the Mexican mainland by the East Pacific Rise, and northward terrane transport along dextral transcurrent faults.

In the rift model, the age progression noted by Duncan is

accommodated by normal sea-floor spreading in the newly opened rift. The contemporaneous opening of the Republic, Chuckanut, and Chiwaukum grabens may represent an inboard expression of this rifting event. (Figure 2)

Wells and others (1984) considered the problem of the strong compressional deformation of the Roseburg Formation (Siletz River Volcanics) in light of the rift hypothesis. Most investigators have considered the deformation to be evidence for the collision of the seamount terrane with North America. They concluded that minor subduction could still be

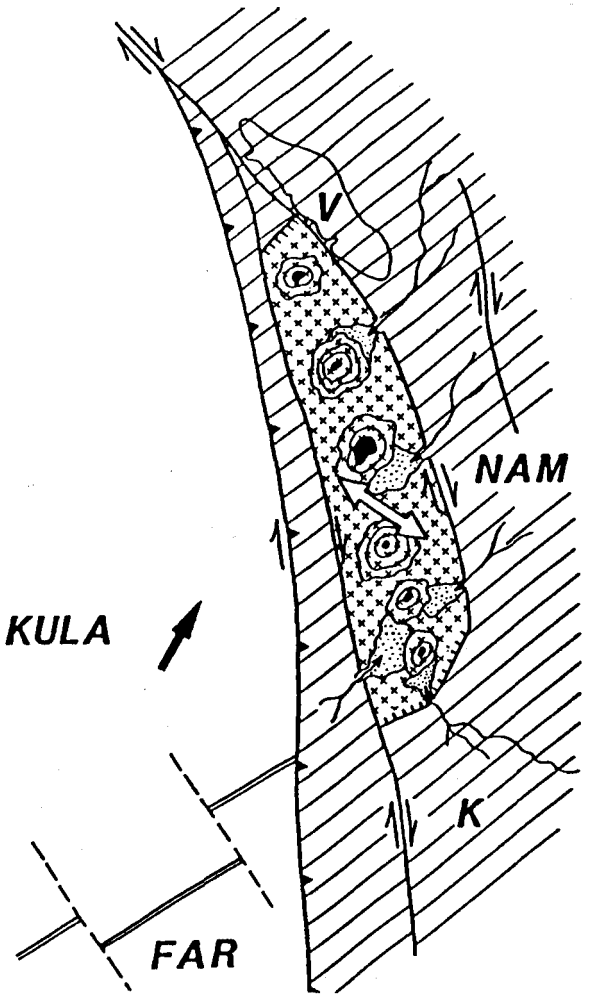

Figure 5. Continental margin rift model for origin of Siletzia seamounts (x pattern). K = Klamath Mountains; V = Vancouver Island; FAR = Farallon plate, Kula = Kula plate; NAM = North American plate. From Snavely, 1987.

consistent with the rifting hypothesis if the Kula-Farallon spreading rate were somewhat greater than the absolute motion between the rifted fragments.

Post-Accretion Tectonics

During the formation of the Siletz River basaltic seamounts and islands, the Farallon plate was subducted at a trench that probably was located near or east of the present Cascade arc. The arc associated with this earlier subduction may be represented by the 50-36 Ma Challis-Absaroka basaltic and andesitic rocks of eastern Washington and Idaho (Armstrong, 1978). The seamount terrane did not subduct, possibly due to its thickness, youth, and buoyancy. In the late middle Eocene the subduction zone shifted to the west near its present position, leaving the seamount terrane stranded in the forearc (Duncan and Kulm, 1989). During and following the accretion of the Siletz seamount terrane, coarse continentally derived clastic sediments of the Umpqua and Lookingglass Formations were deposited unconformably over the northern margin of the Klamath terrane and the folded and faulted Roseburg basalts along the suture (Baldwin, 1974; Snavely and others, 1980). By the latest middle Eocene, subsidence of the accreted seamount terrane began at the site of the present Coast Range, and deposition of the deltaic Flournoy Formation and the deeper water Tyee fan turbidites began in a forearc basin setting (Chan and Dott, 1983).

The earliest Cascade volcanism in the western Cascades began at about 45 Ma, indicated by the influx of volcaniclastic sediments (Baker, 1988; Yeats and others, in prep.), although the oldest dated arc volcanics are slightly younger, with an age of 42 Ma (Lux, 1982).

A period of uplift and deformation in middle to late Eocene time is

indicated by a widespread unconformity on the continental shelf, and along the western margin of the Willamette Valley (Baldwin, 1955; Snavely and others, 1980; Vokes and others, 1954). Strandlines at that time were probably parallel to the boundary with the Klamaths, and with the western Cascades (Baldwin, 1974; Dott, 1966; Niem and Niem, 1984). Alkalic and tholeiitic volcanic centers were active in the forearc at that time, unusual in a forearc setting (Snavely and Wagner, 1961; Snavely and Wells, 1984).

Evidence presented below suggests that a large fault-bounded island was emergent in the east-central Coast Range, and influenced deposition of the Yamhill and Spencer marine strata of the Willamette Valley. This island, along with the broadly correlative Yachats, upper Tillamook, Waverly Heights, Cascade Head and Newport emergent volcanic centers may have constituted a late Eocene Coast Range archipelago composed of both volcanic and tectonic islands.

This period of uplift has been attributed to rapid convergence and increased underthrusting (Snavely and others, 1980), or alternatively to a thermal-mechanical effect created by the passage of the Yellowstone hotspot beneath the forearc region (Duncan and Kulm, 1989). Passage of the Yellowstone hotspot might also explain the unusual and widespread forearc volcanism during this time, which diminished through the late Eocene and early to middle Oligocene.

Gradual rise of the forearc occurred in early to middle Oligocene time, indicated by a shift in strandlines northward and westward from their Eocene positions (Niem and Niem,1984). Filling of the forearc basin by Cascade derived volcaniclastic sediments also contributed to the westward shift. Shallow marine Eugene Formation tuffaceous sandstones interfingering

eastward with the western Cascade marine to non-marine Fisher Formation were deposited in the site of the Willamette Valley (Beaulieu, 1971).

By late Oligocene time, two strandlines were present at the same latitude. A high energy wave dominated delta of the Yaquina Formation built westward over deeper water facies at the present site of the west-central flank of the Coast Range (Niem and Niem,1984; Snavely and others, 1969). To the east, late Oligocene rocky shoreline deposition of the Scotts Mills Formation occurred on the western flanks of the western Cascades (Miller and Orr, 1988). This evidence for two late Oligocene strandlines suggests either a rapid regression in the late Olgocene, or that the Coast Range was present at that time, a configuration similar to that inferred for the late Eocene in this study.

The westward shift in strandlines continued through the mid-Miocene, when strandline and deltaic facies of the Astoria Formation were deposited near the present coastline (Niem and Niem 1984; Parker, 1990).

In middle Miocene time, the voluminous Columbia River Basalts (CRB) were erupted east of the Cascades. Grand Ronde and Frenchman Springs basalts flowed as far as the coast, near the present mouth of the Columbia River (Snavely and Wagner, 1963). Flows are also found in the Willamette Valley as far south as the Lebanon area (latitude 44° 34.1', Beeson, 1979; E.P. Graven, personal communication, 1990). Flows and intrusive rocks identical to the Columbia River Basalts are also found along the Oregon Coast as far south as Cape Foulweather (latitude 44° 45.0). Flows reaching the coast probably invaded unconsolidated marine sandstones and siltstones and flowed out into shallow water, producing volumes of pillow basalts at Depoe Bay, Cape Foulweather and the proposed invasive flows at Cape

Lookout and Cape Meares (Niem and Niem, 1984; Parker,1990). If these flows reached the coast via the present site of the Coast Range, the Coast Range must have been subdued during CRB time. Later uplift has probably removed the intervening CRB's, as none have been found in the central Coast Range (Beeson,1979).

Fault activity along northwest and northeast trends during the eruption of the CRB's is suggested for the Willamette Valley and northeastern Coast Range by the influence of faults with those trends on the distribution of CRB flows (Beeson, 1985). Post- late middle Miocene uplift of the Coast Range along a north-south axis has exposed the core of older Eocene rocks, including the Siletz River Volcanics and Tyee Formation (Niem and Niem, 1984; Snavely, 1987). In the study area, Coast Range uplift has exhumed structures related to the Corvallis fault, and differential erosion has essentially re-created the late Eocene paleotopography.

Tectonic Rotation

Paleomagnetic evidence has demonstrated that the Coast Ranges of Oregon and Washington have undergone varying amounts of clockwise rotation from middle Eocene time until the post-Miocene (Beck and Engebretson, 1982; Globerman and others, 1982; Magill and others, 1981; Wells and others, 1984; Simpson and Cox, 1977). In the central Coast Range, the Siletz River Volcanics have been rotated 65°-75° $\pm$ 12° , the Tyee has rotated 64° $\pm$ 12° (Simpson and Cox, 1977), the Marys Peak sill is rotated 28° $\pm$ 12° (Clark, 1969) and rotations of up to 16° have been described for the middle Miocene Columbia River Basalt (Bentley, 1980; Reidel and others, 1984; Sheriff, 1984). These studies show that rotations decrease in

progressively younger rocks.

Many widely different models have been proposed to explain these rotations. Simpson and Cox (1977) and Duncan (1982) suggested microplate rotation around a southern pivot during collision of the seamount terrane with North America. Magill and others (1981) proposed rotation about a northern pivot in response to basin and range extension to the southeast. Frei and others (1984) combined these two models in a two-stage rotation. Moore (1984) proposed a small plate rotation due to an unstable triple junction between the Kula, Farallon, and North American plates. Beck (1980) suggested the "ball-bearing" model, dating back to Wise (1963), in which the seamount terrane is rotated in a dextral shear-couple between the Pacific and North American plates. Wells and Coe (1985) proposed that rotation is accommodated on sinistral R' shears in a dextral simple shear regime. They suggested that the faults may in part be inherited from a previous tectonic fabric.

Constraints imposed by this large quantity of paleomagnetic data are: 1) Rotations of the post-accretion Tyee turbidites are similar to those of the Siletz River Volcanics. 2) Lesser rotations of rocks as young as middle Miocene have been reported (Reidel and others, 1984). 3) Rotation during accretion is limited to about 20% of the total, the remainder partitioned between effects of dextral shear rotation, and rotation outboard of the extending Basin and Range (Wells and Heller, 1988). The four models most widely cited are illustrated in figure 6.

The limiting factor in distinguishing between the various rotation models seems to be structural evidence from the rotated terrane. In order to test small-block rotation or dextral shear rotation models, detailed mapping of

the rotated rocks must be done in order to locate the structures on which the movements have occurred.

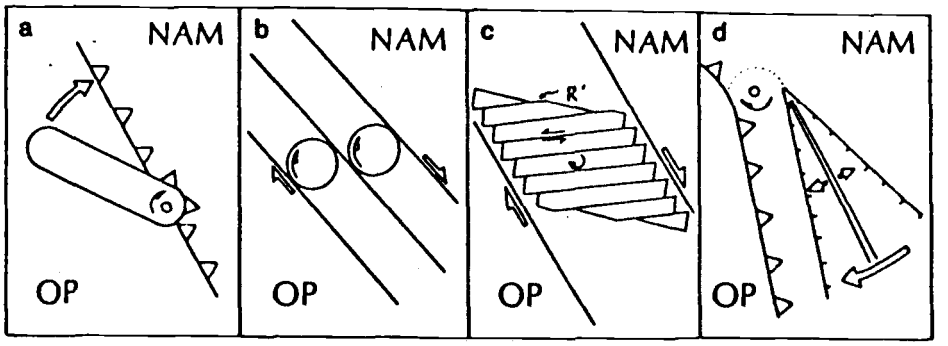

Figure 6. Models for rotation of terranes along western North America continental margin. (a) Oblique collision rotation; (b) ball-bearing model; (c) Riedel shear rotation; (d) asymmetric intra-continental extension; NAM = North American plate; OP = oceanic plate. From Wells and others, 1984.

Convergence History

A final element in the tectonic setting of western Oregon is the convergence history of the North American and Juan de Fuca plates. Verplanck and Duncan (1987) calculated the plate convergence rates through time and suggested that the rate has decreased fivefold, from 16.0 to 3.2 cm/yr since the Eocene, based on a mantle-fixed hotspot reference frame. This is supported by a similar decrease in the relative volumes of volcanic material erupted over that time. They suggest that a decrease in the convergence angle from nearly 90° to less than 30° since the Eocene has further contributed to the reduction in volume of Cascade volcanism.

MAPPING THE CORVALLIS FAULT

Field mapping of the Corvallis fault was conducted during the summer and fall of 1988, and several additional weeks during the summer of 1989. The mapped area covers approximately 335 km^2 (130 mi^2), and is about evenly divided between the eastern flank of the Coast Range, and the western Willamette Valley and adjacent low hills (Figure 7 and Plate 1).

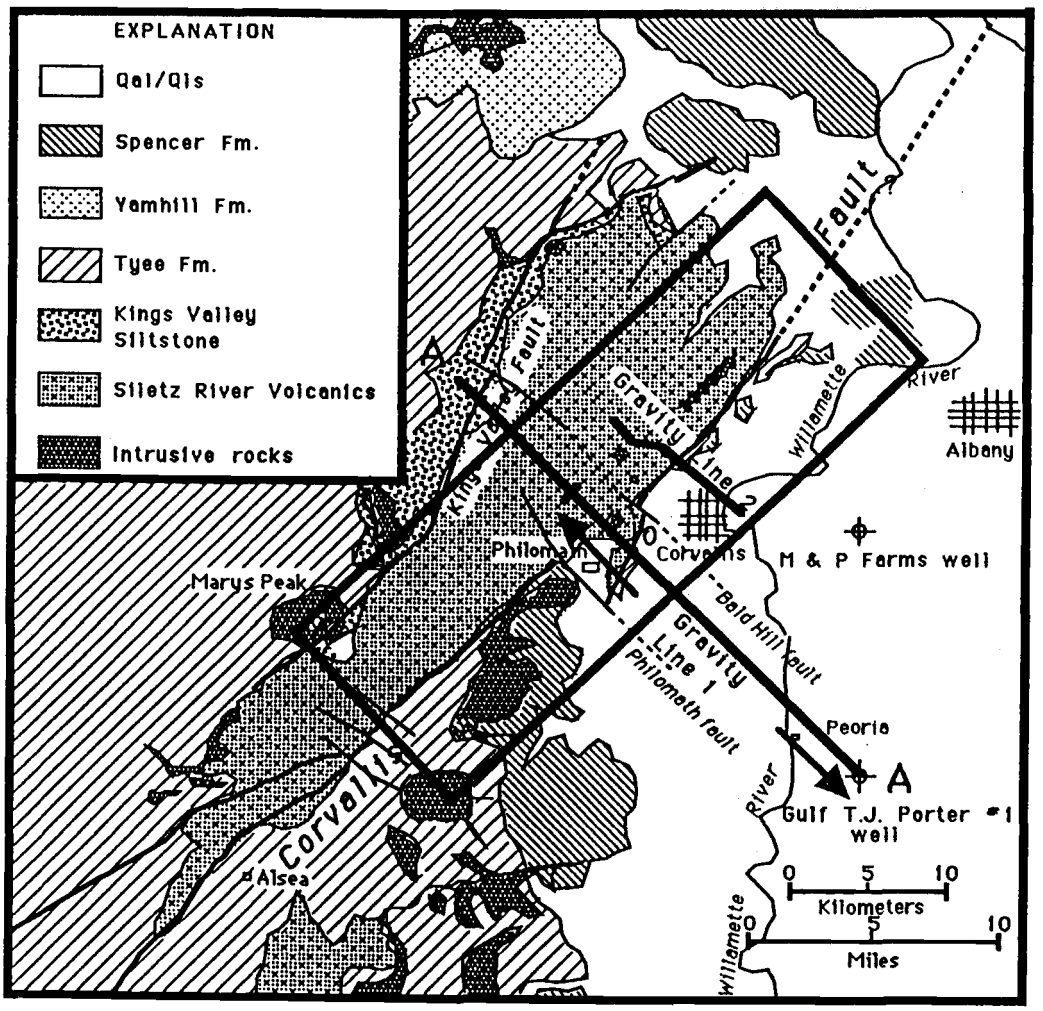

Figure 7. Mapped area of Plate 1, indicated by heavy box.

All the units in the map area have distinguishing characteristics that are most often useable in the field. The Siletz River Volcanics are easily recognizable as zeolitic, usually amygdaloidal, pillow basalt flows, and breccia. Some massive outcrops are present, but in most cases these fine-grained basalts are easily distinguished from the next most common igneous rock in the area, the Oligocene intrusives, on the basis of grain size, texture, and crosscutting relationships. many of the intrusive bodies mappable at 1:24,000 scale are medium to coarse-grained granophyric gabbros, indistinguishable from those of the Marys Peak sill. The largest intrusions, such as the Dike Hill body, are differentiated as is the Marys Peak sill, with ilmenite-rich granophyric diorite making up the upper portion, and some aplite dikes radiating into the baked Spencer sandstones above. The larger intrusions are commonly sills or laccoliths, and show a tendency to intrude the Spencer-Tyee unconformity, which is close to the present surface in much of the area east of the Corvallis fault. Numerous smaller fine-grained intrusions are also present, and these generally are steeply dipping dikes of from 1-5 m in thickness. These smaller intrusions often deformed and upturned Spencer and Tyee sandstones.

Attitudes taken within the Siletz River Volcanics are generally from basaltic sandstone and siltstone interbeds. Some attitudes are from flow contact surfaces, and these include the initial dip of the surface. A few attitudes were taken from the average orientation of individual pillows, where no interbeds or flow contacts were available. Pillow orientation and load features formed in the sand interbeds by the overlying pillow basalts were also used on several occasions to determine stratigraphic tops of flows.

The Tyee Formation is distinguished by graded bedding, abundant

plant and wood debris, sole markings, mudstone rip-ups and the general lack of megafossils. The overlying Spencer Formation is both arkosic and micaceous, and can be similar in appearance to the sandy fraction of the Tyee. However, abundant megafossils, general absence of graded beds (although some were found) and the frequent presence of cross-stratification distinguish it from the Tyee.

The general scarcity of fresh outcrops, particularly within the Tyee and Spencer outcrop areas led to some desperate tactics. Construction sites are found to be excellent sources of fresh outcrops where natural ones are lacking, or too weathered to be of use. Also, municipal projects such as pipe and cable laying usually produced ditches to be examined. Some critical areas simply did not have any outcrops or any hope of there being any in the near future, and so some small excavations were done, probably arousing the curiosity of local residents who wondered at all those holes along Walnut, Circle, and West Hills roads. The problem with mapping geology in construction sites and temporary excavations is that later workers will find it difficult to locate some of the of the structural information depicted on the map, particularly within the city limits of Corvallis. This could not be helped, however, and I had the same difficulty in using older maps, where some of the best described outcrops were undoubtedly construction sites exposed during those studies, and are now covered by buildings. The large study area precluded complete remapping of all areas. Emphasis was given to the structural elements, and areas not well covered in previous investigations.

Interpretation of individual features shown on the geologic map will be discussed in upcoming sections as they relate to the paleogeography, gravity, magnetics, remote sensing, and neotectonic aspects of the study.

EOCENE PALEOGEOGRAPHY

Stratigraphic relationships observed in the study area have shed some light on the local paleogeography during the late Eocene in west central Oregon. Concentrated along the Corvallis fault is a basaltic coarse-grained sandstone to boulder conglomerate with clasts up to 2 m in diameter (see Plate 1 for distribution). These coarse deposits are clearly derived from the Siletz River Volcanics they are in fault contact with. Basaltic clasts are amygduloidal, with zeolite and calcite fillings. Some are recognizable individual pillows. These coarse-grained deposits fine rapidly away from the fault and are (in the finer fraction) richly fossiliferous, with abundant Teredo-bored wood, bivalves and gastropods. The faunas are poorly preserved, and shells are abraded and fragmented. Faunas collected along the fault zone contain Brachydontes (Bivalve) and Polinices (Gastropod). Brachydontes lives in shallow to intertidal waters, but is most commonly found in the intertidal zone (Ellen J. Moore pers. comm., 1989). Teredo-bored wood could be found at any water depth, but the abundance found in these outcrops suggests concentration by wave action.

On the southeastern flank of Logsden Ridge (2 km northeast of Lewisburg), an outcrop of micaceous Spencer sandstone is in high-angle contact with a deposit of basaltic gravel. No evidence of faulting could be found, and this outcrop is interpreted as a channel cut into newly deposited Spencer sand and carrying basaltic debris from the Siletz River Volcanics to the west. The orientation of the channel contact is northwest, suggesting the local topographic slope had a northeast strike. Similar basaltic conglomerates were also found a short distance to the east on the southern

flanks of Spring Hill near Albany (Baker, 1988). The conglomeratic facies found adjacent to the fault zone appears to interfinger with cross-stratified Spencer Formation consisting of arkosic micaceous sandstones immediately to the east, in the Logsden Ridge and Philomath areas, and thus is considered to be a local facies of the Spencer, most likely the lower member.

These data strongly suggest that during deposition of these shallow water high energy sands and conglomerates, a subaerial highland existed to the west that was supplying both arkosic micaceous sand and basaltic debris to the east during deposition of the Spencer Formation, and possibly during deposition of the Miller sand. Concentrations of intertidal fossils, boulder conglomerates, and high concentrations of Teredo-bored wood debris along the trace of the Corvallis fault further suggest that the eastern limit of the highland coincided with the trace of the Corvallis fault (Figure 8).

The presence of Siletz River basaltic debris and arkosic micaceous sands that closely resemble the Tyee along the fault indicate that both Tyee strata and the Siletz River Volcanics acted as secondary sources for the Yamhill and Spencer sandstones, and at least locally were the primary source. The cutting of channels filled with basaltic lag into micaceous sandstones of the Spencer is consistent with the unroofing of the Tyee-SRV highland to the west, and suggests that considerable quantities of Tyee sandstones were eroded and deposited in the Yamhill-Spencer basin to the east.

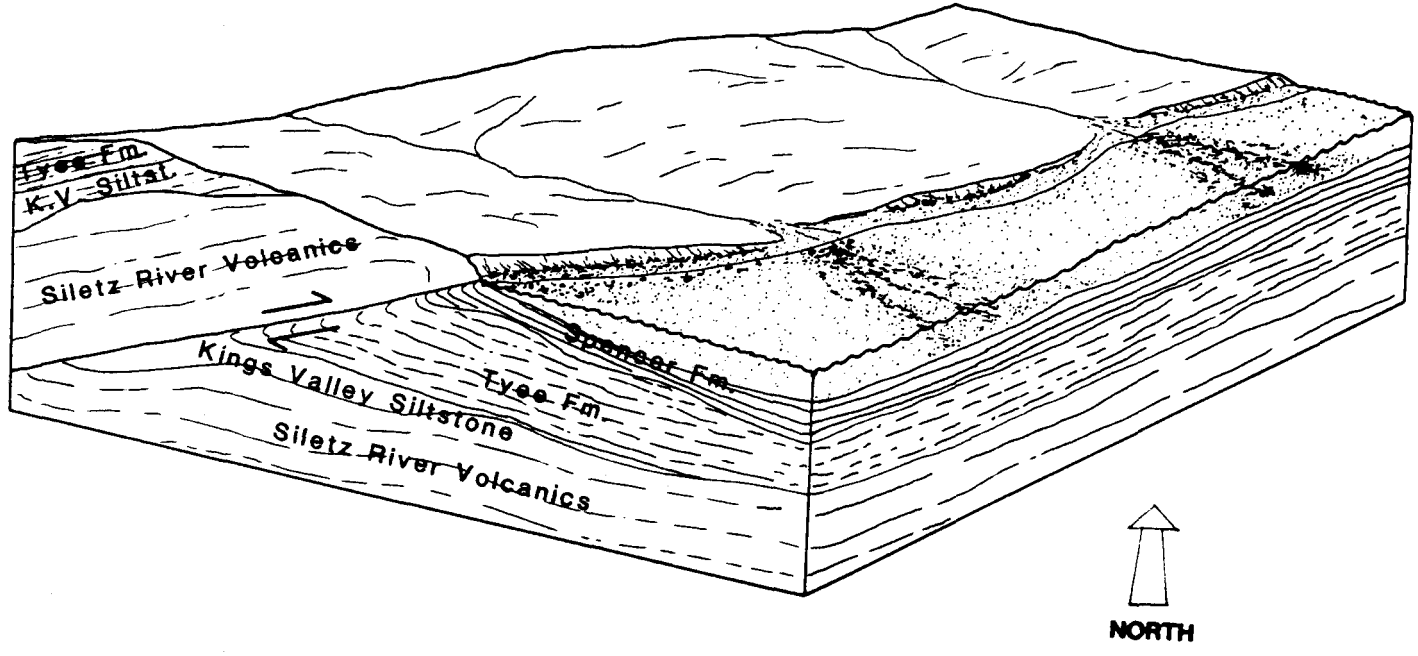

Figure 8. Paleogeography and depositional setting of the Spencer Formation along the Corvallis fault, late Eocene.

Late Eocene Paleogeography of Western Oregon

Other strandlines in western Oregon are well known during late Eocene time. In the Coos Bay area of southwestern Oregon, the late Eocene Coaledo Formation was deposited in a shallow shelf to deltaic environment. From the Coos Bay area the strandline most probably trended northeast, sub-parallel to the Klamath suture, to the Eugene area, where Spencer Formation shallow water to non-marine units interfinger with non-marine volcanic Fisher Formation Beaulieu, 1971; Baldwin, 1974; Vokes and others, 1951). The intervening strandline deposits have largely been removed by erosion during and after the Coast Range uplift, however possible Spencer and Coaledo equivalents are preserved in a synclinal axis mapped in the south-central Coast Range (Baldwin,1961; Niem and Niem, 1989). In the northern Oregon Coast Range, the correlative Cowlitz and Spencer Formations were deposited in similar environments. The strandline location between the Eugene area and the Cowlitz-Spencer deltas is not well known, but most probably lay along the western Cascades, in the present eastern Willamette Valley.

The uplifted Corvallis fault block represents a tectonic island present 10-20 km offshore during the late Eocene. Other islands, mostly volcanic constructions, were also present at about this time. The Yachats Basalt crops out from Alsea Bay to Heceta Head on the central Oregon coast north of Florence. The Yachats Basalt consists of about 750 m of mostly subaerial basalt interbedded with basaltic conglomerate and sandstone that interfingers laterally with sandstones of the Nestucca Formation (Snavely and Macleod, 1974). The Yachats Basalts are underlain and overlain by upper Narizian

Nestucca sandstones and siltstones, which are correlatives of the Spencer, Coaledo and Cowlitz strata (Armentrout and others, 1983; Snavely and MacLeod, 1974). In the Newport area, similar unnamed late Eocene subaerial basalts have been mapped in the lower part of the Siletz River and at Cascade Head (Snavely and MacLeod, 1974).

Farther north, the upper Tillamook Volcanics were subaerial flows supplying minor basaltic sand to the Cowlitz deltas (Niem and Niem, 1985). The Tillamook volcanic islands were emergent during the late Eocene, and may have been a subaerial feature from the middle Eocene through to the end of the late Eocene. Nelson (1985) described volcanic arenites derived from the Tillamooks Volcanics as interbedded with arkosic sands in the lower Cowlitz Formation, analogous to depositional relationships observed along the Corvallis fault. In the northern Willamette Valley, the basalt of Waverly Heights may represent a subaerial correlative of the Tillamooks Volcanics (Yeats and others, in prep.), and may also be present in two wells in the Tualatin Valley area. This basalt likely represents another late Eocene volcanic highland.

Figure 9 is a paleogeographic reconstruction of western Oregon in the late Eocene based on this work and the above evidence. Subsequent erosion and burial would suggest that these highlands were more numerous and extensive than those shown based on the present outcrops. This is supported in the case of the Yachats Basalt by the presence of numerous dikes and sills of Yachats Basalt in the Tyee Formation to the east of the Yachats outcrop area, and by the presence of Yachats basalt extending offshore, as indicated by aeromagnetics (Snavely and MacLeod, 1974).

These islands may not have all been simultaneously exposed as

shown, as the ages of the various units involved are not precisely known. This is due to the potentially large error in radiometric dates on the weathered Eocene volcanic rocks, and the discordance between some of these dates, and those determined from foraminifera.

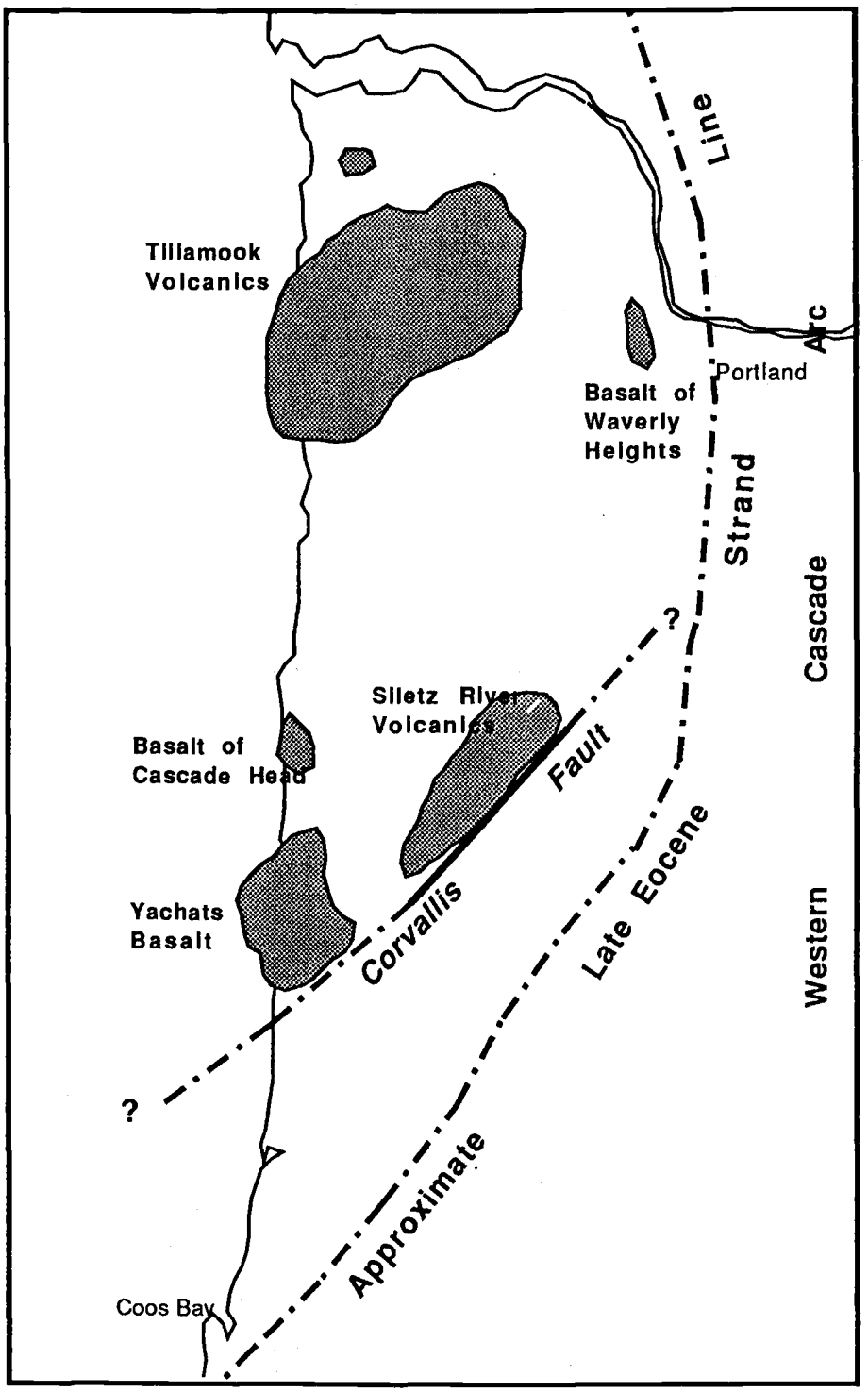

Figure 9. Late Eocene paleogeography of western Oregon.

GRAVITY

A gravity survey was conducted for this study along two traverses oriented normal to the Corvallis fault and the northeast structural grain of the east-central Coast Range.

The first gravity traverse was run from the Gulf Oil T.J. Porter no. 1 well northwest for a distance of 25 km to a point northwest of Philomath (figure 10). The southeast end point was chosen to take advantage of the stratigraphic control available in the Porter well, the only deep well in the area to reach the Siletz River Volcanics. Also, a seismic line located near the Porter well was available and was used to extend subsurface control northwest to the Willamette River. The remainder of the traverse route was selected to take advantage of a gravity base station located at the Corvallis airport, and a series of benchmarks for elevation control (Rinehart and others, 1964). Elevation control between benchmarks was by leveling lines and loops between benchmarks. Maximum elevation error is estimated to be $\pm$ 0.15 m based on loop closure. Although the benchmarks used were surveyed by a variety of agencies over several decades, elevation differences were commonly on the order of 5-10 cm, well within the precision needed for the gravity survey.

Although gravimeters are sensitive enough that elevation control is always the limiting factor in gravity work, station spacing sets a practical limit on the size of the structures that can be resolved with gravity measurements, regardless of instrument precision. Station spacing varied along Line 1, being 200-300 m in the area of interest near the fault, and increasing away from the fault. This was due mainly to time and cost

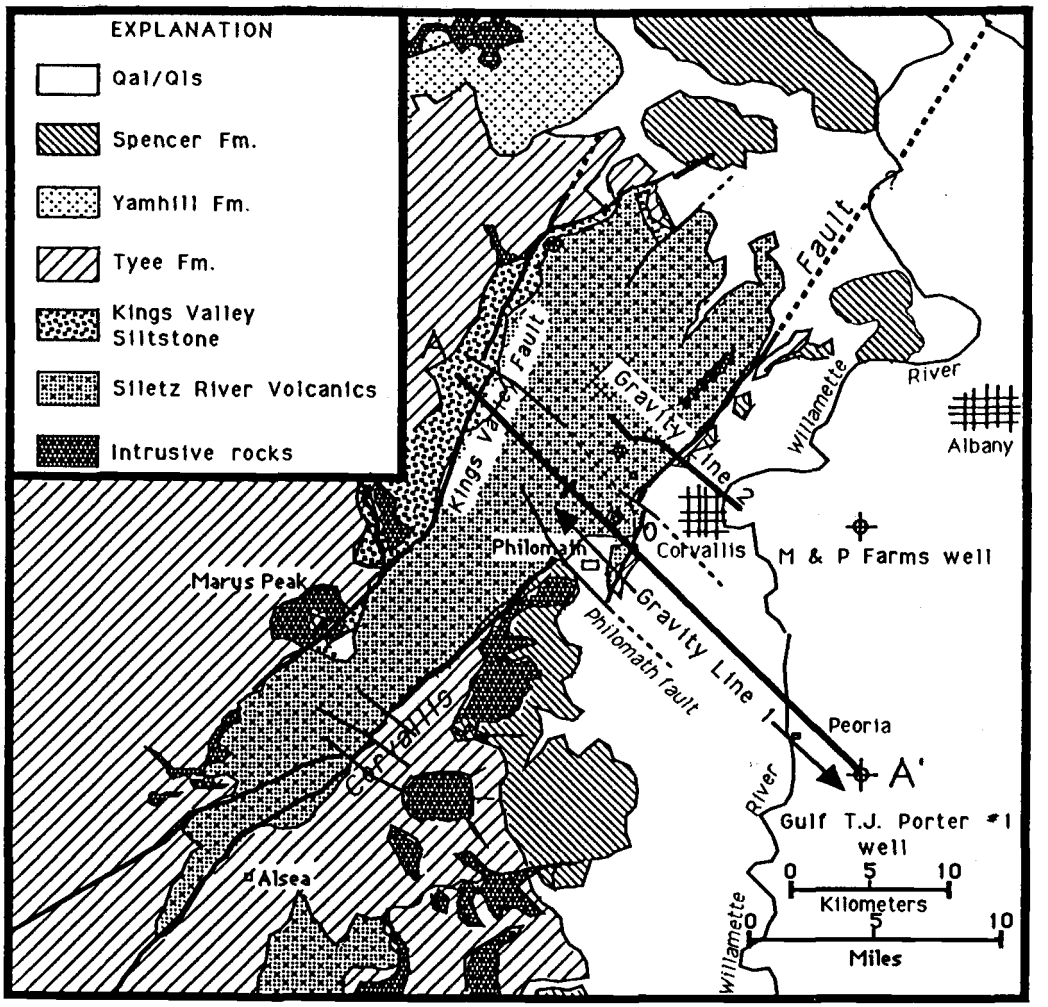

Figure 10. Location map showing the two gravity lines, the cross section line A-A', and wells used for subsurface control.

constraints that would not permit closer spacing along the entire 25 km length of the line.

A shorter second line, Line 2, was completed in order to verify the unexpected results of Line 1. Line 2 runs from a point on State Highway 34 east of the Willamette River, 10 km northwest through the City of Corvallis to a point in the Coast Range. The route was chosen to take advantage of a dense network of benchmarks located within the city limits. As before,

leveling lines were done where elevation data were unavailable. Station spacing along Line 2 averaged about 250 m. A base station at the Oregon State University Oceanography building was used for Line 2.

Gravity measurements were made with a LaCoste and Romberg model G gravimeter #707, looping back to the base station every two hours during the survey. No tears occurred on Line 1, and all airport base station values were plotted to obtain a combined earth tide and drift curve from which a correction was derived and applied to all values on Line 1. The same procedure was followed for Line 2. A tear occurred on Line 2 between stations 33 and 34. Repeated measurements between that location and the base station established the magnitude of the tear, and a correction was applied to the preceding stations. Terrain corrections were made to both lines using the modified method of Hammer (1939) in Telford and others (1976), and free air and Bouguer slab corrections were made using the method of Tsuboi (1983), based on IGSN 1971.

Modeling of both lines strongly indicates a surprising result. A sharp increase in gravity was expected across the fault as previously interpreted, as the density contrast is 0.3-.04 g/cc. With an estimated minimum vertical separation on the fault of 1500 m, a 7-10 mgal increase, with a steep gradient was expected. However, the increase across the fault was only 2-3 mgal, and a very gradual increase was seen to occur west of the fault. Modeling of these data suggested that the fault contact between the Siletz River basalts and younger Eocene strata dipped shallowly to the west, rather than steeply, as field observations and previous mapping indicated. The principal structure of the Corvallis fault is a low-angle thrust.

For the remainder of this paper, this low-angle contact will be referred

to as the Corvallis thrust, a structural relation not readily apparent at the surface. The high-angle structure observed in outcrop, as will be discussed below, is considered to be a younger feature that has truncated the leading edge of the thrust along a parallel trend. This structure will be referred to as the Corvallis fault.

The Gravity Models

Geologic Constraints on the Gravity Models

Constraints on the models come from surface geology, multichannel seismic lines at the eastern ends of both lines, and lithologic, dipmeter, and neutron density logs from the T.J. Porter, and M&P Farms, wells. In the Porter well the Siletz River Volcanics are found at a depth of -2060 m msl. Overlying the SRV are 320 m of Tyee Formation, and 1048 m of the Yamhill Formation. Surface geology to the west in the field area shows just the opposite relation, with an estimated 1200-2400 m of Tyee strata along the Corvallis fault, and the Yamhill absent (1200 m is the minimum thickness of the Tyee based on a measured section along West Hills Road, 2400 m is estimated for the Tyee in the Marys Peak area from mapping in this work and from the mapping and descriptions of Baldwin, 1955). The Tyee was modeled as thickening uniformly to the west in the absence of other information, and likewise the Yamhill is shown thinning uniformly to the west.

A unit shown in the models but not seen at the surface along the gravity traverses is the Kings Valley Siltstone. This unit has been estimated to be 1000 m thick in Kings Valley (Vokes and others, 1954), making it a significant low-density body at the scale of the gravity models. It has been included in the models, thinning uniformly to the east, where it is not recognized in deep

wells. The surface location of the Corvallis fault itself is well constrained to within a few meters, based on both surface geology and magnetics (Plate 1 and Figure 18).

Formation densities were obtained from a variety of sources. Neutron density logs were used where available from deep petroleum test wells in the Willamette Valley, and these were supplemented by lab determinations for the Siletz River Volcanics and the Tyee Formation (Bromery and Snavely, 1964; Couch and Braman, 1979). A density value for the Kings Valley Siltstone was unavailable, so a value was selected from a table of typical rock densities in Telford and others (1976).

Each method is subject to error in terms of estimating the actual bulk densities of rock units. Neutron logs and lab determinations sample localized rock units, and may not account for fracturing and porosity on a larger scale. Density determinations for the Siletz River Volcanics fail to account for the effect of sand interbeds and fracturing, and only sample the uppermost unit, which is more likely to be weathered and altered. The available density data for each rock unit were considered, and densities were assigned to reflect my best estimate of realistic bulk densities.

No regional correction or long wavelength filtering was applied to either line. The regional gravity gradient is not clearly separable by wavelength from the signal of mid to upper crustal structures such as the target of this study. Lack of well established constraints on the crustal geometry made it possible that filtering or regional corrections would degrade rather than improve the models. Additionally, as will be discussed below, modeling the unfiltered data acted as a conservative influence on the possible interpretations. Neither a regional correction nor long wavelength

filtering would be likely to significantly alter the principal conclusion that a shallow-dipping thrust is present west of the Corvallis area. A regional correction of this type would reduce the slope of the gravity profiles somewhat, but could not produce the steep gravity gradient across the Corvallis fault that would be expected if it were a high-angle structure.

Gravity Interpretation

Gravity modeling was done on an IBM AT using G-M SYS, a proprietary gravity and magnetics modeling program developed by Northwest Geophysical Associates of Corvallis, Oregon (Figs.11 and 12). The computational basis for the program is the method of Talwani and others (1959). Maximum model depth was set at 5 km, selected to best model the upper crustal structure. The target of interest in these models was the geometry of the Siletz River basement. Structure higher in the sedimentary section was considered secondary, due in part to the relative lack of density contrasts between the upper Eocene and younger sedimentary units. In modeling Line 1, good density and depth controls were available from the Porter well at the eastern end of the line, so the calculated gravity was fixed at that end while geometry and structure was iteratively changed along the rest of the line until a satisfactory fit to the observed data was obtained. Line 2 was modeled the same way, however, the fixed east end of the line was not as well constrained as on Line 1. The M&P Farms well was used to constrain densities and thicknesses in the upper 1200 meters of section, the total depth of this well. Seismic control was used to constrain the lower section, down to the Siletz River Volcanics.

The models show the Corvallis fault dipping shallowly to the northwest.

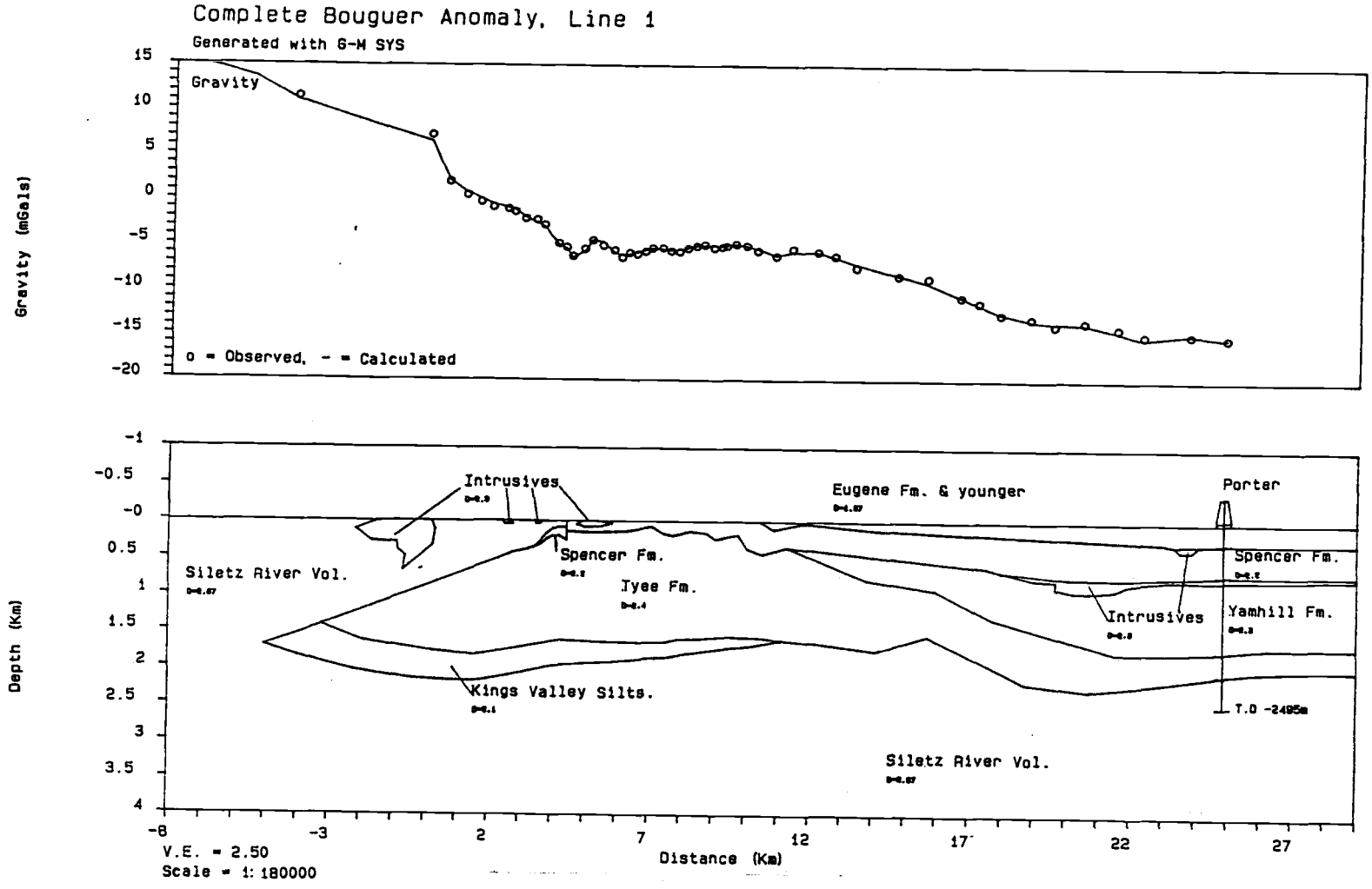

Figure 11. Gravity Line 1. See Figure 10 for location.

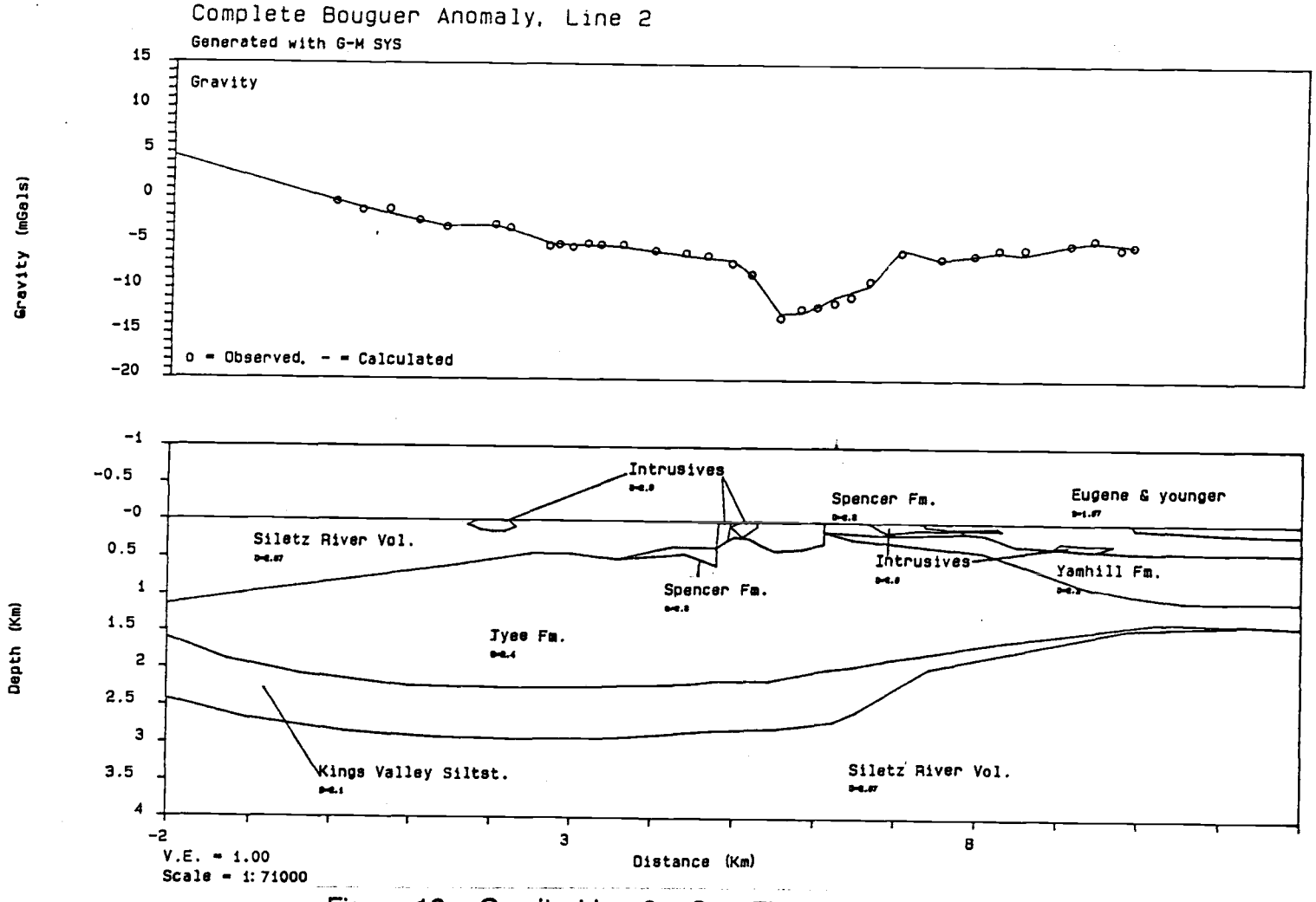

Figure 12. Gravity Line 2. See Figure 10 for location.

Independent modeling of the two lines produced nearly identical dips of about 10°. Initially I was concerned that 3D effects, due to the proximity of the large right step in the main fault trace near Line 1, might be the reason for the unexpectedly low dip. However modeling of Line 2, which was located far from any major offset, confirmed the low-angle of this interface, and thus 3D considerations are believed to be negligible. With such a low dip, the density contrast across the Philomath fault is relatively low, as only the thin leading edge of the upper plate is offset, rather than a thick block of Siletz River Volcanics as would be expected if the Corvallis fault were a high-angle fault.

The location of the footwall cutoff is poorly constrained in both lines. If the fault cuts steeply across the Tyee-Kings Valley Siltstone contact, the footwall cutoff should be marked at the surface by a rapid rise in observed gravity. Alternatively, if the angle between the fault surface and the contact is a shallow one, the footwall cutoff may go unobserved on the gravity profile. On Line 1, The location of the cutoff may be suggested by the high observed value of station 1, the westernmost station. Some public domain gravity data are available to the west of Line 1, however modeling including these data is inconclusive due to the large gaps in the data. Alternatively, the increase at station 1 could also be due to the near surface presence of large intrusions. Small intrusions have been mapped in that area (Plate 1), and intrusive bodies are inferred for the area based on aeromagnetics, however, poor exposure makes determination of the size of the intrusion(s) impossible. On Line 2, no sharp rise in observed gravity occurred toward the west end of the line, and it is probable that the line did not extend far enough to the west to include the footwall cutoff. The cutoff in Line 2 is placed beyond the limit of the data and should be considered schematic.

The low-angle thrust interpretation is surprising, as the straight surface trace and other aspects of the surface geology suggest a steeply-dipping contact. A feature of the gravity models supporting this interpretation is the concave upward shape of the gravity curve in the area of the inferred thrust. This appears on both lines and is suggestive of a low-density body beneath the Siletz River Volcanics. The wavelength of the low is too short to be reproduced by introducing anomalous densities below the model depth, or to the west.

An analogy the the gravity models of this study comes from gravity models of the Wind River thrust of the Wyoming foreland thrust belt, a structure with a gravity profile of similar form to that of the Corvallis fault, although roughly double in amplitude (Berg and Romberg, 1966; Smithson and others, 1978). Figure 13 shows two gravity models for the Wind River thrust system. Model A is based on the geometry interpreted for the structure based on seismic reflection. Density control of both the sedimentary section and the crystalline rocks is good, with deep well data from industry. Model A produced a curve with a steeper gradient near the thrust tip, and a Bouguer curve higher overall than the observed values. Model B resolved the mass excess of model A by reducing the dip of the thrust and increasing the amount of horizontal displacement. The authors suggested that perhaps the discrepancy in the fault dip between the seismic and gravity interpretation was the result of misinterpretation of the reflectors picked as the fault plane in the seismic section. Rather than the fault plane, the dipping reflectors may have been the overturned Paleozoic sediments thought to underlie the thrust plane, and thus the thrust plane would be somewhat higher in the section and have a shallower dip.

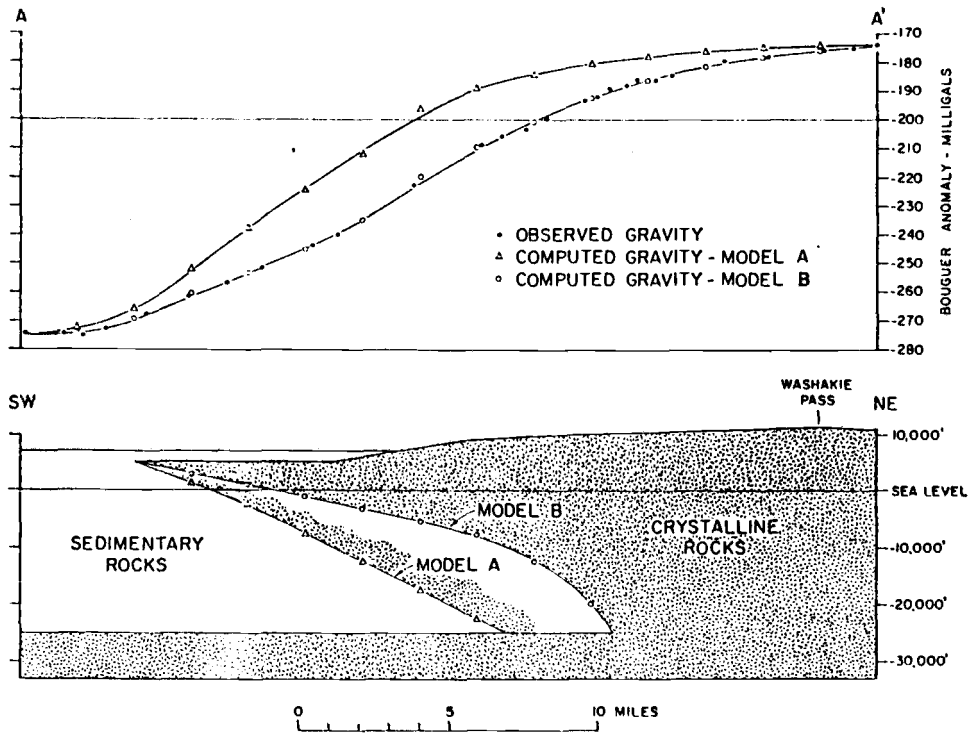

Figure 13. Gravity models of the Wind River thrust. See text for discussion. From Berg and Romberg, 1966.

The process of modeling the Corvallis fault was very much analogous to that described for the Wind River thrust. Holding densities constant, fixing the east ends of the lines at the well controls, and the west ends to points in the central Coast Range, the dip and sub-thrust geometry were iteratively changed until a best fit was obtained.

The Siletz River Volcanics as modeled show considerable structural relief in both models. Seismic lines in the Willamette Valley show similar antiformal and synformal morphology to the east of the study area (Graven, in prep). The basement topography could be the result of either folding and

faulting, or topography developed during formation or erosion of the seamount province prior to deposition of the overlying sedimentary sequence.

Intrusions mapped at the surface have in most cases been included in the models where they are of sufficient mass to appear on the observed data. These are modeled using a density of 2.90 g/cc, a typical value for intrusive gabbros (Telford and others, 1976). The subsurface configuration of these intrusive bodies is not known, with the exception of the eastern portions of the three sills at the east end of Line 1. These sills appear on seismic reflection profiles and were also penetrated in the Porter well. Several other intrusive bodies are shown in the subsurface where short wavelength gravity anomalies are observed. Some of these suggested intrusives correlate to aeromagnetic highs, supporting the interpretation of subsurface intrusives.

The Geologic Section

The geologic section A - A' was constructed along gravity Line 1 using the surface geology, available well and limited seismic data described above, and the gravity models, which were used to constrain the overall geometry of the Siletz River Volcanics and basement depths (Plate 2). The line was extended west to Kings Valley to include the ramp geometry and décollement (see fig. 10 for location of A-A').

Field mapping shows that both the Tyee and Spencer Formations are involved in a set of sub-parallel east vergent folds. (Lawrence and others, 1980), (Plates 1 and 2). Fold trends in the Spencer-Tyee section are generally northeast, parallel to the Corvallis fault. A basement high at km 11 in Line 1, and near the east end of Line 2 may also be a northeast trending fold. A fold axis projected northeastward from the high in Line 1 at the same

average azimuth as folds in the sedimentary section intersects Line 2 at the high at the east end of the line. This antiform runs northeastward from Muddy Creek to the vicinity of the Willamette River, immediately east of Corvallis. This structure is also evident in a proprietary seismic line, and highly disrupted Spencer and Tyee strata suggest a fault at its crest. Although no information is available to confirm the trend of this fault, its presence on the crest of the northeast trending subsurface antiform suggests that it may also follow a northeast trend. At the surface along this trend, both Muddy Creek, the lower Marys River, and a portion of the Willamette River bend sharply and follow the surface projection of this structure, suggesting the possibility of structural control of those drainages. Southwest of the map area, Baldwin (1955) mapped the northeast-trending Prairie Peak anticline parallel to, and several km east of the Corvallis fault. This structure continues to the northeast in Tyee strata in the southeastern part of the geologic map. The northeast-trending basement structure suggested by the gravity models may the extension of the Prairie Peak anticline in the subsurface.

The Tyee Formation is shown as making up nearly all the stratigraphic section below the fault tip. Gravity suggests a thickness of 2.15 km for the Tyee, consistent with field estimates. The location of the Spencer-Tyee unconformity is near the surface in the area adjacent to the fault, and dips at an average of about 20-25° to the east or southeast. Although outcrops are sparse, the highly variable angular unconformity between the Spencer and the Tyee, the intertidal fossils in the Spencer, and the folding of both units suggests that there was an irregular erosional surface on the Tyee before deposition of the Spencer. The eastward extent of this unconformity is not known, however Yamhill strata in deep wells to the east have slight angular

unconformities with the Tyee and Spencer Formations.

Erosion or non-deposition of the Yamhill Formation along the fault and for some distance to the east suggests that the uplifted Corvallis fault block was a source for the Miller sand member of the Yamhill as suggested by Baker (1988), as well as for the Spencer (above). Thinning or erosion of the Yamhill probably occurred during early stages of fault movement, with non-deposition or erosion of the Yamhill as the uplifted block emerged prior to Spencer deposition.

The geometry of the Corvallis thrust is consistent with a fault-propagation fold geometry. Consistent northwesterly dips in the hanging wall average 20° between the Corvallis and Kings Valley faults in the northern half of the SRV uplift (Plate 1). The homoclinal dip, supported by the gravity results, suggests that the SRV uplift overlies a ramp at depth. Vertical separation of the top of the SRV across the fault is calculated to be about 6.7 km along the line of section by projecting this contact eastward at the average surface dip. The projected height above ground is then added to the calculated depth to the SRV below the Corvallis fault from the gravity model (method of Yeats, 1988). This method includes the contribution of both faulting and folding, without differentiating between the two. The Corvallis thrust was then modeled as a fault-propagation fold (Suppe 1985, 1988), using a backlimb dip of 20°, and a ramp height of 6.7 km, equal to the calculated vertical separation. Given the ramp height, the backlimb dip and the depth to the décollement, Suppe's models will calculate the forelimb dip and horizontal displacement along the detachment. For the Corvallis thrust, the forelimb dip was calculated to be 70° (overturned), in good agreement with the 65°-75° dips observed in the field. Horizontal displacement is 13-15

km. The depth to the décollement was calculated by assuming that the exposed section of SRV between the Kings Valley and Corvallis faults represents the total thickness of the section above the detachment at the base of the ramp. Thickness of this section is 4.6 km, using a dip of 20°, and assuming no other significant faulting. The base of the ramp is located approximately at the Kings Valley fault, where the average northwesterly dip changes from 20° to 3°-7° (Plate 2).

Surface dips are projected into the air to show the overall geometry of the hanging wall block. The details of the overturned Tyee beds in the footwall are somewhat schematic at depth. Overturned 65°-80° west dipping Tyee beds are observed near the line of section, as well as other places along the fault zone, suggesting the interpretation as drawn. A proposed sequence of events to produce the relations seen at the surface is: 1) Thrusting and formation of the fault-propagation fold. 2) A breakthrough along a décollement in the Tyee transfers some of the shortening to the east, folding Tyee and Spencer strata. 3) A breakthrough occurs along the trajectory of the original ramp, thrusting the hanging wall block further east. Depiction of the eastward decreasing fold train in the Tyee is here shown as the result of thrusting along a detachment within the Tyee. No direct evidence for this detachment has been found, however the common mudstone intervals within the Tyee make likely candidates for such a detachment. These folds verge to the southeast, and are sub-parallel to the Corvallis fault, suggesting this connection to the thrust event. Additionaly, there is a suggestion of this geometry, and of a detachment on a proprietary seismic line.

Additional support for the existence of a low-angle thrust comes from water well data, magnetics, and aerial photographs. Nearly all the water

wells drilled within 1.5 km west of the fault zone in the Corvallis-Philomath area are found to contain some combination of "hard blue sandstone" (sic) and "basalt" or "lava rock" (sic). These wells should contain only basalt, with some sandstone and siltstone interbeds, which are usually black or brown. Although water well logs are not consistent, or necessarily correct in rock identification, the sandstone interbeds in the SRV are usually described in well logs as black or brown when drilled west of the fault. The description "hard blue sandstone" is typical of wells drilled in Tyee or Spencer sandstones, and several fresh outcrops match this description as well. A possible explanation for the anomalous well logs is that the leading edge of the thrust sheet is broken up and very thin in some places immediately west of the surface expression of the fault. In some of these wells, no basalt at all is recorded down to depths of several hundred feet, suggesting that there are windows through the thin upper plate into Tyee or Spencer strata below. Further support for this can be found in magnetic line 18, in the Philomath area (figure 17. Magnetics are fully discussed in a later section). The flat response along much of this line, which is entirely west of the fault zone, may be due to a window in the Siletz River Volcanics.

The homoclinal northwest dipping hanging wall is critical to a thrust fault interpretation, and is much of the basis for the interpreted ramp, along with the gravity results. Dips from the field are somewhat sparse (Plate 1), however additional support for this interpretation is found in the oblique aerial photograph shown in figure 14. This view is looking southwest along the trend of Vineyard Mountain, immediately northwest of the Corvallis fault. The fault is in the extreme left of the photograph (not visible), and runs toward Marys Peak in the background. In this view, the northwest dipping slopes of

the west flank of Vineyard Mountain are seen to be dipping at a constant angle, in contrast to the irregular southeast flank of the mountain. The slope angle is about 15°, similar to the average dip of the Siletz River Volcanics measured in the field. These slopes are interpreted as dip slopes, and have been observed at several other locations in the hanging wall block west of the Corvallis fault (e.g. the west side of Coffin Butte, northwest facing slopes in the Paul Dunn Forest, and others).

The presence of these dip slopes supports the thrust fault/ramp interpretation, and their abrupt termination at the anticlinal axis and sharp

Figure 14. Dip slopes on the western flanks of Vineyard Mountain. View is to the southwest, Soap Creek valley in the center. The Corvallis fault is not visible in this view, but extends from the extreme left, toward the southeastern slopes of Marys Peak in the background.

bend to overturned atttudes supports the inference of relatively straight-limbed Suppe-style folding.

Regional Gravity

Werner (in prep) has produced complete Bouguer and residual Bouguer gravity contour maps of the Willamette Valley, including the eastern Coast Range and the western Cascades. The complete Bouguer map uses all available public domain gravity data, including the stations from this study, and is in general similar to the less detailed map of Berg and Thiruvathukal (1967). The southeast dipping gradient associated with the mapped extent of the Corvallis fault is apparent on the new map, as on the old. However, longer wavelength gradients obscure the gravity expression (if any) to the northeast of the area of this study.

The residual map, the first of its kind in the public domain, reveals several significant trends after long wavelength filtering (greater than 50 km) (Figure 15). The gradient of the Corvallis fault anomaly is somewhat reduced after filtering. The resulting reduced gradient requires some combination of reduced dip on the thrust, greater volumes of Kings Valley Siltstone in the subsurface, or greater amounts of Tyee and/or Spencer strata beneath the thrust. Any of these options will produce greater horizontal displacement on the fault. In this way, modeling of the unfiltered Bouguer anomaly (as in figures 11&12) provides a conservative estimate of vertical and horizontal displacements on the Corvallis thrust.

Another significant feature of the residual map is a northeast trending gravity high extending well beyond the mapped extent of the Corvallis fault. This anomaly continues northeastward to the range front of the Waldo Hills,

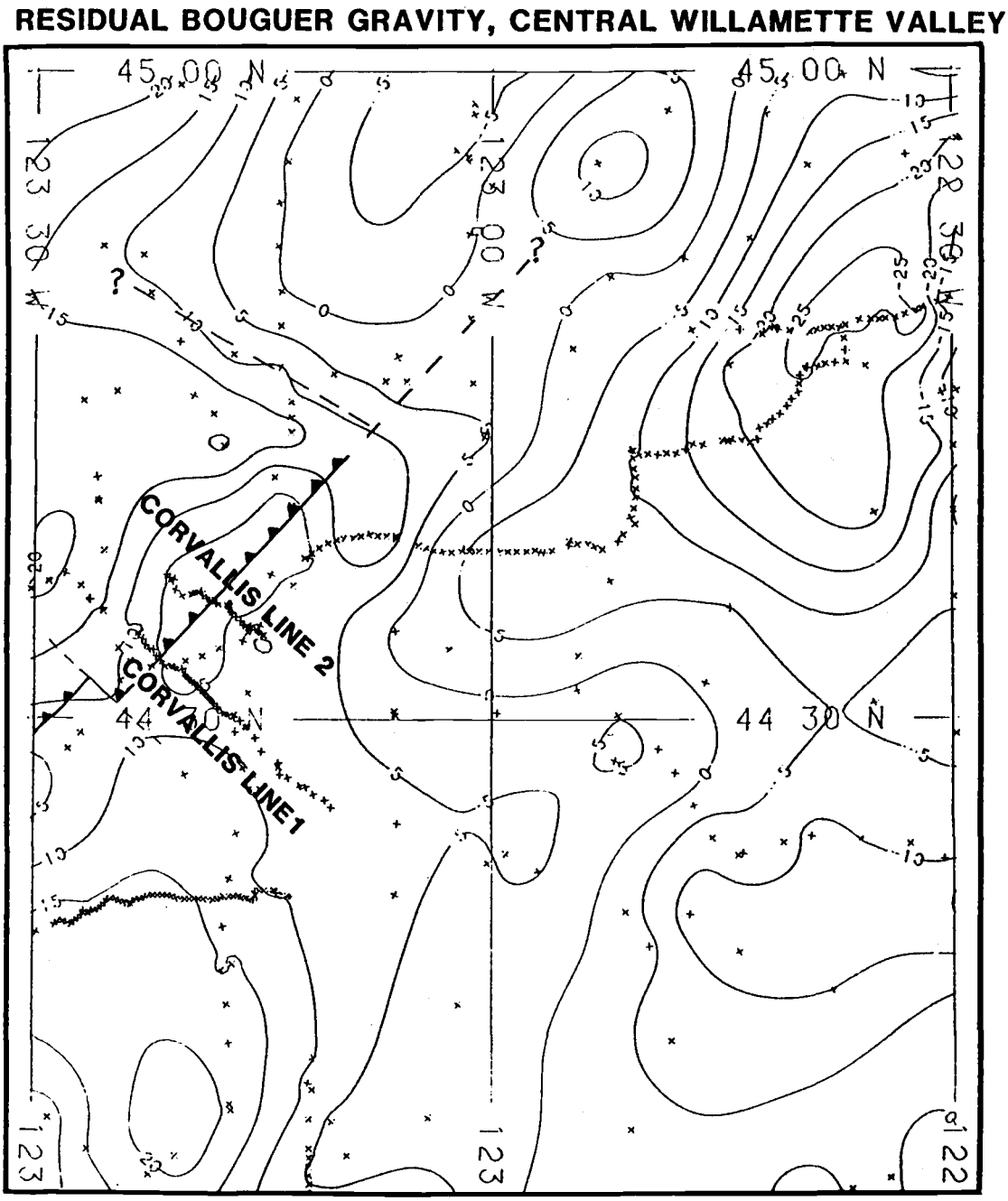

Figure 15. Residual Bouguer gravity of the central Willamette Valley. From K.S. Werner (in prep).

east of Salem, another northeast trending linear feature on trend with the Corvallis fault. This high, along with an intervening fault shown by Walker and Duncan (1989) tends to support a continuation of the Corvallis fault northeastward to the western Cascades.

The residual map also reveals a sharp (90°) bend to the northwest of the gravity gradient associated with the Corvallis thrust, just north of the map area. The northwest trending gravity gradient corresponds to the southern boundary of the Luckiamute structural basin, immediately north of the uplifted Corvallis fault

block. These data strongly suggest that displacement on the Corvallis thrust does not die out to the northeast into the valley, but is taken up along another northwest trending structure that has produced the bend in the gravity contours. Possible explanations for the observed data could include termination of the thrust in a tear fault, or offsetting by a cross fault.

The presence of two divergent anomalies associated with the mapped Corvallis fault and inferred Corvallis thrust suggests that the two structures diverge near Coffin Butte, at the extreme northern end of the map area. The thrust probably dies, bends northwest or is offset at the northern end of the uplifted block, while the throughgoing northeast-trending anomaly may be associated with the high-angle Corvallis fault.

On a larger scale, Blakely and Jachens (1990) have published new residual and isostatic residual gravity maps of Oregon which feature several large northeast-trending anomalies in western Oregon. The largest of these extends along the western front of the Blue Mountains southwestward to the Klamath mountains (Fig. 16). Several other subparallel anomalies cross most of western Oregon. The anomaly associated with the Corvallis fault is a

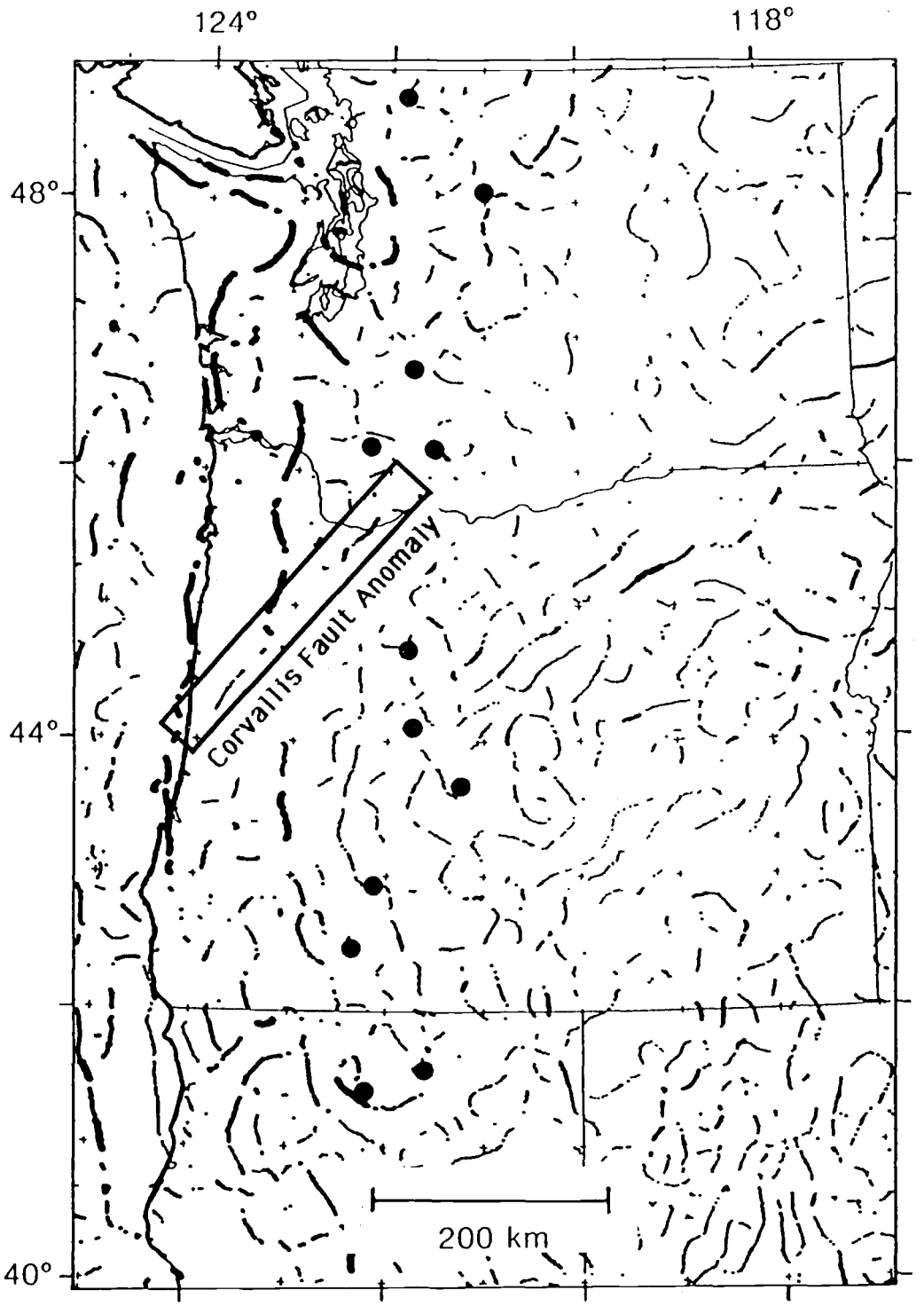

Figure 16. Plot of points of maximum isostatic gravity gradient taken from an isostatic residual gravity map of Oregon. Prominenent northeast trending lineament associated with the Corvallis fault/Waldo hills lineation shown in box. From Blakely and Jachens (1990).

similar feature, parallel to those shown by Blakely and Jachens (1990). The origin of these northeast trending anomalies is unknown, however the throughgoing nature of these features as they crosscut the Siletzia terrane and the Cascades suggests they are older structures, possibly related to rifting or accretion along the former continental margin (Rick Blakely, personal communication,1990).

The association of the Corvallis thrust with a series of regional gravity anomalies suggests that it may represent the late reactivation of a deeper structure related to the formation of the Siletzia terrane. The contrasting association of a low-angle thrust with a linear structure of more regional extent suggests that perhaps the limited Corvallis thrust is an anomalous segment of a larger structure.

MAGNETICS

In areas with poor surface exposure, 24 magnetic traverses were done using a portable GeoMetrics model G-846 proton precession magnetometer (Figure 17). These traverses were primarily used to locate the fault at the surface, but they were also useful in mapping the numerous intrusive bodies in the area. The magnetic lines allowed the trace of the fault to be mapped accurately in farmland and pastures where other methods would not have done as well. Test lines in the Timberhill area and Chip Ross Park, where the fault crops out, helped calibrate the other lines. Some areas are not conducive to mapping with magnetic traverses due to high cultural noise, mainly from power lines, but also from roads with buried pipe, and railroad tracks. Some of these areas were not covered, while others were traversed in unfavorable orientations to avoid magnetic sources. South of Philomath, magnetic traverses were not used as the fault was fairly easily located in the field.

The traverses were done with varying length and station spacing according to the uncertainty of the location of the fault in a given area. Four readings were taken at each location and averaged to obtain the station value. Drift measurements were made before and after each line and drift corrections made where drift exceeded 5 gammas for a given line. Proton precession magnetometers make absolute measurements of total field intensity, and are accurate to ± 1 g (Breiner, 1973; Telford and others, 1976. 1 g = 10^{-5} Gauss, a convenient unit for magnetic intensity in geophysical exploration). Each line is an independent relative profile of the total magnetic intensity for the date and time the traverse was done.

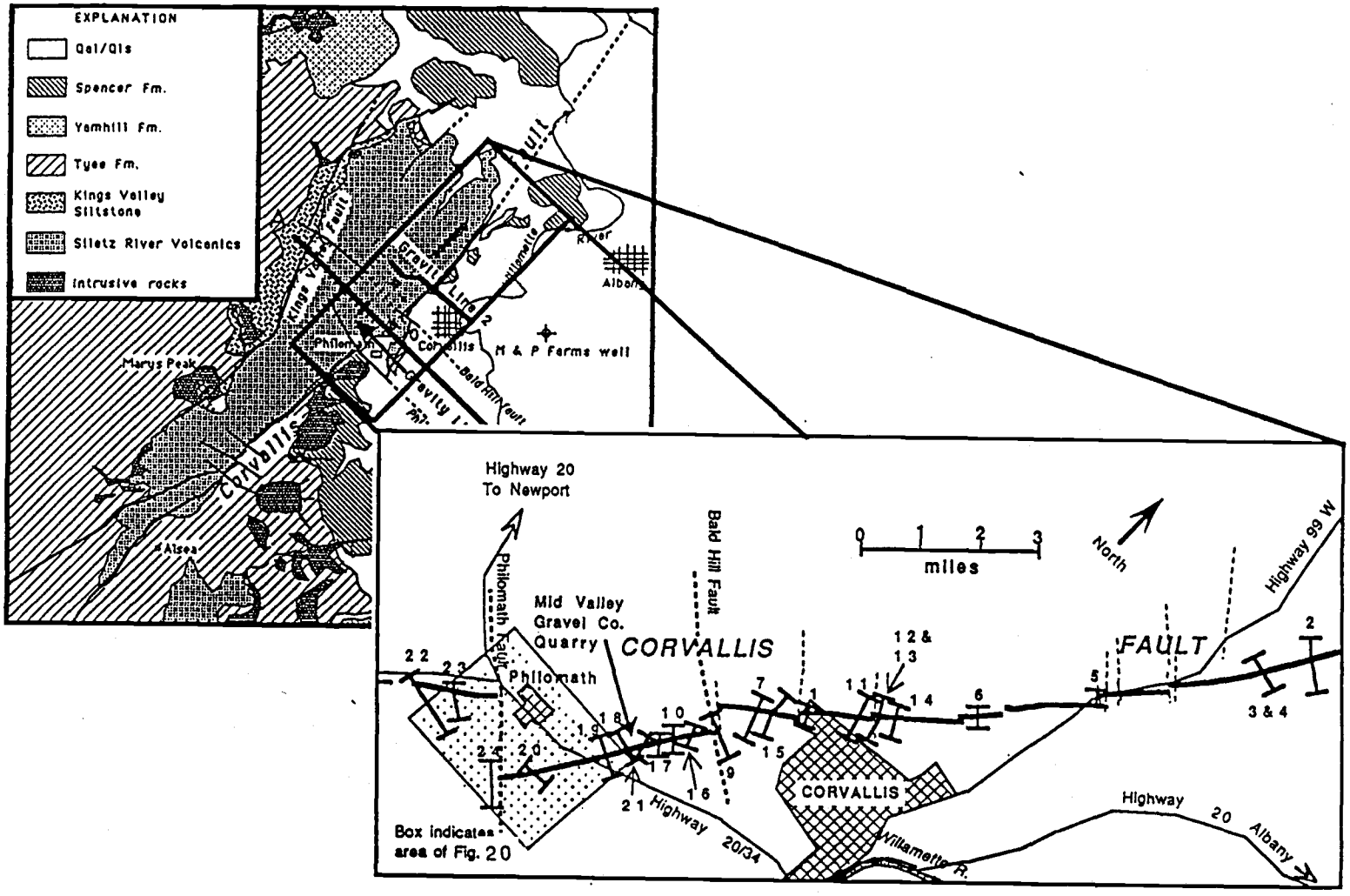

Figure 17. Location map showing the location of 24 magnetic traverses. Shaded box indicates area of 2-D magnetic survey.

A magnetic area survey was also performed in the Philomath area in order to investigate the area of a 2.5 km right step in the fault trace. The aeromagnetic data could not resolve this feature, probably due to the influence of a massive intrusion adjacent to the fault offset. The survey covered 20.7 km^2 (see outlined box 1 on Plate 1), using 423 data points, for a coverage of about 20.4 points/km^2. For this survey, a base station was established at the Philomath Middle School and was occupied at approximately two hour intervals each day the survey was in progress. Each days diurnal corrections were made to the data from that day, and successive days were normalized to an arbitrary standard value. Neither major sun activity and nor any major magnetic excursion occurred during the collection of this data.

It was originally planned to use the magnetic data to construct two dimensional models of the Corvallis fault and associated structures, however, several complications made this impractical. The unexpectedly high concentration of intrusive bodies and associated high-amplitude magnetic signatures obscure the response of the Siletz River Volcanics. In addition the remanent magnetization is relatively strong in the Siletz River basalts. Thus, complicated structures will cause strong fluctuations in the total intensity recorded at the surface, as the remanent vectors will be oriented so as to cause both constructive and destructive interference over short distances. Available magnetic modeling methods do not take the remanent component into consideration (Patterson and Reeves, 1985). These complications, along with the post-Eocene 70° clockwise rotation of the Siletz River Volcanics, precluded modeling the magnetic data for subsurface structure.

Magnetics Interpretation

Figure 18 is a compilation of all the magnetic traverses arranged in order from north to south. A typical plot from east to west shows a relatively flat response across areas of alluvium and Eocene sedimentary exposure, with some variations that may be minor faults (Lines 2, 3, 4, 7, 15, and 16), or intrusives (Lines 1, 3, 6, 9, and 20). The main fault trace was easily identifiable on nearly all the magnetic plots, and allowed location to within 5-50 m. The fault zone picks were added to the geologic map to augment other field observations in refining the map pattern. Magnetic response in the fault zone and farther to the west varied, but typically the flat response abruptly terminated in a series of high amplitude peaks and valleys as the fault was crossed, with the first response a high peak or series of steps up to a peak in all cases except Line 10. The longer traverses typically showed reduced total intensity farther to the west, also with high amplitude variations, but less dramatic than in the area of the fault zone. This is interpreted as being the result of dikes intruding the fault zone, producing the initial high and the first series of peaks. The low to the west is interpreted as the response of the Siletz River Volcanics, which are reversely polarized in the study area. Strong remanent magnetization can be an order of magnitude greater than induced magnetization in its contribution to the disturbance of the Earth's field (Telford and others, 1976). Reverse polarity in the Siletz River Volcanics has apparently masked the expected enhancement of the total field strength due to the induction component, resulting in a negative anomaly.

The high peaks in and near the fault zone are known to coincide with intrusives in Lines 1, 6, 7, 9, 10, 11, 12, 13, 14, 15, 16, 17, 18, and 21 based on surface mapping, and are inferred for the remainder of the lines.

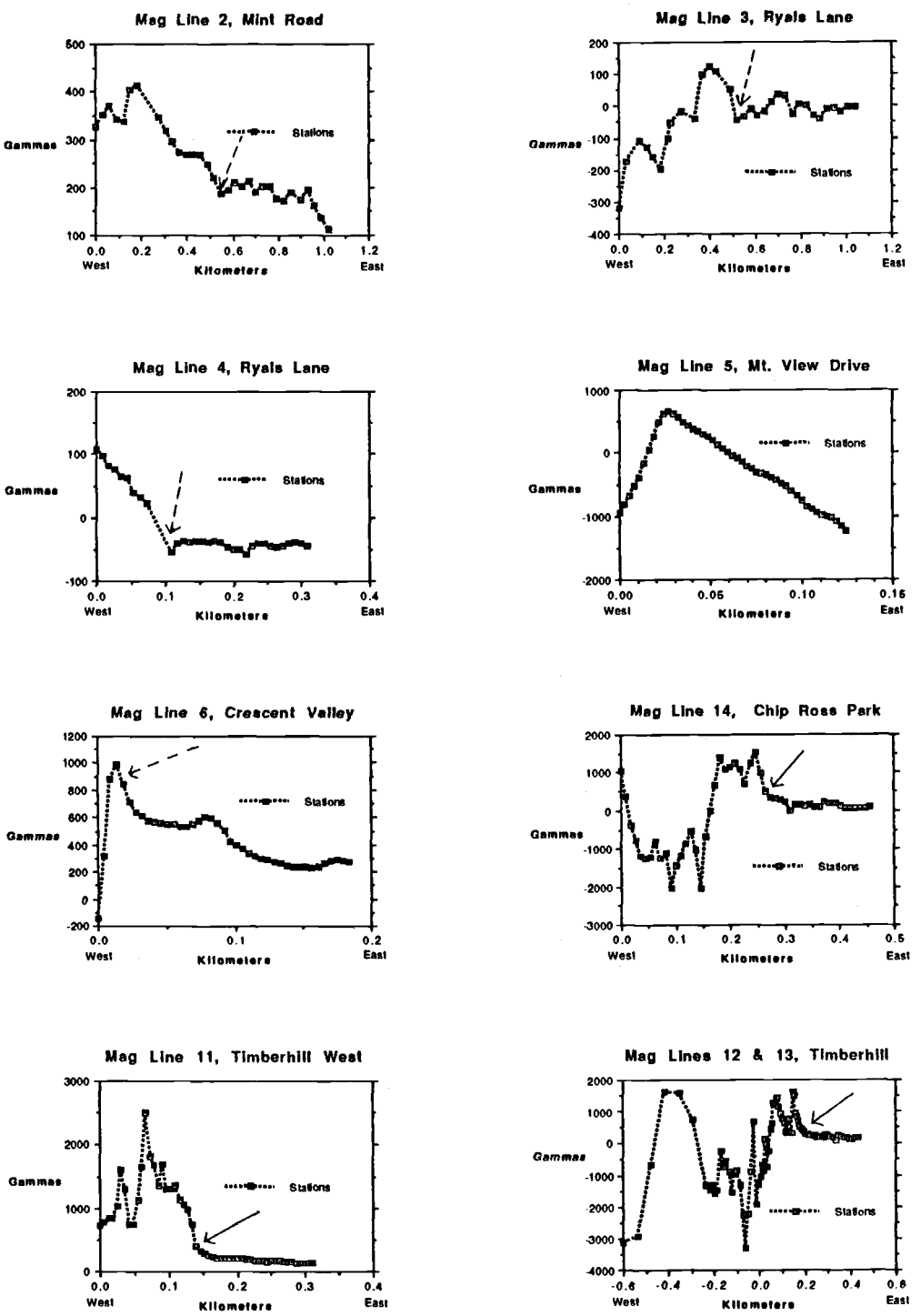

Figure 18. Magnetic traverses of the Corvallis fault. Lines are arranged in order from north to south. All values are in gammas, total field intensity. Intensities are normalized to an arbitrary value. Solid arrows indicate known Corvallis fault locations, dashed arrows indicate inferred locations.

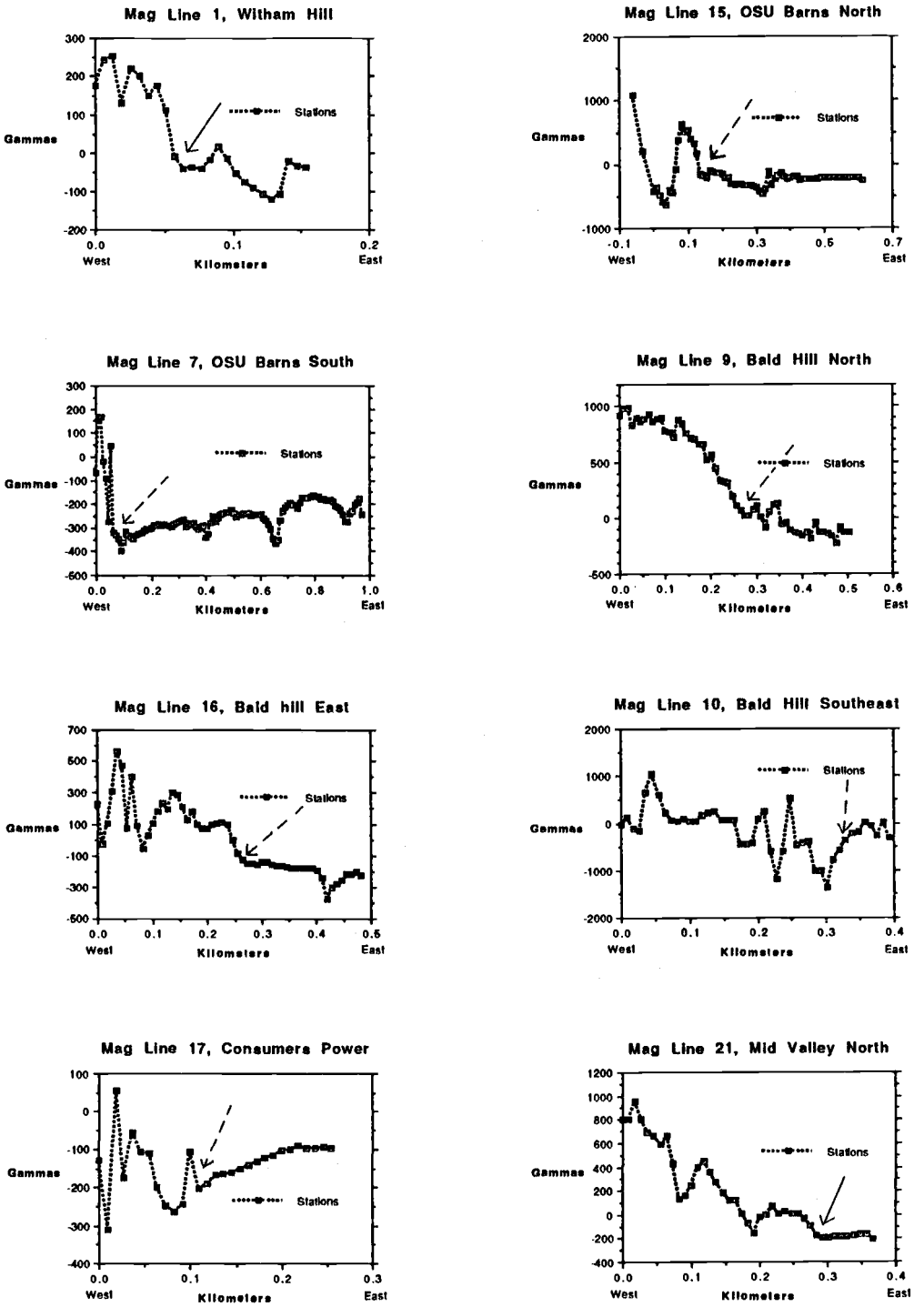

Figure 18 (continued). Solid arrows indicate known Corvallis fault locations, dashed arrows indicate inferred locations.

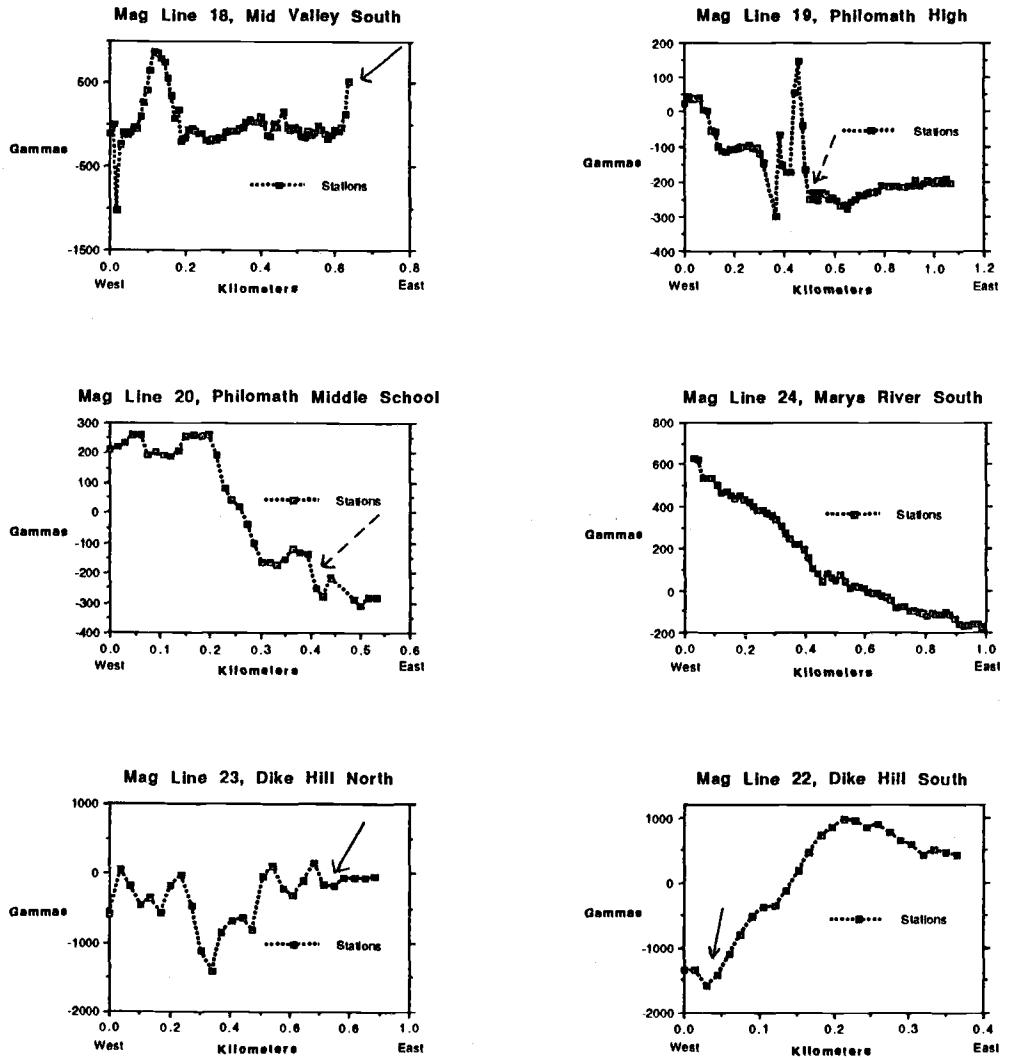

Figure 18. (continued). Solid arrows indicate known Corvallis fault locations, dashed arrows indicate inferred locations.

The Corvallis fault strikes N40-50E, and is fortuitously oriented to allow some further interpretation of the magnetic data. Because the strike of the fault is within 20°-30° of the declination of the magnetic field in the area (19° E), the magnetic traverses normal to the fault are close to normal to the field direction. The result of this orientation is that edge effects are reduced to a minimum (Briener, 1973; Telford and others, 1976), and total field intensity is a better reflection of the combined TRM and IM influences of the rock. The high amplitude peaks associated with the fault zone intrusives are most likely due to the additive effects of normally polarized rocks, with little influence from edge effect. Field checks of these rocks with the portable magnetometer (field method in Breiner, 1973) confirm that the rocks tested were normally polarized. This circumstantial evidence, along with similar lithology and similar cross-cutting relations supports a correlation of these intrusives with other normally polarized intrusives of mid-Oligocene age in the Coast Range. The consistent polarization also supports the contention of Snavely and Wagner (1961) that the mid-Oligocene intrusive episode was relatively short.

Faults that are not intruded, as is the main Corvallis fault, may often be identified on magnetic traverses as sharp lows over the fault traces. The lows are thought to be due to shearing and brecciation, which disrupts coherent viscous or thermal remanent magnetization, or to percolation of groundwater (Bailey, 1974). Groundwater flow alters the magnetic minerals (usually magnetite, Fe_3O_4, or ulvospinel, Fe_2TiO_4) to non-magnetic iron-hydroxides such as hematite (Tarling, 1971).

Line 7 in particular has three distinct lows which correspond to splays of the Corvallis fault, and which are visible on air photos. (Figure 19)

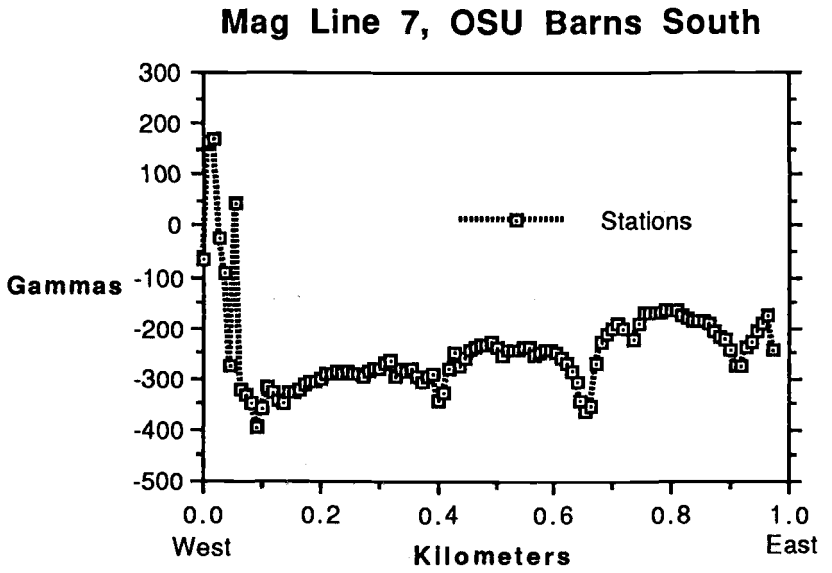

Figure 19. Line 7, arrows indicate splay faults corresponding to air photo lineations shown on Plate 1, box 2.

Lines 15 and 16 have similar lows east of the main fault.

The survey of the Philomath area (figure 20) confirmed the large right step in the Corvallis fault trace suggested by Lawrence and others (1980), and indicated by field mapping. The nature of this step is significant in the structural interpretation of the fault. Four possibilities are; a right-lateral tear fault; a younger right-lateral cross-fault offsetting the originally straight trace of the Corvallis fault; a normal fault, down to the north, shifting the trace of a low-dipping Corvallis fault to the east; or a salient of the Corvallis thrust, with no offsetting fault. The area survey data can be used to eliminate several of these possibilities. Figure 20 (and Plate 1) shows that the Corvallis fault trace is abruptly terminated as it reaches the offset area, rather than bending smoothly to the west, so an original bend in the trace is rejected. The offset is marked by a lineation that extends into the sedimentary units to the east,

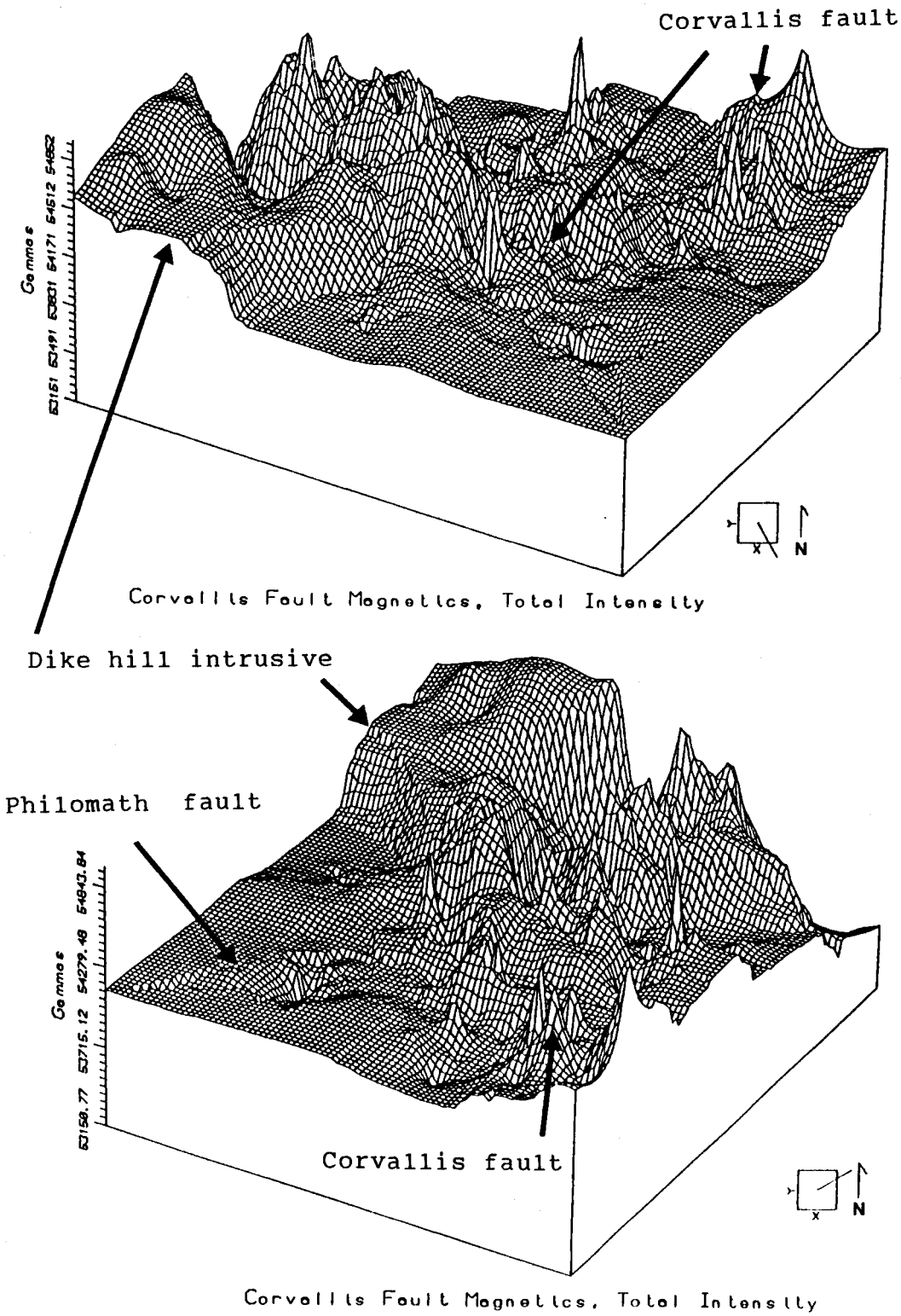

Figure 20. Two views of magnetic data from the Philomath area. Plots are perspective views of total field intensity. Upper view is from the southeast, lower view is from the northeast. See text for discussion.

suggesting that the offset is a younger feature, and probably not a tear fault. The offsetting lineation is also the site of a long intrusive body, marked by a row of high intensity peaks, with the same trend and location as the offset. This was confirmed in the field where the intrusion crops out along the Marys River. Thus the offset is a cross-fault, here named the Philomath fault, younger than the Corvallis fault and older than the mid-Oligocene gabbro that intrudes it.

The map pattern of the Corvallis fault suggests that the Philomath fault could either be a normal fault, north block down, or a right-lateral strike-slip fault. One possible interpretation is that the Philomath fault is the southern boundary of an asymmetric graben bounded on the north by the Bald Hill fault. Between these two faults the trace of the Corvallis fault changes azimuth to the east, consistent with a low-angle fault downdropped between the two cross faults. Greater slip on the Philomath fault would explain the greater horizontal separation, and a southerly tilt to the block.

The Philomath fault also is marked by distinct lineaments observed on aerial photographs, and appears to extend to the surface in young sediments, as will be discused in a later section. The perspective view net diagram shows the offset, the continuation of the offset to the southeast, and the strong peaks caused by normally-polarized intrusions plugging both the Corvallis fault and the Philomath fault. Further evidence that the Philomath fault is a pre-intrusive structure is that the massive intrusive body forming Dike Hill south of Philomath (Plate 1), apparently does not extend to the north of the Philomath fault. Magnetics indicate that it is not present in the subsurface in the Philomath area, nor is it offset by the Philomath fault. The abrupt termination of this large intrusion suggests that intrusion occurred subsequent

to initiation of the Philomath fault, and that the more resistant SRV to the north may have acted to limit the emplacement of the gabbros to the less resistant Spencer and Tyee sandstones to the south.

Aeromagnetics

A published aeromagnetic survey (Bromery and Snavely, 1964) covering approximately the northern 2/3 of the field area was used to improve the mapping of intrusive bodies in the study area. The Corvallis fault is clearly delineated by steep magnetic gradients, and by the high amplitude terrane typical of exposed Siletz River Volcanics west of the fault. Also observed on the aeromagnetic data are numerous irregularly shaped highs, some of which correspond to intrusive bodies previously mapped at the surface. In an attempt to better define the extent of the intrusions in the area, a correlation was made between these magnetic highs and the intrusions. In order to test the correlation, several intrusives were selected whose dimensions were known from field study. These intrusions were plotted on the aeromagnetic map and the magnetic contour that best represented the map pattern of each was selected. The magnetic values were in good agreement with each other, and that contour was selected as a value which if exceeded elsewhere on the map, was suggestive of the presence of an intrusive body (A similar method that plots points of maximum gradient is currently used in both gravity and magnetics interpretation, Blakely and Connard, 1989). This method was tested on several unknown magnetic highs (McCulloch Peak and Dimple Hill) that were suspected of being intrusions. Subsequent field checking confirmed the presence of intrusions in those locations. Other anomalies that indicate probable intrusions are shown on Plate 1 surrounded by thin solid

lines broken at intervals by M's (for magnetics).

Correlation of these highs with other mapped intrusive bodies is good as shown on Plate 1. Circumstantial evidence for the presence of some of the unconfirmed intrusions lies in the observation that nearly every topographic high in the field area that has exposure is held up by resistant intrusions, whether in the SRV or the sedimentary outcrop belt. Many of the unconfirmed magnetic highs also occupy topographic highs, and this supports the notion that they also correspond to intrusive bodies.

It should be noted that the largest magnetic highs occur in a belt trending northeastward along the northwest border of the mapped area. These highs do not show any correlation with topography, and have no ground confirmation of intrusions cropping out within them, thus they may be related to some other magnetic source such as a band of normally polarized basalts within the Siletz River Volcanics.

REMOTE SENSING

Field work in Western Oregon is hindered by dense foliage, and mostly heavily weathered outcrops. A variety of remote sensing imagery was studied to aid in geologic interpretation of the field area. A lineament map was constructed at 1:24,000 scale using Landsat imagery; U-2 high-altitude photos; medium-altitude black and white, color and color infra-red images; side looking real aperture radar images; and low-altitude oblique aerial photos acquired for this study.

Lineaments from each image type were compiled separately. These were then superimposed on a combined lineament map using different colors to represent the image type. The most significant and frequently observed lineaments are included on Plate 1.

Interpretation

The main structural element visible in most images is the prominent northeast trending lineament associated with the Corvallis fault. It is visible at all scales from Landsat down to low-altitude photos. The fault is made visible at high altitude by the change in weathering and topography marked by the fault contact between Siletz River Volcanics on the west and Tyee and Spencer sandstones to the east. In lower altitude images, the fault is visible as vegetation changes, soil color changes, and vegetation lines outlining the fault trace, presumably due to increased moisture in the fractured rocks of the fault zone (figure 20). The lineament map was used to aid in location of the fault trace in some areas such as Crescent Valley, where no outcrops were available, and location by magnetics was precluded by high cultural noise.

Figure 21. Low altitude oblique aerial photo of the Corvallis fault in the Timberhill/Chip Ross Park area of north Corvallis. This view to the northwest shows the subtle color change across the fault, as well as vegetation growing along the trace, and along a small northwest trending offsetting fault.

Many small left offsets or left steps in the fault trace are visible at medium to low altitudes, and others were suggested by ground mapping and magnetics. Left steps mapped on the ground were correlated with those visible on the lineament map, and are shown as lineament symbols on the field map. Several others, such as the Bald Hill fault, were confirmed as faults by subsequent field mapping. Many other left steps remain unconfirmed by means other than imagery interpretation, however, one representative example was chosen for ground study in order to confirm the left step. Several closely spaced magnetic traverses were run normal to the Corvallis

fault trace in the Timberhill area in order to confirm the presence of the interpreted offset. The profiles did confirm that an offset of about 140 meters was present at the same location as that inferred from low-altitude imagery. This supports the interpretation of left steps or offsets made elsewhere along the main trace.

The nature of these steps is not entirely clear. The largest and best mapped of these is the Bald Hill fault, which offsets the trace of the Corvallis fault by 0.6 km in a left-lateral sense. This offset was also inferred from the results of magnetic lines 9, 7 and 16 (Figure 18). Mapping suggests a connection between this offset and a northwest-trending left-lateral fault mapped immediately to the east, and these have been linked and named the Bald Hill fault.

The lineament map provides an important piece of evidence concerning the relative timing of faulting along the Bald Hill and Corvallis faults. Although the main trace of the Corvallis fault is located along the base of the hills north of the Bald Hill fault, other weaker lineaments lie to the east as shown in box 2 on Plate 1. These appear to connect the main trace of the Corvallis fault across the Bald Hill fault without a break, bypassing the left step. The pattern suggests that the Bald Hill fault offsets the Corvallis thrust, but that strike-slip motion on the Corvallis fault post-dates that on the Bald Hill fault, and the left offset has been bypassed by a *younger* through-going trace of the Corvallis fault. The prominent salient of the Corvallis fault between the Bald Hill and Philomath faults may also have been bypassed by a younger throughgoing trace, west of the town of Philomath. A lineation is present along a straight line connecting segments of the Corvallis fault north and south of these offsetting faults.

Low-altitude oblique aerial photos of the Philomath area revealed a series of linear and sinuous depressions along the location inferred for the Philomath fault based on magnetics. These features are best viewed on photographs taken shortly following a heavy rainfall, as they were full of water and stood out from the surrounding farmland. They are also visible in medium and high-altitude vertical images. The sinuous form of some of these depressions is due to meander scars of the Marys River, which generally trends northwest in this area. Several of the depressions are straight, however, and parallel the inferred Philomath fault, thus they may be a surface expression of the Philomath fault.

Other Lineaments

Prominent in all types of imagery were several northeast lineations which are generally subparallel to the Corvallis fault. Ground investigation found no exposures to reveal the nature of these features. They may be faults in a shear zone related to the Corvallis fault, or they may be other faults that have ramped up through the Tyee and Spencer. Other northeast trending folds and faults have been identified to the east in the subsurface by well and seismic data (Graven, in prep; Yeats and others, in prep.) and by gravity data (this study). Alternatively, one of these prominent lineations may be due to the topographic slope change where Quaternary sediments onlap the resistant northeast-trending hills adjacent to the fault zone.

In an investigation of the Holocene activity of the Corvallis fault, low-sun angle aerial photographs were taken to attempt to identify neotectonic features in Pleistocene to Holocene deposits. Many of the features previously discussed were visible in these images. Most of the visible features were in

older rocks and pediment surfaces that had only a thin veneer of Holocene material, most of that being derived from the underlying Eocene formations.

The previously discussed Philomath fault is marked at the surface by lineaments in the overlying Pleistocene to Holocene gravels, and similar lineations are visible in the Muddy Creek area. Whether these lineations represent disruption of the gravels by faulting, or represent some form of differential erosion due to the shallow subsurface presence of an old fault zone could not be determined in this study. Several other northwest trending faults/lineaments continue into Quaternary alluvium, and similarly the activity on these structures could not be evaluated.

A unique opportunity to search for neotectonic features in the area presented itself in January 1989, when a major storm deposited a foot or more of snow on the valley and surrounding hills. Good weather following the snow permitted a flight to obtain more low-sun angle photographs with the area still blanketed in snow. The advantage of this photography is that the normally present cultural "camouflage" of farm fields, and roads is subdued or eliminated by the snow cover. Examination of these photographs revealed clearly the intertwining and overlapping depositional patterns of the Willamette River, but no neotectonic features were discovered.

DETAILED DESCRIPTION OF THE CORVALLIS FAULT ZONE, AND ANALYSIS OF ASSOCIATED MINOR STRUCTURES

The Mid Valley Gravel Co. Quarry

The Corvallis fault zone is only infrequently exposed along its mapped trace. A single unparalleled exposure does exist 2 km northeast of Philomath at the Mid-Valley Gravel Co. quarry. This fortuitous exposure has made it possible to examine, if only in a single location, the detailed structure of the fault zone (figure 22).

The exposed pillow basalt is moderately to highly sheared throughout the pit, with shearing decreasing away from the core of the fault zone. A sandstone interbed in the basalt, traceable for some distance in the area, dips 60°-70° to the west and is overturned, based on graded bedding and pillow load structures. At the base of the sedimentary interbed is a black siltstone and mudstone lens 3-4 m thick that apparently fills an original depression in the basalt surface. Bedding in the SRV and pillow geometry also indicate that the SRV in this location is overturned and dipping to the west. Several high-angle minor faults cut the Siletz River Volcanics in the western part of the pit.

The main fault zone consists of a series of subparallel planar surfaces with predominantly sub-horizontal slickensides. These fault surfaces dip 60°-90° to the northwest, and are developed in both the boulder conglomerate facies of the Spencer, and in two small intrusions, one fine-grained and the other medium-grained. The discovery of these slickensides was somewhat unexpected given the indications from folding and other field relations that the Corvallis fault is a reverse fault.

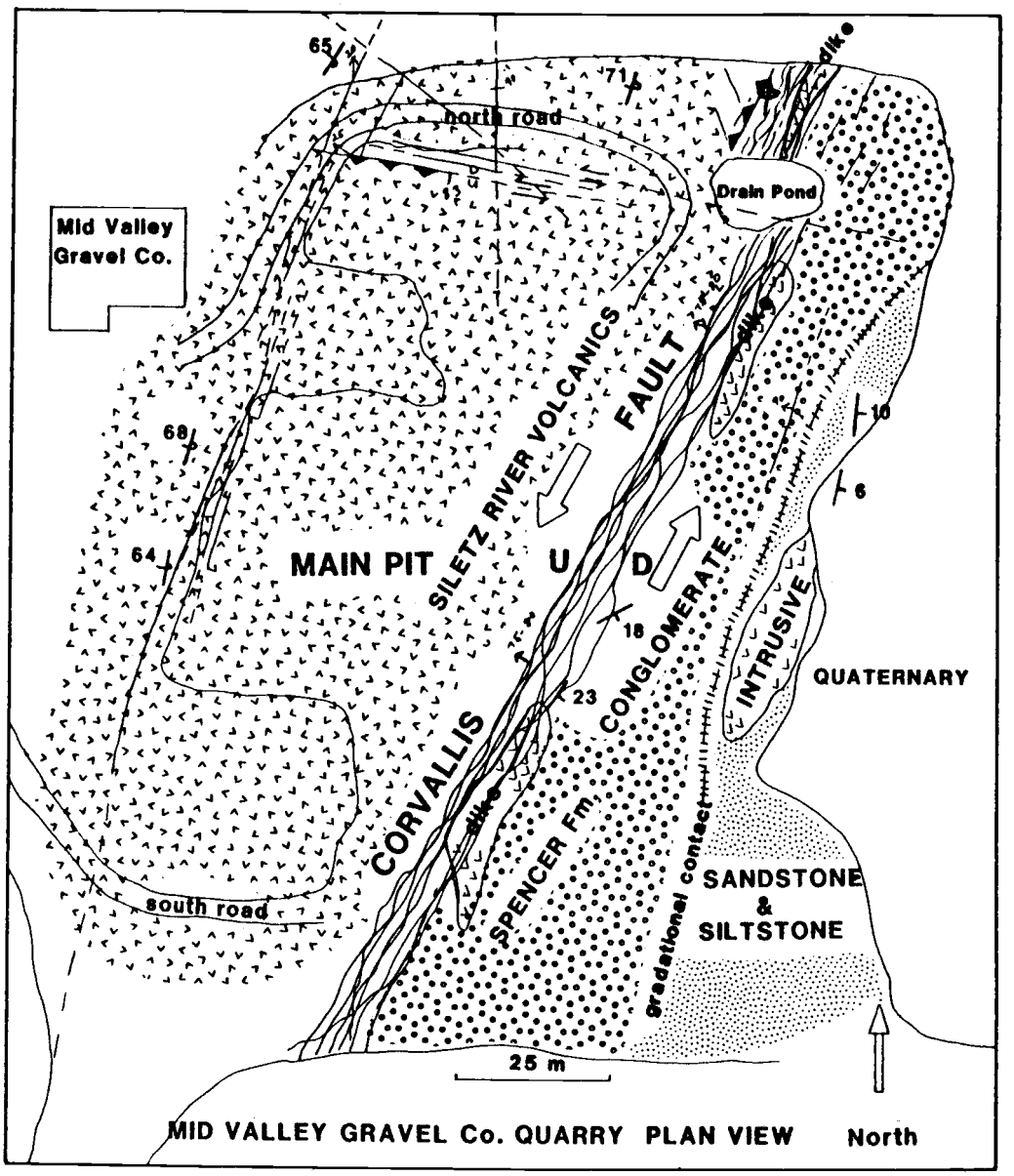

Figure 22. Plan view of the Mid Valley Gravel Co. Quarry, Philomath, Oregon. U/D indicates sense of vertical motion. Arrows indicate sense of lateral motion.

The core zone of the fault is offset left-laterally about 10 m by a N80W trending fault. This minor fault has sub-horizontal slicks, and an up to the south component of reverse motion. Immediately west of the core fault zone, a small portion of a second fault is exposed. The second fault is a thrust plane with SRV thrust over basaltic sandstones and siltstones that may be part of the Spencer fault zone facies. These beds show grading, and are drag folded into a tight overturned east-verging syncline beneath the fault plane (Alternatively they may be a graded basaltic sand interbed in the Siletz River Volcanics). This second fault surface is deformed, and dips vary from 30° to the west to 70° to the east (fig. 21). Deformation along this second surface is minimal, with a gouge zone only about 10-30 cm thick. This small exposure is interpreted as the only known outcrop of the major thrust fault described in previous sections (The exposure described by Allison in 1953 is considered to be analogous, but is now too badly weathered for study).

Intruded into the fault zone is a fine-grained platy-jointed basaltic body that dips at 40° to 50° to the east, and widens to a sill-like configuration at the top of the exposure. Slickensides are developed in this intrusion, indicating that strike-slip motion occurred following the intrusive episode.

The main fault zone separates sheared Siletz River Volcanics on the west from highly sheared basaltic sandstone and basalt boulder conglomerate of the Spencer Formation on the east. Included in this facies of the Spencer is the overturned basaltic sandstone in the footwall of the thrust, and fine-grained brown to grey tuffaceous sandstone and siltstones in the eastern part of the pit. The fine-grained phase grades rapidly westward into coarse basaltic conglomerate. The sandstone is intruded by a larger, medium-grained basaltic body, and both are cut by minor fault surfaces sub-

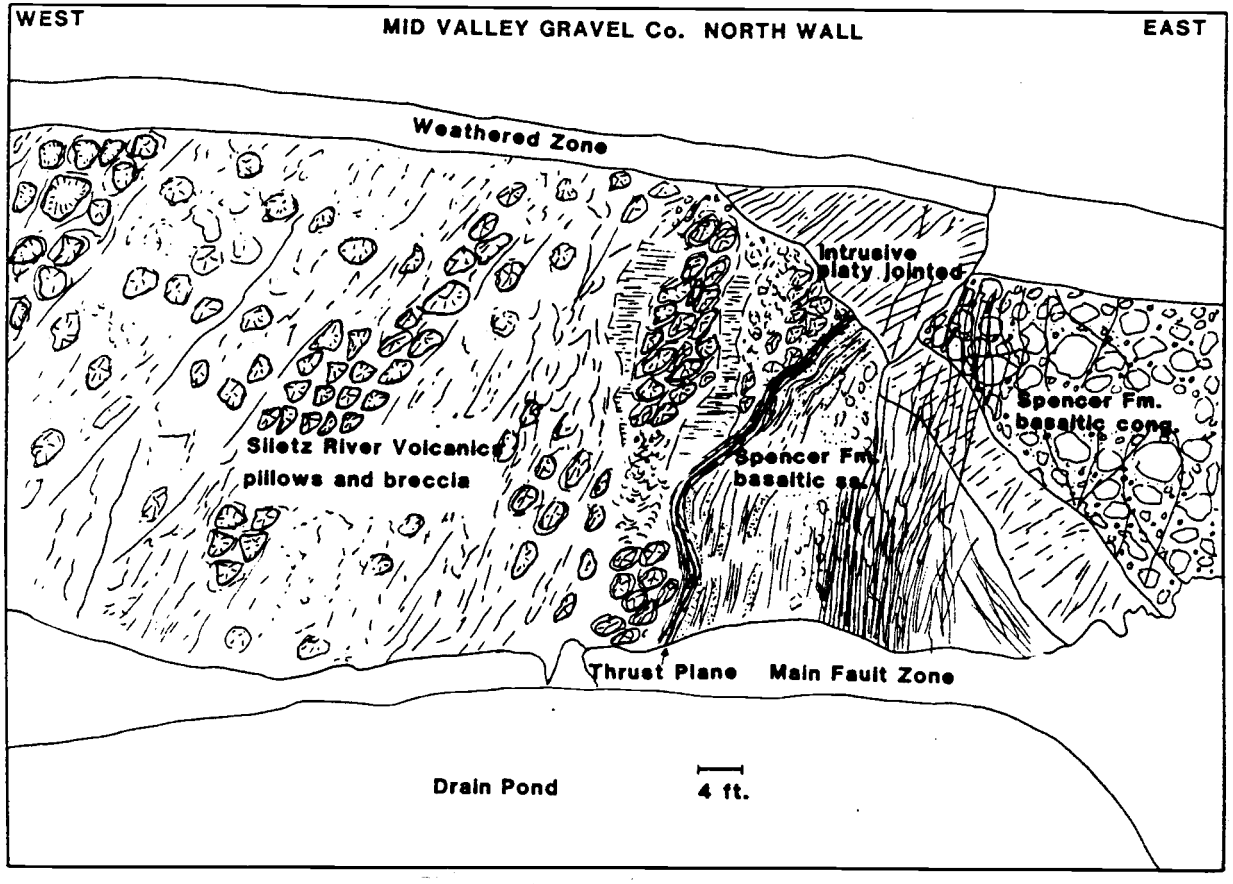

Figure 22. Sketch of the north wall of the Mid Valley Gravel Co. quarry, drawn from a photograph. Bedding in the basaltic sandstone is verturned (based on graded beds) below the deformed thrust plane in the right center if the view. Pillows are also overturned and bedding in the SRV dips 60°-70° to the northwest.

parallel to the main trace. Slickensides in the second intrusion pitch 90° on a surface dipping 78° to the northwest, indicating a period of dip-slip motion.

Overlying both the Spencer and the intrusion are interbedded sands, silts, and gravels most probably of the Linn gravels (Allison, 1953). These late Pleistocene deposits are part of the Quad geomorphic surface of Balster and Parsons (1968). Overlying the Linn gravel is a thin silty deposit of the Willamette Formation, probably the Irish Bend or Malpass Member (Balster and Parsons, 1969), containing several erratic quartzite boulders. Bedding in the terrace deposits appears undisturbed, and dips 6° to the east or southeast. The terrace deposits terminate against the low hill occupied by the main fault trace, and bedding of the terrace deposits is cut by the present erosion surface, which slopes 10°-12° in the same direction.

Shear Sense Determination

For a determination of the shear sense of the Corvallis fault, the methods and terminology of J.P. Petit (1987) were adopted, ashis descriptions of minor structures closely matched those observed in the exposure at Mid Valley Gravel. Petit has categorized the various types of shear-sense indicators observed on over 4000 striated surfaces of known slip direction, and in varying lithologies. Figure 24 illustrates three categories of secondary fractures recognized by Petit, and the terminology, which is based on Reidel shear experiments (Tchalenko and Ambraseys, 1970; Wilcox and others,1973). Slickensides were examined in detail for shear-sense indicators, and the orientations of minor structures were recorded. Secondary fractures in the Corvallis fault zone closely resembled the R criteria of figure 24e. This type of fracture pattern was the dominant one in

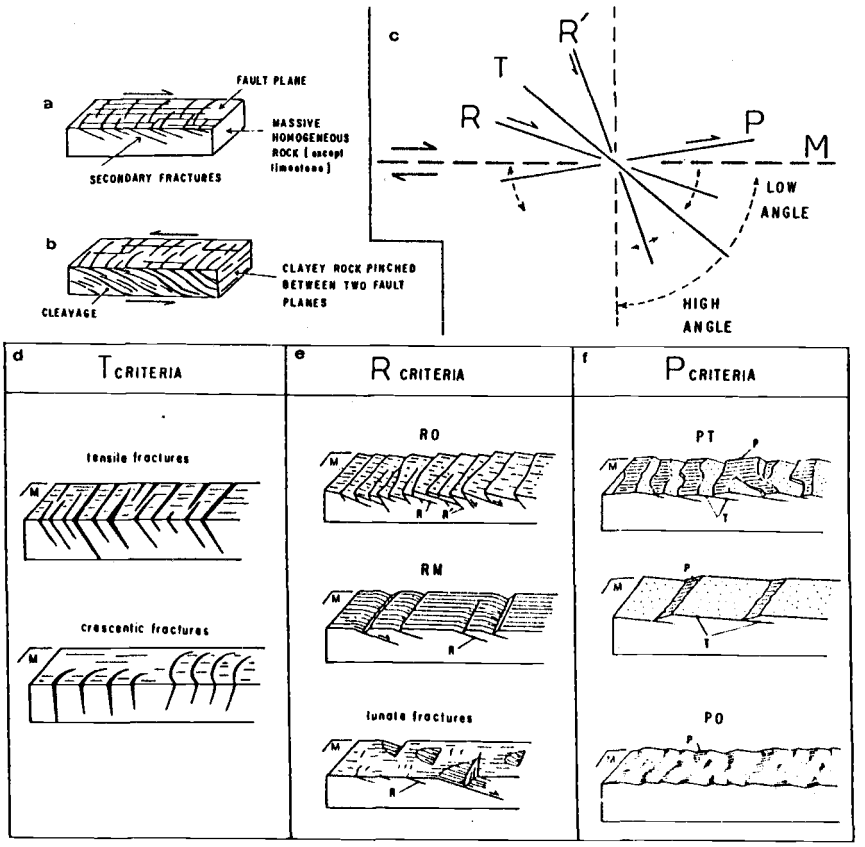

Figure 24. Minor structures as shear sense indicators. (a) and (b) are indicators similar in appearance, but opposite in motion sense; (d), (e), and (f) are three classes of shear sense criteria due to secondary fracturing. From Petit, 1987.

over half of the cases studied by Petit, and is most common in sandstones and igneous rocks.

The most common secondary fractures observed were of the RO and RM type. RO (R only) fractures appear on the main fault plane as a dihedral formed by the intersection of R shears, dipping shallowly into the main surface, and R' shears dipping more steeply (Fig. 24 d). This type of structure was very common, and was the primary shear sense indicator used for the

Corvallis fault. Also common were fractures corresponding to the RM type. RM fractures form steps in the fault surface caused by the breakage of the tip of the dihedral at the intersection of R shears and the main fault surface. Less commonly observed, but also consistent with the RM and RO fractures were lunate fractures, formed by the intersection of the main surface and R fractures that are concave toward the main fault plane. Lunate fractures are convex toward the direction of motion.

It should be noted here that all three of these fracture types produce a fault surface that is composed of incongruous steps, that is steps that face against the direction of motion of the missing block. At first glance, these

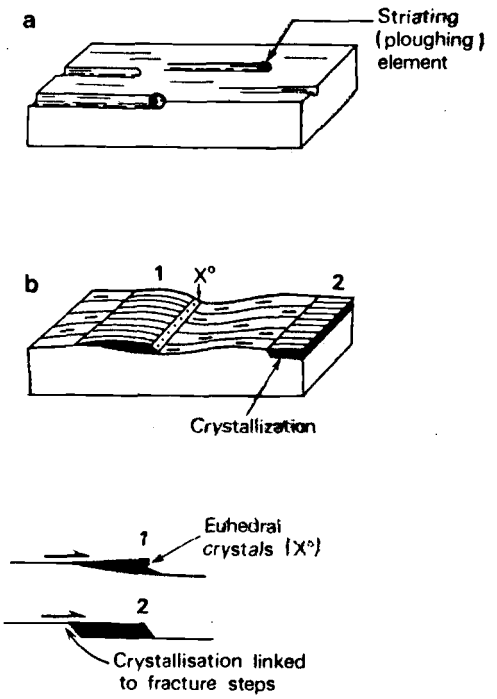

Figure 25. (a). Striation due to a ploughing element (asperity ploughing) (b). Fracture steps and associated crystallization on the lee side of the steps. From Petit, 1987.

steps are often interpreted as fracture steps (figure 25 b) which face in the direction of motion of the missing block, leading to an incorrect determination of shear sense.

A final category of features that is rare, but also consistent with the other three, were plough marks or tool marks. These are grooves on the fault surface that have a termination. The end of the groove points in the direction of motion of the missing block. Several of these were found, as well as an example of a tool, a resistant clast in the conglomerate, around which smaller tool marks diverged (figure 26). The lee side of the tool was fractured and partly missing, resembling a glacial roche moutonée. Like the other three

Figure 26. Resistant tool embedded in a slickensided fault surface. Smaller tools made by the now missing block diverge around the resistant clast, and the lee side is plucked away, both indicating left-lateral motion on this surface. Arrow is approx. 6" long.

shear sense indicators, plough marks indicate left-lateral motion. These four criteria indicate that left-lateral motion produced the dominant slickensides in the Mid Valley exposure.

On a larger scale, a plot of the slickensided surfaces in the core of the fault zone mirrors the results previously discussed for single surfaces. Three groupings of striated surfaces are evident on the stereo plot shown in figure 27. These represent R, R', and P shears. Shear sense determinations were done on these as described above, and the results are consistent with the studies of Freund (1974), Tchalenko and Ambraseys (1970) and others in the development of both R and R' shears. These experimental studies showed that the R and R' shears may develop equally, or either set may be dominant. A contour plot of slip surfaces in the Mid Valley pit shows that both are developed about equally, and that both have a slight plunge to the north. Added to the plot are the approximate stress axes, with s_1 bisecting the angle between R and R'.

The amount of displacement on the fault during the strike-slip episode is not known. No piercing points have yet been discovered at the surface or in the subsurface to give an indication of horizontal separation. In the available outcrops, and particularly at the Mid Valley pit, it is clear that the cobble to boulder conglomerates that were shed from the upthrown block to the west are still adjacent to the source block, so very large strike-slip

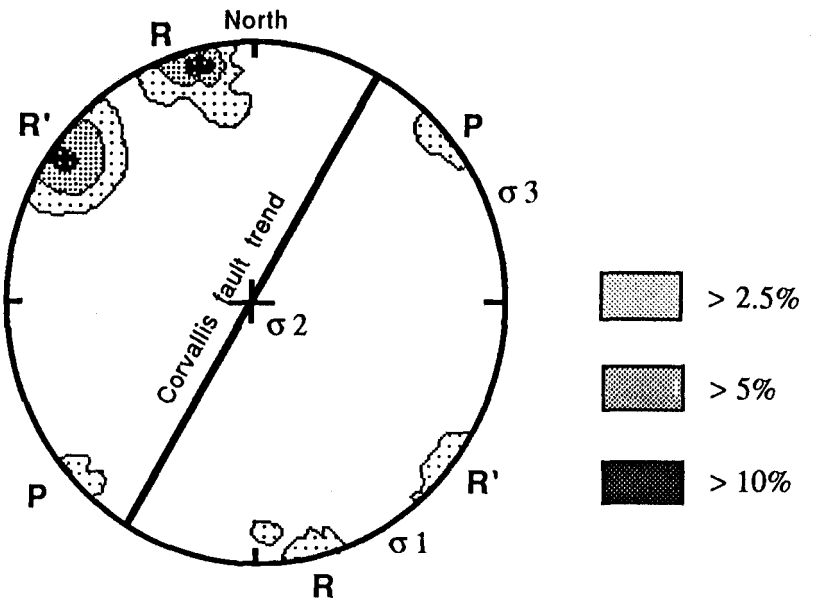

Figure 27. Equal-area contour plot of shear surfaces in the Mid Valley exposure. Maxima correspond to R, R', and P shears.

displacements are ruled out. Movements on the order of ten to fifteen km however are possible without separating the colluvial deposits from their source. Inasmuch as the original extent of the fault zone conglomerates is not known, this is only a weak constraint on the amount of net horizontal slip.

In addition to the horizontal, striated surfaces, one large surface of sub-vertical slickensides was found developed in an intrusion 10 m east of the core fault zone. It could not be determined exclusively whether the dip-slip or strike-slip motion was the latest episode, nor could the motion sense be determined for the vertical slicks. The overall dominance of the horizontally developed shear zone suggests, however, that strike-slip motion was the latest episode, destroying evidence of a previous dip-slip history.

If the fault zone intrusions correlate with the Marys Peak sill and other

local intrusives at about 30 Ma, the strike-slip motion on the Corvallis fault is constrained to be post mid-Oligocene.

NEOTECTONICS

The neotectonics of the Willamette Valley and the central Oregon Coast Range remain poorly known. Rapid weathering, high erosion rates, and dense vegetative cover make detailed surface mapping difficult at best. Yeats and others (1990), have found that the pervasive northwest and northeast pattern of faults recognized in the Coast Range continues into the Willamette Valley in the subsurface. Some of these structures may offset sedimentary units in the valley that are as young as late Pleistocene. Several northwest and northeast-trending faults are recognized immediately to the east of the study area in the subsurface (Graven, in prep.). The northwest trending faults display a right separation of structure contour lines, which could indicate right-lateral motion or dip-slip motion, with the southwest sides down. The northeast trending faults appear to be up to the east.

Evidence for neotectonic activity on the Corvallis fault and associated structures is somewhat ambiguous. Clearly the major episode of faulting was in the late Eocene, and the present exposure of these structures suggests that post-middle Miocene uplift has exhumed the older dead structures that now are transverse to the present structural grain (Lawrence and others, 1980). On a gross scale, along most of the fault trace, the base of the Coast Range hills is set back several km from the trace, with little evidence that would suggest Quaternary activity. Late Pleistocene Linn (?) gravels were examined along the Marys River and Oak Creek for evidence of post-Pleistocene deformation in the areas where the streams cross the Corvallis fault. These gravels contain silt and sand interbeds, and are overlain by massive silts of the Willamette Formation. Bedding and contacts dip from 0° to

12° to the east or southeast, averaging about 6°. No evidence for faulting was found along these two streams, however the banks were 50-70% covered by foliage, so offsets could easily have been missed, particularly as faults would likely be the sites of slumping and dense vegetation along the banks.

Despite these negative indicators for neotectonic activity, there are also indications that the Corvallis fault may have been active at least in a minor way since the late Pleistocene. Three earthquakes have been felt along the general trend of the fault since the 1940's, located approximately in Alsea in 1957, intensity III, in Albany in 1961, intensity III-IV, and the largest, an intensity V shock (modified Mercalli scale) reportedly felt strongly in Corvallis on May 12, 1942 (Berg and Baker, 1963). No instruments were available to precisely locate these shocks, thus no instrument magnitudes or focal plane solutions are possible. (The date of this shock is incorrectly reported as May 12, 1942 in both U.S. Dept. of Commerce *United States Earthquakes,* 1942, and Berg and Baker, 1963. The correct date is unknown, but was probably in 1946 or 1947). Local resident Ray Ellis, an amateur geologist, recalls that at the time of the Corvallis earthquake, a ground break occurred where highway 99W crosses the Corvallis fault between Lewisburg and Camp Adair, a now abandoned military base. The location described is on flat to gently sloping ground in a shallow northeast trending valley occupied by the Corvallis fault. The break is reported to have been visible for about a year. The location of the break makes it unlikely that the scarp was a slump feature triggered by the seismic event, and its location on the trace of the fault suggests minor motion on the Corvallis fault.

At the Mid Valley pit, a contact separates gravels of probable late Pleistocene age from an overlying silty unit, interpreted as the Willamette silt

as it contains several exotic boulders. The contact is perfectly planar, and dips 6° to the east. The fine-grained silts would likely have been deposited without any appreciable slope to the deposition surface, so 6° of eastward tilt is inferred for the late Pleistocene deposits adjacent to the fault. In a study of the geomorphic surfaces of the Willamette Valley, Balster and Parsons (1969) described the Quad surface (named for the OSU Quad), which probably includes the above described gravels and silts as a continuation of the Calapooyia surface to the east. As the elevation of the surface is 30-40 m higher than the remainder of the Calapooyia surface, they concluded that it had probably been uplifted by faulting. The Willamette Formation is generally found overlying the Linn gravels at elevations of between 60 and 90 m above sea level in the Willamette Valley (McDowell and Roberts, 1988). In the Willamette River channel immediately east of the study area, the contact is found at an elevation of 68 m. At the Mid Valley location, the contact is at 107 m elevation, close to the highest elevation at which the silts have been found (McDowell and Roberts, 1988). The silts overlie only 2-3 m of gravel, which directly overlie the Spencer Formation. Absent is the Monroe or Corvallis clay usually found between the Spencer and the Linn Gravels (Roberts and Whitehead, 1984; Yeats and others, in prep.). The thinning and absence of some Pleistocene units, as well as their relatively high elevation are also suggestive of minor Quaternary uplift in the vicinity of the Corvallis fault.

The Mid Valley pit is located on the crest of an elongate ridge that is associated with the main trace of the fault. The ridge is a curious feature, and it and several others along the fault trace have the appearance of "mole tracks", surficial compressional features associated with strike-slip faults, often the expression of positive flower structures (Sylvester, 1988). It is not entirely

clear if the ridges result from differential erosion, as the fault zone contains both resistant intrusions and well-cemented sandstone and conglomerate, or from faulting and compression.

One other location offers possible evidence for Quaternary activity. In the Timberhill development of north Corvallis, the main trace of the fault crosses Walnut Blvd and strikes northeast through a saddle at the entrance to Chip Ross Park. About halfway between Walnut and the saddle, a small scarp, striking N50°-60°E, ranging in height from a few inches to 1 m, marks a sharp break in slope at the fault. A small hand trench was dug across the scarp at its maximum height, and it was found to be underlain by a steeply east-dipping minor fault with the southeast block down. This scarp may well be a mass movement feature, as the hill slope is steep at that point, but none of the other features usually associated with slumps were observed nearby. Although most of the northwest trending probable faults observed on the aerial images were located in areas of Eocene outcrop, some of these extended into the high terrace deposits of Pleistocene age at the edges of the valley. The subtle continuation of these structures into areas of Quaternary to Holocene outcrop suggests that some of the northwest trending structures may be active. The most prominent of these structures is the Philomath fault, previously discussed. Possible expressions of this structure were visible in the 5-8 m thick Pleistocene gravels near the Marys River southeast of Philomath, and are suggestive of modern control of the river by the Philomath fault.

Finally, geodetic evidence based on nine east-west leveling routes indicates that the Coast Ranges of Oregon and Washington are undergoing a contemporary eastward tilt of about 3.3×10^{-8} rad./yr. (Adams, 1984; Reilinger

and Adams, 1982; Vincent and others, 1990). Reilinger and Adams (1982) report an anomaly to the tilt pattern on the Newport-Albany leveling route between the Kings Valley and Corvallis faults. Benchmarks located on the block between the two faults are apparently rising at about 2 mm/yr relative to the Coast Range and Willamette Valley.

Present State of Stress, Strain Accumulation and Faulting in Western Oregon

In situ stress determinations in western Oregon from borehole elongations (Werner and others, 1990) suggest that the principal horizontal stress is oriented N-S to NNE-SSW. Similar stress orientations are reported for eastern Oregon, Washington, western British Columbia, parts of Idaho and northern California (Zoback and Zoback, 1980; 1990). However, the plate convergence direction is calculated to be N50E (Riddihough, 1984), conflicting with N-S compression in western Oregon. Deformation presently occurring in the accretionary wedge offshore consists of a series of N-S trending imbricate thrust faults involving Eocene to Holocene sediments (Kulm and Fowler, 1974), indicating that the dominant stress being transmitted to the upper plate at its leading edge is E-W (or alternately that the orientation of these structures is controlled by a N-S trending buttress farther landward under the continental shelf). Also, fold axes, thrust faults and Holocene subsidence in the Coos Bay area indicate Quaternary to Holocene E-W to ENE-WSW compression (Adams, 1984; Peterson and Darienzo, 1989). Farther to the south, intense deformation associated with convergence along the southern Cascadia subduction zone occurs onshore and offshore as folds and thrust faults oriented normal to the expected plate convergence direction (Kelsey and Carver, 1988; G.A. Carver, personal communication,

1990). Evidence for onshore deformation associated with plate convergence is seen from the Coos Bay area south to the Mendocino triple junction. Apparently, where the coast is within 60-70 km of the deformation front, onshore deformation consistent with plate convergence is observed. Where the distance to the trench is greater than 60-70 km, no onshore deformation is seen, and it is replaced by N-S compression. There may exist a zone of transition between the two stress domains, approximately 60-70 km landward from the deformation front, and this is inferred to be the limit to which stress transferred to the upper plate at the plate boundary is transmitted landward.

This transition zone may shift its position east or west according to the convergence rate, thus parts of western Oregon may have been alternately subjected to north-south and east-west compression due to changes in the convergence rate with time. Kelsey (1990) found in the Cape Blanco region that Holocene uplift has taken place on an east-west trending anticline, and that this deformation is superimposed on older structures trending NNW. The older deformation is parallel with that in the subduction related fold belt offshore, thus the younger anticline may represent a late Quaternary shift in the transition zone to a position farther offshore. A westward shift in this transition zone in the late Tertiary is consistent with field evidence in this paper, and will be discussed in the next section.

The source of the present N-S compression is unknown, however fault patterns in western Oregon and in this study may be related to the present stress orientation. The left-lateral most recent motion on the Corvallis fault is consistent with the present N-S stress orientation. Several east-west trending thrust faults have also been mapped in northwestern Oregon (Niem and Niem, 1985; Parker, 1990), and northwest trending right lateral faults may be

responsible for a pull-apart structure in the Portland basin (Yelin and Patton, 1989). This evidence, coupled with possible seismic activity, indicates that the Corvallis fault may be active. High erosion rates that tend to rapidly remove evidence of scarps, and lack of abundant seismicity make it difficult to evaluate the seismic potential of the Corvallis fault. However, deformation of Pleistocene strata is gentle, and therefore activity on the fault, if any, is judged to be minor.

STRUCTURAL SYNTHESIS

Summary and Discussion

Mapping of the Corvallis fault, combined with gravity modeling, has shown that the major structure is a northwest dipping low-angle thrust fault in the study area. A dip of between 10° and 20° is inferred for the structure, based on both surface geology and gravity. Both the gravity results and field mapping are consistent with a fault-propagation fold geometry. Using a field-determined dip of 20°, vertical separation and horizontal displacement are calculated to be 6.7 km and 13-15 km respectively.

In contrast, the detailed structure of the fault zone at the Mid-Valley locality indicates that the most recent motion on the Corvallis fault was along a high-angle fault. This younger structure is inferred to have truncated the older thrust tip. Both dip-slip and strike-slip motions have occurred in the post-middle Oligocene, indicated by slickensides of both types developed in the fault zone intrusives. The latest motion was probably the strike-slip event, indicated by the dominance of sub-horizontal slickensides on the Corvallis fault. Analysis of the slickensides and associated shear fractures indicates that the strike-slip episode was left-lateral.

Normal motion, or possibly oblique-slip motion, displacing the east block up, is inferred to have caused exposure and erosion of the truncated leading edge of the Corvallis thrust, such that the original tip is no longer exposed at the surface. This is supported by the gravity models, which were improved by the incorporation of this structure, and by the Mid Valley exposure, where the original thrust surface appears to be drag folded against

the younger fault.

A possible explanation for the coincidence of these two faults at the same location may be that following thrusting, a down to the west normal fault developed, due to the gravitational load of the thrust sheet. Such an interpretation has also been suggested for the association of the Wind River thrust and the Continental fault. The Continental fault is a normal fault with the same orientation as the tip of the Wind River thrust, and is down to the northeast, or thrust sheet side. Berg (1962) interpreted this fault as being the result of gravitational collapse of the toe of the Precambrian thrust wedge (figure 28). Berg (1962) noted a
similar association of normal faults with other thrusts in the Wyoming/Montana foreland. These thrusts are of large horizontal displacement, and include the Crooks Gap fault north of the Sheep Creek thrust, and the Pathfinder fault north of the Seminoe thrust (Carpenter and Cooper, 1951).

A possible alternative explanation for the combination of a low-angle thrust, and the high-angle structure seen in outcrop, could be the steepening of the fault surface near the tip. This is a common feature of the Laramide thrusts of Wyoming that have good well and seismic control (fig. 28) (Berg, 1962; Berg, 1981). Later reactivation to produce the horizontal slickensides could also be consistent with the observed data.

A further analogy is drawn here with the Wind River thrust and other similar Laramide structures of the Wyoming and Colorado foreland. The cross-section presented here bears a strong resemblance in general style to those presented by Berg (1962; 1981). Gravity data indicate that the Siletz River Volcanics dip toward the root zone beneath the thrust sheet, as observed in the Wind River, Immigrant Trail, and EA thrusts. Also common in

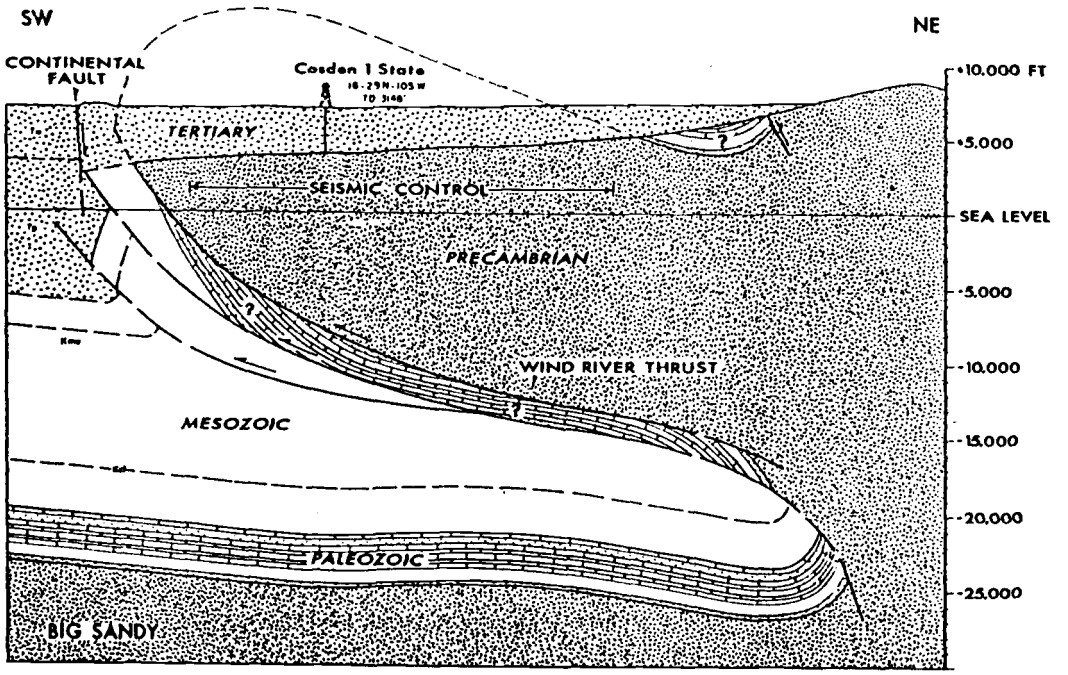

Figure 28. Interpreted (but not balanced) cross section of the Wind River thrust based on seismic reflection and drilling data. See text for discussion. From Berg, 1962.

the Laramide structures is an overturned sedimentary section beneath the thrust, and this is often cut by secondary leading thrusts. The overturned Tyee sandstones mapped east of the Corvallis fault may be the result of similar processes, their present exposure due to the uplift and erosion of parts of the footwall. The folding ahead of the thrust may be due to a "bulldozer effect" from a steepened fault tip, or may be due to unmapped or blind thrusts leading the main surface, as documented for the Laramide structures. Plate 2 is shown with this option as the cause of the folds east of the main thrust.

Regional Extent of the Corvallis Fault and the Corvallis Thrust

This study has mapped in detail the trace of the Corvallis fault from near Camp Adair in the northeast, to Alsea summit at the southwestern map boundary. Mapping the fault farther to the northeast and southwest becomes difficult due to the scarcity of subsurface data to the northeast, and to the poor exposure, rugged terrain and lack of lithologic contrast to the southwest. In the subsurface, one proprietary seismic line shows a high noise response at the approximate projected location of the fault, northeast of the map area, but the structure at that location is not discernable. Other available well and seismic data are insufficient to locate the northeast extension if it is present in the subsurface. Farther to the northeast, 23 km from the point at which the trace is lost in the valley, two possible indicators of a northeast extension are found. Walker and Duncan (1988) and Graven (in prep.) have shown a fault (the Turner fault) trending N 50 E in Columbia River Basalt south of Salem, on trend with the Corvallis fault. 8 km farther northeast, the outcrop pattern of the Columbia River Basalt, east of Salem, is terminated for 36 km along a northeast trending lineation marking the range front of the Waldo Hills, also on trend with the Corvallis fault (Wells and Peck, 1961; Yeats and others, in prep.). As previously mentioned, the residual Bouguer gravity map of the Willamette Valley reveals a northeast trending anomaly extending from the mapped Corvallis fault to the area of the Waldo Hills lineament. Along this lineation the CRB's are exposed to the southeast, and covered by Quaternary alluvium to the northwest. Grand Ronde flows of the Columbia River Basalt are found to be at a lower elevation on the northwest side of this lineation (Marvin Beeson, personal communication, 1990 Graven, in prep.). Side

looking radar images of the Waldo Hills lineament show a prominent linear feature extending the full length of the CRB/Quaternary contact, and extending southwest through the southern Salem hills. (figure 29) At present there is no direct evidence of this probable fault, however its linearity and location on trend with the Corvallis fault suggest a possible correlation. Southwest of the field area, Baldwin (1955) mapped the Corvallis fault as continuing some 19 km to the southwest of the present mapping, then dying out in the Tyee Formation. Farther to the southwest, mapping is hindered

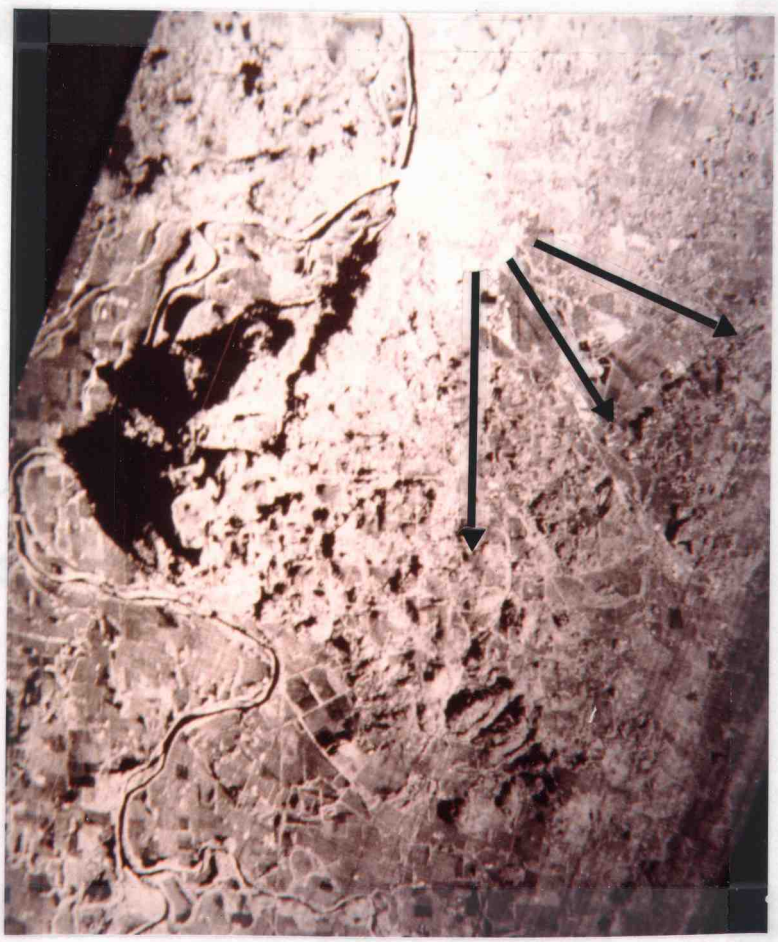

Figure 29. Real aperture side-looking radar image of the central Willamette Valley. Bright return in upper center is the city of Salem. Waldo Hills lineament is shown by the arrows. This feature is on trend with the Corvallis fault, slightly ofset to the northwest. Image courtesy of C. Rosenfeld, OSU Geosciences.

as only Tyee strata are exposed along the projected extension of the fault, and the area is heavily forested. Snavely and Wells (1984), Snavely (1987) and Walker and Duncan (1989, based on the mapping of Snavely and Wells 1984) show an extension of the Corvallis fault some 50 km farther to the southwest based on shear zones and opposing dips in the Tyee (Parke D. Snavely Jr., personal communication, 1990). At the coast north of Florence, the late Eocene Yachats Basalt outcrop pattern is controlled by northeast and northwest trending faults (Snavely, 1976b, Snavely and MacLeod, 1974). Snavely has mapped a northeast trending fault that crops out near the southern boundary of the Yachats Basalt and has correlated this fault with the Corvallis fault. He has also tentatively identified it offshore, on the basis of a seismic reflection line, and has extended it to the mid-continental shelf (Parke D. Snavely Jr., personal communication, 1990). Seismic lines on the inner shelf southwest of Florence confirm a structure along the southwest projection of the Corvallis fault (LaVerne D. Kulm, unpublished data).

Regional gravity contours (Berg and Thiruvathukal, 1967) support the continuation of a northeast-southwest trending structure between the present mapping and the Oregon Coast. Although the main signature of the thrust sheet bends northwestward and merges with the eastern flank of the Coast Range gravity high, a weaker anomaly trends northeast into the western Cascades via the Waldo Hills. The gravity maps of Blakely and Jachens (1990) suggest that a continuous lineament extends from the Oregon coast into the Cascades.

Perhaps the strike-slip fault that is presently coincident with the leading edge of the Corvallis thrust, or the thrust itself, represents the reactivation of a deeper major structure that is responsible for the throughgoing gravity

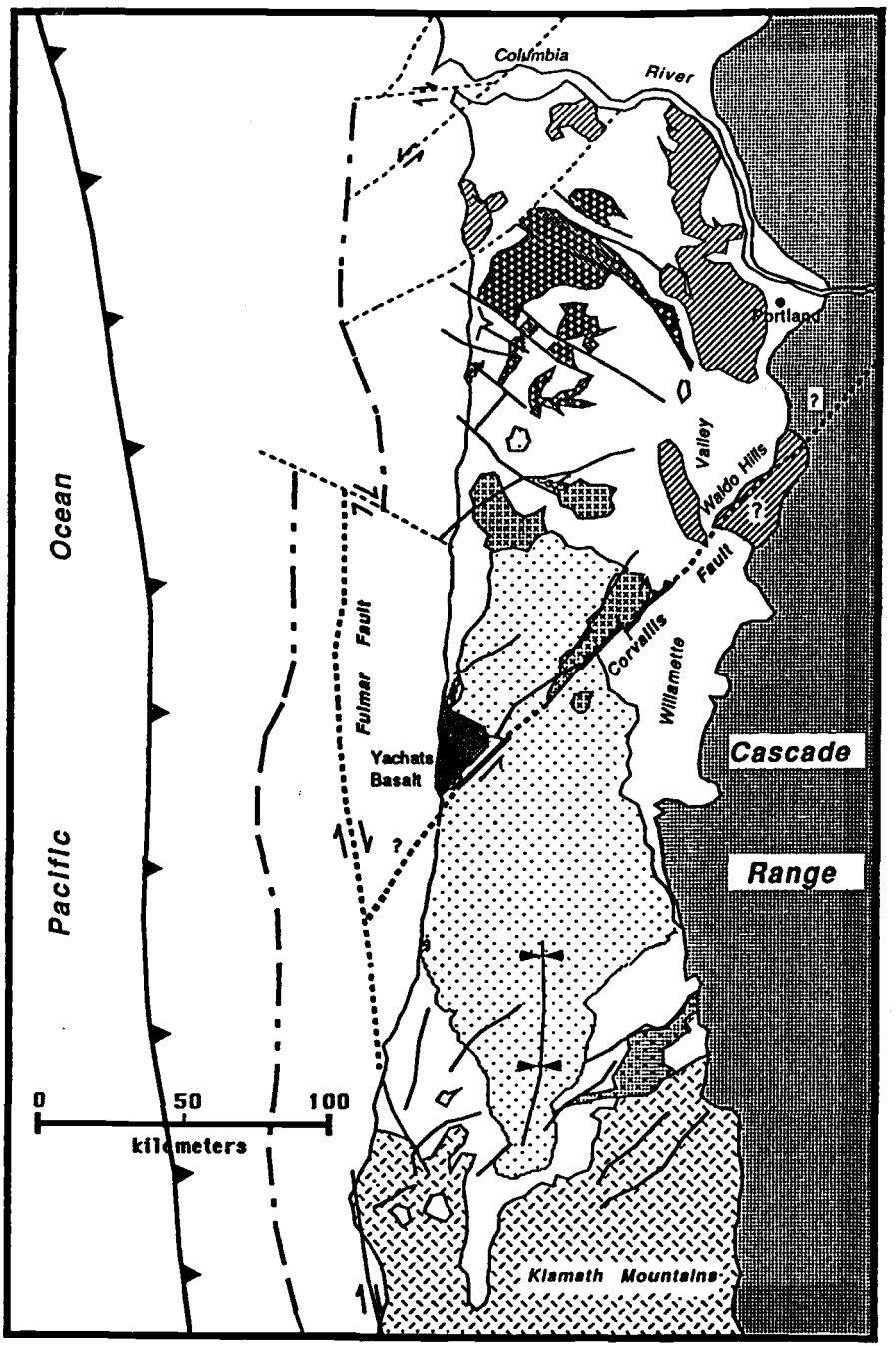

Figure 30. Possible extensions of the Corvallis fault along the Waldo Hills lineation, and southwest onto the continental shelf. Modified after Snavely, 1987.

anomaly.

While a throughgoing anomaly appears to exist beyond the study area, the gravity contours suggest that the thrust tip turns sharply or is offset to the northwest. The associated gradient then merges with the east flank of the Coast Range gravity high (Fig. 15). This may reflect termination of the thrust along a tear or series of tears similar to the southern termination of the Wind River thrust (Berg, 1962), and the Beartooth thrust near Red Lodge, Montana (Foose and others, 1961).

Alternatively, the thrust may be offset by a northwest trending fault. A fault with this orientation has been mapped in the subsurface east of the study area (Graven, in prep; Yeats and others, in prep.), and may be related to the termination of the Corvallis thrust.

The gravity gradient along the Coast Range high is steeper both to the north and south of the map area, suggesting that if this boundary is a structural one, it probably has a steeper dip than the Corvallis thrust.

The association of the Corvallis thrust, probably of limited extent, with a regional lineament, suggests that perhaps the low-angle thrust represents an anomalous segment of a regional structure. The low angle of the Corvallis thrust may be due to the local presence of a weak unit within the Siletz River Volcanics that promoted the local formation of a décollement. Elsewhere, the regional structure may be a high angle reverse fault. In the Tillamook area, Ray Wells has mapped a Kings Valley Siltstone equivalent informally named the Trask River Siltstone. This unit is variable in thickness, up to 1500 m, and lies between basalts equivalent to the SRV at the type locality, and younger Siletz River basalts (R. E. Wells, personal communication, 1990). The presence of these two similar siltstone units in the SRV suggests that others

may also exist, and that the seamount terrain may be characterized by overlapping shield cones, with several interbedded siltstone intervals. An episode of compression in the forearc may have detached some of these separate components of the SRV along weak siltstone intervals, producing the Corvallis thrust and possibly other unrecognized thrusts.

That the Corvallis fault is relatively prominent may be the result of a fortuitous combination of location and lithologic contrast, or it may be that an older structural fabric was only partially reactivated in the late Eocene, leaving pre-Tyee structures still buried by Tyee and younger marine sediments.

Relation to Forearc Models.

The Oregon Coast Range, along with the continental shelf and slope of Oregon and Washington are part of an unusually broad forearc ridge, within which are several forearc basins. Two somewhat different models have been suggested for the structure of the arcward part of forearc ridges. Pavlis and Bruhn (1983), in a comparison of broad forearc ridges such as the Aleutian arc, and the Barbados ridge, proposed that the uplift of these broad ridges is accomplished by melange accumulation and duplexing at deep levels, arcward of the active accretionary wedge. The trenchward tilt that characterizes these accretionary systems results from the accumulation of melange at deep levels at the contact between the "backstop" and the downgoing plate. They suggested that the arcward limit of this uplift is marked by a major fault (Fig. 31).

Other investigators have observed that a backthrust often separates the uplifted ridge from the forearc basin (Reed and others, 1983, Silver and Reed, 1988, Westbrook, 1982). Byrne and others (1988) suggested a structure

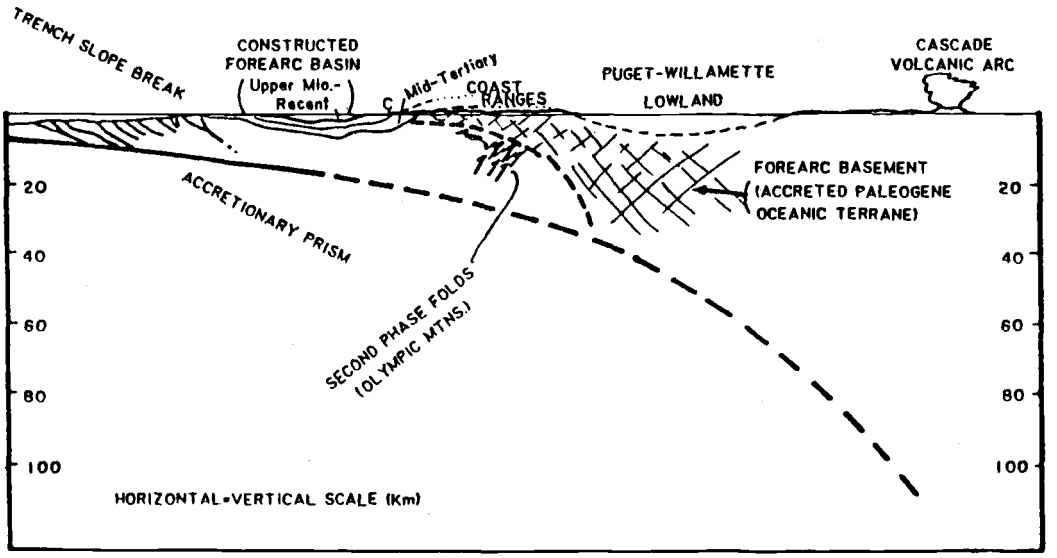

Figure 31. East-west cross section across the Cascadia arc-trench system about 45° N. Geology generalized from Snavely and others, 1980. From Pavlis and Bruhn, 1983. See text for discussion.

based on the mechanics of accretion against a backstop. In their sandbox forearc model, an arcward vergent backthrust develops at the landward limit of the active forearc ridge, and separates the ridge from a relatively undeformed forearc basin. This structural boundary marks the seaward limit of the seaward dipping "backstop" (Figure 32). Both models feature a relatively undeformed forearc basin landward of the ridge, and separated from it by a major fault.

The Oregon Coast Range uplift may be composed of elements of both of these models. Gravity and refraction data suggest that a density and velocity inversion may underlie the Siletz River Volcanics at depth (Dehlinger

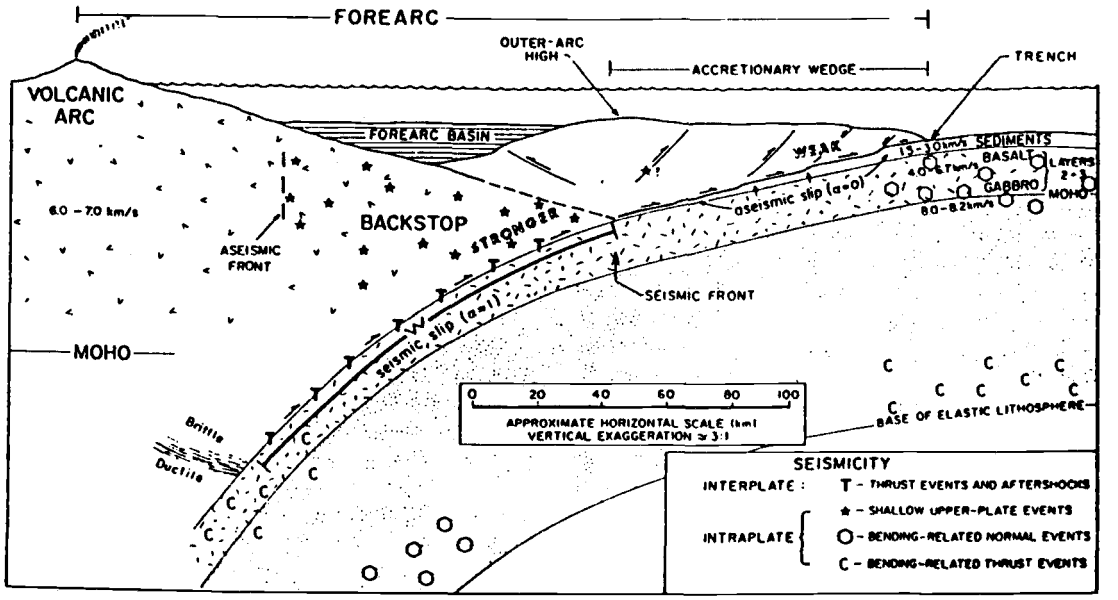

Figure 32. Schematic cross section of the upper 50 km of an arc-trench system. Backthrust develops as an expression of the seaward limit of the "backstop" at depth. From Byrne and others, 1988.

and others, 1968; Keach and others, 1989; Langston, 1981). In the Olympics of Washington, Crescent Formation oceanic crust is thrust over a melange of lower density and velocity (Cady, 1975). Couch and Braman (1979) proposed that the velocity and density anomaly inferred at depth beneath the Coast Range might be due to an equivalent of the melange underlying the Olympics. Lawrence and others (1980) suggested that much of the Oregon Coast Range may be an allochthonous sheet overlying low-density sediments or melange. These observations suggest that the understuffing and relatively passive mechanism of Pavlis and Bruhn (1983) may be a factor in the uplift of

the Coast Range.

Evidence from this paper indicates that a portion of the boundary between the forearc ridge and the forearc basin is bounded by a low-angle thrust fault. Unrecognized thrusts may mark the boundary elsewhere along the western Willamette Valley, as suggested by regional gravity data. The cross-section constructed for this work bears a remarkable resemblance to the experimental results of Byrne and others (1988), suggesting that the mechanism of reversal of thrust vergence at the forearc ridge/forearc basin boundary may also be applicable to the Cascadia forearc. The Corvallis thrust may have been such a structure in the late Eocene. Silver and Reed (1988) argue that the controlling influence on which of these mechanisms is operative in a forearc system is the dip of the "backstop". They suggest that an arcward dipping backstop should promote understuffing and uplift of the forearc. In contrast, a seaward dipping backstop would limit understuffing, and the growth of the wedge would be controlled by wedge taper considerations.

In the Oregon Coast Range, there may be two backstops in operation. The Siletz River microplate represents a rigid crustal element embedded within the broad forearc ridge. Its seaward edge acts as a backstop against which an active submarine accretionary wedge has accumulated from the middle Eocene to the present. The thrust fault described in this paper suggests that a second and older backstop may be located farther landward, probably beneath the Willamette Valley. This second backstop may consist of Siletz River crust and seamounts, thickened by imbrication during the accretion of the terrane in the Eocene. This thickened crust may be responsible for the deepening gravity low beneath the central and eastern

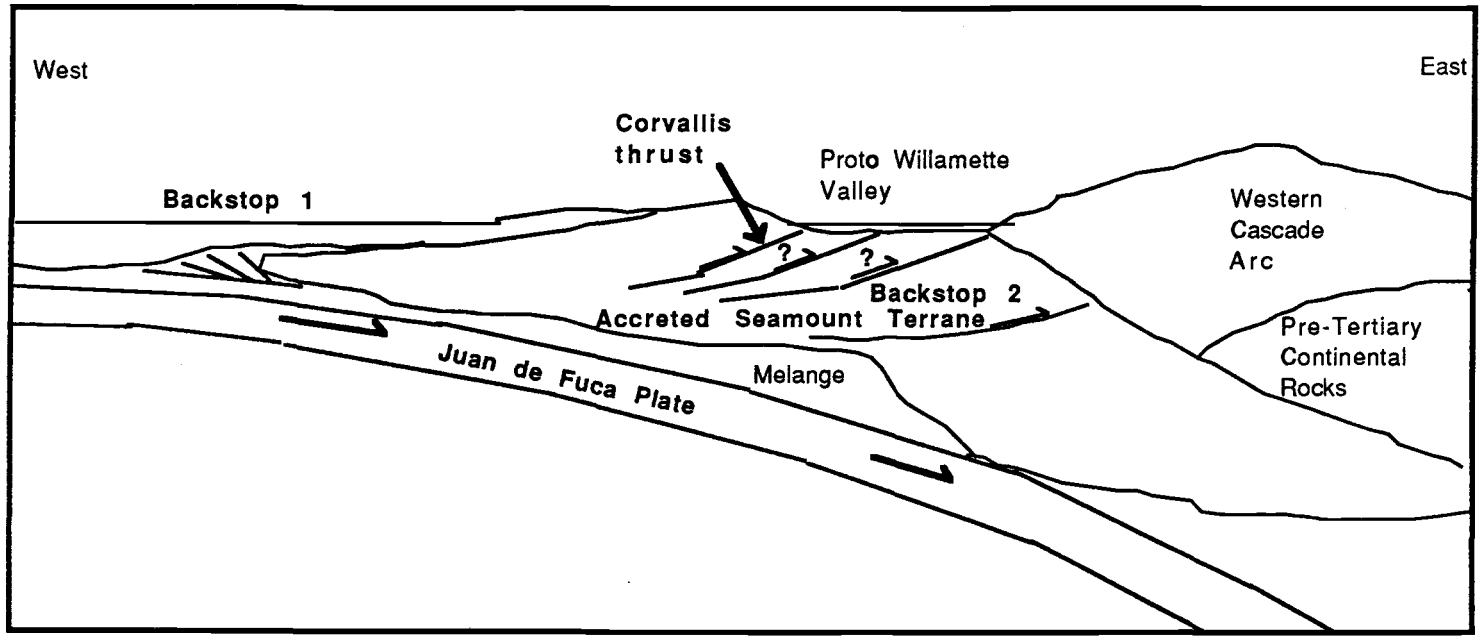

Figure 33. Cartoon showing proposed crustal configuration of the Cascadia arc subduction system.

Willamette Valley. The regional low is probably due to the effect of the deepening Moho, however the Siletz River Volcanics are found to underlie the Willamette Valley (Graven, in prep.; Yeats and others, in prep.). Thus the thickened crust responsible for the gravity low may be imbricated Siletz River Volcanics, rather than older North American continental crust.

If the mechanical model of Byrne and others (1988) is valid, it may have been this earlier backstop that controlled the location of the Corvallis thrust during the late Eocene. The second backstop could be composed of imbricated and thickened SRV, stacked up during collision with the pre-Tertiary continental margin (Fig. 33).

Relation of Structure to Rotation Models

A pervasive pattern of northwest and northeast trending faults is evident in the east-central Coast Range from this study, and a similar pattern is well documented in most of the central and northern Oregon Coast Range and in southwest Washington (Snavely and others, 1976 a, b, c; Niem and Niem, 1985; Wells and Coe, 1985). Several models have been proposed to fit these faults into a tectonic picture which includes the previously discussed clockwise rotation, and the contemporary borehole elongation studies indicating north-south compression. Niem and Niem (1985) and Werner and others (1990) suggest that the fault patterns can be explained in terms of conjugate fracture patterns associated with pure shear in a north-south direction. In their model the northeast-trending faults must be left-lateral, and the northwest faults must be right-lateral.

In contrast, Wells and Coe (1985), using the faults mapped in southwest Washington, suggested that the observed patterns can be ex-

plained by a Reidel shear model in which rotations were accommodated by numerous left-lateral northwest trending faults. Domains of differing rotation were bounded by more northerly trending right-lateral faults. Wells' model attempts to integrate the observed fault pattern, paleomagnetic rotations, and the oblique subduction occurring in the Pacific Northwest (Fig. 34).

The key to solving the structural problems observed in western Oregon is accurate field data, which are difficult to come by. This paper presents evidence that is in general consistent with present day north-south pure shear in that the latest motion of the northeast-trending Corvallis fault was left-lateral.

The numerous left steps in the trace of the Corvallis fault suggest a somewhat different stress orientation. Wells and Coe (1985), and Terres and Sylvester (1981) have demonstrated that clockwise rotations can be accommodated on R or R' shears in a dextral shear couple. It is here proposed that the left-lateral faults offsetting the Corvallis fault are analogous to those found in southwest Washington by Wells and Coe (1985). These faults were probably active during an episode of more rapid convergence, which has slowed about 60% since the Pliocene (Riddihough, 1984; Spence, 1989).

The bypassing of at least one of these left steps (at Oak Creek) suggests that they are somewhat older than the latest motion on the Corvallis fault. I propose that prior to the present episode of north-south compression, the Oregon Coast Range was dominated by convergence-normal compression and dextral shear rotation. Fault patterns were controlled by a dextral shear couple in which clockwise rotations were accommodated on the northwest-trending left-lateral faults. With decreasing convergence rates in

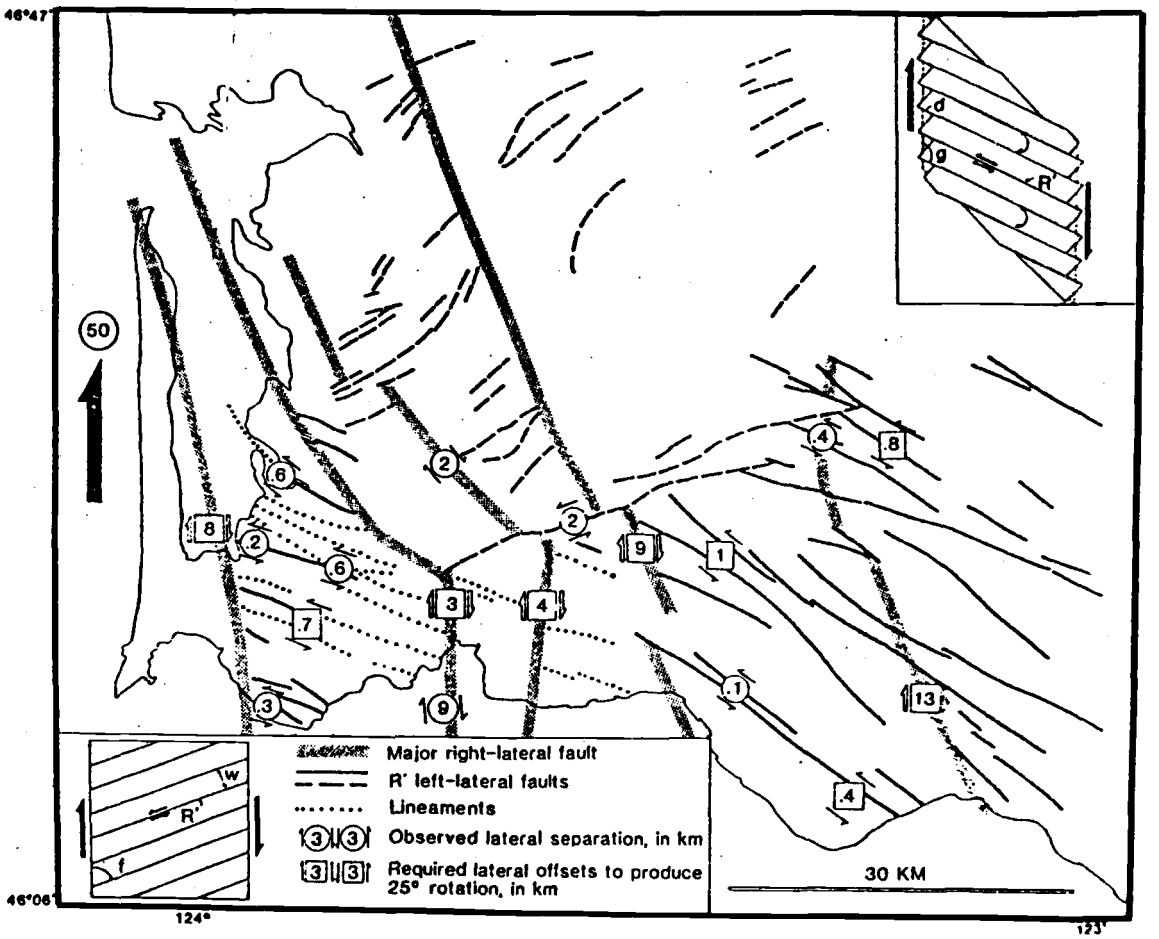

Figure 34. Fault pattern in southwest Washington, and proposed rotation mechanism. From Wells and others, 1984.

the late Tertiary, the transition zone between plate convergence compression and the north-south prevailing stress in western North America shifted seaward, possibly in the Pliocene. Thus the clockwise rotation of the Oregon Coast Range may have ceased in the last several million years, replaced by contemporary north-south compression.

CONCLUSIONS

Evidence presented in this study suggests that the nature of the Corvallis fault differs significantly from previous interpretations.

1) Gravity and surface geologic data suggest the Corvallis thrust is a low-angle thrust, dipping 10°-20° to the northwest. Horizontal and vertical separations are estimated to be13-15 km and 6-7 km respectively.

2) The geometry of the Corvallis thrust is consistent with a fault-propagation fold model, with multiple episodes of deformation required to produce the observed field relations.

3) The Corvallis thrust was active during the late Eocene, and was probably the eastern boundary of a tectonic highland in the forearc. Other broadly synchronous volcanic and tectonic highlands may have formed a discontinuous archipelago in the position of the present Oregon Coast Range.

4) A high-angle fault (the Corvallis fault) is closely associated with the thrust, and is interpreted a west block down normal fault. This fault may be the result of gravitational collapse of the footwall sediments beneath the high density thrust sheet. Later reactivation of this structure as a left-lateral strike-slip fault has produced the abundant horizontal slickensides observed in outcrop.

5) The Corvallis thrust may have been a late Eocene backthrust related to the developing accretionary wedge, and may have marked the boundary between the wedge and a proto Puget/ Willamette forearc basin.

6) Lineaments in both gravity anomalies and radar and photgraphic imagery, field mapping, and offshore seismic data suggest a connection between the Corvallis thrust/Corvallis fault and a larger structure of regional extent. The nature of this suggested regional structure is unclear at this time, but this and other northeast trending regional lineations parallel the Siletzia/Klamath Mountains suture in southwest Oregon. This relation suggests a possible connection to accretion/collision related structures that may underlie the Cascade arc and post accretion sediments in western Oregon.

7) Numerous left offsets of the trace of the Corvallis fault suggest small block rotations have occured in the study area. This supports the hypothesis that such small block rotations may be responsible for much of the observed paleomagnetic rotation of post-middle Eocene rocks in western Oregon. Latest motion on the Corvallis fault suggests that these left offsetting faults have themselves been cut by the Corvallis fault, suggesting a late cessation of small block rotations.

REFERENCES

Adams, J., 1984, Active deformation of the Pacific northwest continental margin: Tectonics, v. 3, p. 449-472.

Al Azzaby, F.A., 1980, Stratigraphy and sedimentation of the Spencer Formation, Yamhill and Washington Counties, Oregon: Unpublished M.S. thesis, Portland State University, Portland , Oregon, 104 p.

Allison, I.S., 1953, Geology of the Albany quadrangle, Oregon: Oregon Department of Geology and Mineral Industries Bulletin 37, 18 p. 1 map, scale 1: 62,500.

Armentrout, J.M., Hull, D.A., Beaulieu, J.D., and Rau, W.W., 1983, Correlation of Cenozoic stratigraphic units of western Oregon and Washington: Oregon Department of Geology and Mineral Industries Oil and Gas Investigation 7, 90 p.

Armstrong, R.L., 1978, Cenozoic igneous history of the U.S. Cordillera from lat. 42° to 49° N, *in* Smith, R.B. and Eaton, G.P., eds., Cenozoic tectonics and regional geophysics of the western Cordillera: Geological Society of America Memoir 152, p. 263-282.

Bailey, A.D., 1974, Near surface fault detection by magnetometer: California Geology, v. 38, p. 274-277.

Baker, L.J., 1988, The stratigraphy and depositional setting of the Spencer Formation, west-central Willamette Valley, Oregon: a surface-subsurface analysis: Unpublished M.S. thesis, Oregon State University, Corvallis, 171 p.

Baldwin, E.M., 1947, Geology of the Dallas and Valsetz quadrangles, Oregon: Oregon Department of Geology and Mineral Industries Bulletin 35, 61 p.

Baldwin, E.M., 1955, Geology of the Marys Peak and Alsea quadrangles, Oregon: U.S. Geological Survey Oil and Gas Investigations Map OM-162, scale 1:62,500.

Baldwin, E.M., 1961, Geologic map of the lower Umpqua River area, Oregon: U.S. Geological Survey Oil and Gas Investigations Map OM-204, scale 1:62,500.

Baldwin, E.M., 1964, Geology of the Dallas and Valsetz quadrangles, Oregon revised: Oregon Department of Geology and Mineral Industries Bulletin 35, 52 p.

Baldwin, E.M., 1974, Eocene stratigraphy of southwestern Oregon: Oregon Department of Geology and Mineral Industries Bulletin 83, 40 p.

Baldwin, E.M., 1975, Revision of the stratigraphy of southwestern Oregon: *in* Weaver, D.W., Hornaday, G.R., and Tipton, A., eds., Paleogene Symposium and Selected Technical Papers, annual meetings AAPG, SEPM, SEG, Long Beach, California, p. 49-64.

Baldwin, E.M., 1981, Geology of Oregon, Kendall/Hunt, Dubuque, Iowa, 170 p.

Baldwin, E.M., Brown, R.D.,Jr., Gair, J.E., and Pease, M.H., Jr., 1955, Geology of the Sheridan and McMinnville quadrangles: U.S. Geological Survey Oil and Gas Investigations Map OM-155. scale 1:62,500.

Balster, C.A., and Parsons, R.B., 1968, Geomorphology and soils Willamette Valley, Oregon: Oregon State University Agricultural Experiment Station, Special Report 265, 17 p.

Balster, C.A., and Parsons, R.B., 1969, Late Pleistocene stratigraphy, southern Willamette Valley, Oregon: Northwest Science, v. 43, p. 116-129.

Beaulieu, J.D., 1971, Geologic formations of western Oregon, west of longitude 121° 30': Oregon Department of Geology and Mineral Industries Bulletin 70, 72 p.

Beck, M.E., 1980, Paleomagnetic record of plate-margin tectonic processes along the western edge of North America: Journal of Geophysical Research, v. 85, p. 7115-7131.

Beck, M.E., and Plumley, P.W., 1980, Paleomagnetism of intrusive rocks in the Coast Range of Oregon: Microplate rotations in Tertiary time: Geology, v. 8, p. 573-577.

Beeson, M.H., Perttu, R., and Perttu, J., 1979, The origin of the Miocene basalts of coastal Oregon: an alternative hypothesis: Oregon Geology, v. 41, p. 159-156.

Beeson, M.H., Fecht, K.R., Reidel, S.P., and Tolan, T.L., 1985, Regional correlations within the Frenchman Springs Member of the Columbia River Basalt Group: New insights into the middle Miocene tectonics of northwestern Oregon: Oregon Geology, v. 47, p. 87-96.

Beeson, M.H., and Tolan, T.L., 1989, The Columbia River Basalt Group in the Cascade Range: a middle Miocene reference datum for structural analysis, *in* Muffler L.J.P., Weaver, C.S., and Blackwell, D.D., eds., Workshop XLIV, Geological, Geophysical, and Tectonic setting of the Cascade Range, U.S. Geological Survey Open-File Report 89-178, p. 257-290.

Bela, J.L., 1979, Geologic hazards of eastern Benton County, Oregon: Oregon Department of Geology and Mineral Industries Bulletin 98, 122 p.

Bentley, R.D., 1980, Wrench tectonic model for the late Cenozoic evolution of Oregon and Washington: Geological Society of America Abstracts with Programs, v. 12, p. 385.

Berg, J.W., and Baker, C.D., 1963, Oregon earthquakes, 1841 through 1958: Bulletin of the Seismological Society of America, v. 53, p. 95-108.

Berg, J.W., and Thiruvathukal, J.V., 1967, Regional Bouguer gravity map of Oregon: Oregon Department of Geology and Mineral Industries GMS-4a.

Berg, R.R., 1962, Mountain flank thrusting in Rocky Mountain foreland, Wyoming and Colorado: American Association of Petroleum Geologists Bulletin, v. 46, p. 2019-2032.

Berg, R.R., 1981, Review of thrusting in the Wyoming foreland: Contributions to geology, University of Wyoming, v. 19, p. 93-104.

Berg, R.R., and Romberg, F.E., 1966, Gravity profile across the Wind River Mountains, Wyoming: Geological Society of America Bulletin, v. 77, p. 467-656.

Berkman, T.A., 1990, Surface-subsurface geology of the middle to upper Eocene sedimentary rock units, western Columbia County. northwest Oregon: M.S. Thesis, Oregon State University, Corvallis, Oregon, 410 p.

Bird, K.J., 1967, Biostratigraphy of the Tyee Formation (Eocene), southwestern Oregon: PhD Thesis, University of Wisconsin, Madison, Wisconsin. 209 p.

Blakely, R.J., and Connard, G.G., 1990, Crustal studies using magnetic data: *in* Pakiser, L.C., and Mooney, W.D., Geophysical framework of the Continental United States, Geological Society of America Memoir 172, p. 45-61.

Blakely, R.J., and Jachens, R.C, 1990, Volcanism, isostatic residual gravity, and regional tectonic setting of the Cascade volcanic province: Journal of Geophysical Research, in press.

Breiner, S., 1973, Applications manual for portable magnetometers: Geometrics, Sunnyvale, California, 58p.

Bretz, J.H., 1969, The Lake Missoula floods and the channeled scabland: Journal of Geology, v. 77, p. 503-543.

Bromery, R.W., and Snavely, P.D., Jr., 1964, Geologic interpretation of reconnaissance gravity and aeromagnetic surveys in northwestern Oregon: U.S. Geological Survey Bulletin 1811-N, 13 p.

Brownfield, M.E., 1982, Geologic map of the Sheridan quadrangle, Polk and Yamhill Counties, Oregon: Oregon Department of Geology and Mineral Industries, GMS-23, scale 1:24,000.

Bruer, W.G., Alger, M.P., Deacon, R.J., Meyer, H.J., Portwood, B.B., and Seeling, A.F., 1984, Correlation section 24, northwest Oregon: Pacific section, American association of Petroleum Geologists.

Byrne, D.E., Davis, D.M., and Sykes, L.R., 1988, Loci and maximum size of thrust earthquakes and the mechanics of the shallow region of subduction zones: Tectonics, v. 7, p. 833-857.

Carpenter, L.C., and Cooper, H.T., 1951, Geology of the Ferris-Seminoe Mountain area; Wyoming Geologic Association 6th Annual Field Conference Guidebook, p. 108-111.

Clark, H.C., 1969, Remanent magnetization, cooling history, and paleomagnetic record of the Marys Peak sill, Oregon: Journal of Geophysical Research, v. 74, p. 3143-3160.

Cady, W.M., 1975, Tectonic setting of the Tertiary volcanic rocks of the Olympic Peninsula, Washington: U.S. Geological Survey Journal of Research, v. 3, p. 573-582.

CH2M Hill (Niem, W.A., Macleod, N.S., and Priest, G.R.), 1987, Superconducting super collider site proposal: University site, Oregon: Geology and tunneling, v. 3, 46 p.

Chan, M.A., and Dott, R.H., Jr., 1983, Shelf and deep sea sedimentation in Eocene forearc basin, western Oregon--fan or non fan?: American Association of Petroleum Geologists Bulletin, v. 67, p. 2100-2116.

Couch, R.W., and Braman, D. ,1979, Geology of the continental margin near Florence, Oregon: Oregon Geology, v. 41, p. 171-179.

Dehlinger, P., Couch, R.W., and Gemperle, M., 1968, Continental and Oceanic structure from the Oregon coast westward across the Juan de Fuca Ridge: Canadian Journal of Earth Sciences, v. 5, p. 1079-1090.

Dott, R.H., 1966, Eocene deltaic sedimentation at Coos Bay, Oregon: Journal of Geology, v. 74, p. 373-420.

Duncan, R.A., 1982, A captured island chain in the Coast Range of Oregon and Washington: Journal of Geophysical Research, v. 87, p. 10,827-10,837.

Duncan, R.A., and Kulm, L.D., 1989, Plate tectonic evolution of the Cascades arc-subduction complex, *in* Winterer E.L., Hussong, D.M., and Decker, R.W., eds., The eastern Pacific Ocean and Hawaii: Boulder, Colorado, Geological Society of America, The Geology of North America, v. N., p. 413-437.

Foose, R.M., Wise, D.U., and Garabarini, G.S., 1961, Structural Geology of the Beartooth Mountains, Montana and Wyoming: Geological Society of America Bulletin, v. 72, p. 1143-1172.

Frank, F.J., and Johnson N.A., 1972, Ground water data in the Corvallis-Albany area, central Willamette Valley, Oregon: Oregon State Engineer, ground water report 17, 46 p.

Frei, L.S., Magill, J.R., and Cox, A.V., 1984, Paleomagnetic results from the central Sierra Nevada: Constraints on reconstructions of the western United States: Tectonics, v. 3, p. 157-178.

Freund, R., 1974, Kinematics of transform and transcurrent faults: Tectonophysics, v. 21, p. 93-134.

Glenn, J.L., 1965, Late Quaternary sedimentation and geologic history of the north Willamette Valley: Unpublished PhD thesis, Oregon State University, Corvallis, Oregon. 231 p.

Globerman, B.R., Beck, M.E., Jr., and Duncan, R.A., 1982, Paleomagnetism and tectonic significance of Eocene basalts from the Black Hills, Washington Coast Range: Geological Society of America Bulletin, v. 93, p. 1151-1159.

Graven, E.P., 1990, Structure and tectonics of the southern Willamette Valley, Oregon: M.S. Thesis, Oregon State University, Corvallis, Oregon. In prep.

Hammer, S., 1939, Terrain corrections for gravimeter stations: Geophysics, v. 4, p. 184-194.

Heller, P.I., and Dickinson, W.R., 1985, Submarine ramp facies model for delta-fed, sand-rich turbidite systems: American Association of Petroleum Geologists Bulletin, v. 69, p. 960-976.

Heller, P.L., Peterman, Z.E., O'Neil, J.R., and Shafiqullah, M., 1985, Isotopic provenance of sandstones from the Eocene Tyee Formation, Oregon Coast Range: Geological Society of America Bulletin, v. 96, p. 770-780.

Keach, R.W., II, Oliver, J.E., Brown, L.D., Kaufman, S., 1989, Cenozoic active margin and shallow Cascades structure: COCORP results from western Oregon: Geological Society of America Bulletin, v. 100, p. 783-794.

Kelsey, H.M., and Carver, G.A., 1988, Late Neogene and Quaternary tectonics associated with northward growth of the San Andreas transform fault, northern California: Journal of Geophysical Research, v. 93, p. 4797-4819.

Kelsey, H.M., 1990, Late Quaternary deformation of marine terraces on the Cascadia subduction zone near Cape Blanco, Oregon: EOS, v. 71, p. 367.

Kulm, L.D., and Fowler, G., 1974, Oregon continental margin structure and stratigraphy: A test of the imbricate thrust model, *in* Burk, C.A., and Drake, C.L., The geology of continental margins, Springer-Verlag, New York, p 261-284.

Kulm, L.D., and Duncan, R.A., 1989, Plate tectonic evolution of the Cascades arc-subduction complex *in* Winterer, E.L., Hussong, D. M., and Decker, R.W., eds., The eastern Pacific Ocean and Hawaii, v. N, The Geology of North America, The Geological Society of America, Boulder, Colorado, p. 413-437.

Langston, C.A., 1981, Evidence for the subducting lithosphere under southern Vancouver Island and western Oregon from teleseismic P wave conversions: Journal of Geophysical Research, v. 86, p. 3857-3866.

Lawrence, R.D., Livingston, N.D., Vickers, S.D., and Conyers, L.B., 1977, Field guide to the geology of Corvallis and vicinity, Oregon: Ore Bin, v. 39, p. 53-71.

Lawrence, R.D., Rosenfeld, C.L. and Ruddiman, W. III, 1980, Marys Peak field trip: Structure of the eastern flank of the central Coast Range, Oregon: *in* Geologic field trips in western Oregon and southwestern Washington, Oregon Department of Geology and Mineral Industries Bulletin 101, p. 121-131.

Lovell, J.P., 1969, Tyee Formation: Undeformed turbidites and their lateral equivalents: mineralogy and paleogeography: Geological Society of America Bulletin, v. 80, p. 9-22.

Lux, D.R., 1982, K-Ar and ^{40}Ar-^{39}Ar ages of mid-Tertiary volcanic rocks from the western Cascade Range, Oregon: Isochron/West, v. 33, p. 27-32.

Magill, J.R., Cox, A.V., and Duncan, R.A., 1981, Tillamook Volcanic series: Further evidence for tectonic rotation of the Oregon Coast Range: Journal of Geophysical Research, v. 86, p. 2953-2970.

Mallory, V.S., 1959, Lower Tertiary biostratigraphy of the California Coast Ranges: American Association of Petroleum Geologists, Tulsa Oklahoma, 416 p.

McDowell, P.F., and Roberts, M.C., 1987, Field guidebook to the Quaternary stratigraphy, geomorphology and soils of the Willamette Valley, Oregon: Field trip no. 3, Association of American Geographers annual meeting, 1987, Portland, Oregon, 75 p.

McKeel, D.R., 1984, Biostratigraphy of exploratory wells, northern Willamette basin, Oregon: Oregon Department of Geology and Mineral Industries Oil and Gas Investigation 12, 19 p.

McKeel, D.R., 1985, Biostratigraphy of exploratory wells, southern Willamette basin, Oregon: Oregon Department of Geology and Mineral Industries Oil and Gas Investigation 13, 17 p.

McWilliams, R.G., 1973, Stratigraphic and biostratigraphic relationships of the Tyee and Yamhill Formations in central-western Oregon: The Ore Bin, v. 35, p. 169-186.

Miller, P.R., and Orr, W.N., 1988, Mid Tertiary transgressive rocky coast sedimentation: central western Cascade Range, Oregon: Journal of Sedimentary Petrology, v. 58, p. 959-968.

Molenaar, C.M., 1985, Depositional relations of Umpqua and Tyee Formations (Eocene), southwestern Oregon: American Association of Petroleum Geologists Bulletin, v. 69, p. 1217-1229.

Moore, G.W., 1984, Tertiary dismemberment of western North America: Third Circum-Pacific Energy and Mineral resources Conference Transactions, p. 607-612.

Moore, J.C., Byrne, T., Plumley, P.W., Reid, M., Gibbons, H., and Coe, R.S., 1983, Paleogene evolution of the Kodiak Islands, Alaska: Consequences of ridge-trench interaction in a more southerly latitude: Tectonics v. 2, p. 265-293.

Nelson, D.E., 1985, Geology of the Fishhawk Falls-Jewell area, Clatsop County, northwest Oregon: M.S. thesis, Oregon State University, Corvallis, 360 p.

Niem, A.R., and Niem, W.A., 1984, Cenozoic geology and geologic history of western Oregon: *in* Ocean Margin Drilling Program regional atlas series, Atlas 1: Western North America continental margin and adjacent ocean floor off Oregon and Washington, sheets 17 and 18, Marine Science International, Woods Hole, Ma.

Niem, A.R., and Niem, W.A., 1985, Oil and gas investigations of the Astoria Basin, Clatsop and northernmost Tillamook Counties, northwestern Oregon: Oregon Department of Geology and Mineral Industries Oil and Gas Investigation 14.

Niem, A.R., Niem, W.A., and Baldwin, E.M., 1989, Geology and oil, gas and coal resources, southern Tyee basin, southern Coast Range, Oregon: Oregon Department of Geology and Mineral Industries Open-File Report O-89-3.

Niem, A.R., Niem, W.A., Martin, M.W., Kadri, M.M., and McKeel, D.R., 1985, Correlation of exploratory wells, Astoria basin, northwest Oregon: Oregon Department of Geology and Mineral Industries Oil and Gas Investigation 14, 8 p.

Parker, M.J., 1990, Oligocene and Miocene geology of the Tillamook embayment, Tillamook County, northwest Oregon: M.S. thesis, Oregon State University, Corvallis, Oregon, 524 p.

Patterson, N.R., and Reeves, C.V., 1985, Applications of gravity and magnetics surveys: The state of the art in 1985: Geophysics, v. 50, p. 2558-2594.

Pavlis, T.L., and Bruhn, R.L., 1983, Deep-seated flow as a mechanism for the uplift of broad forearc ridges and its role in the exposure of high P/T metamorphic terranes: Tectonics, v. 2, p. 473-497.

Penoyer, P.E., and Niem, A.R., 1975, Geology and ground water resources of the Kings Valley area, central Oregon Coast Range, Oregon: Oregon State University Water Resources Institute Paper WRRI-39, 92 p.

Peterson, C.D., and Darienzo, M.E., 1989, Episodic, abrupt tectonic subsidence recorded in late Holocene deposits of the South Slough syncline: An on-land expression of shelf fold belt deformation from the southern Cascadia margin: Annual meeting, Geological Society of America Abstracts with Programs, v. 21, p. 129.

Petit, J.P., 1987, Criteria for the sense of movement on fault surfaces in brittle rocks: Journal of Structural Geology, v. 9, p. 597-608.

Plumley, P.W., Coe, R.S., and Byrne, T., 1983, Paleomagnetism of the Paleocene Ghost Rocks Formation, Prince William Terrane, Alaska: Tectonics, v. 2, p. 295-314.

Rarey, P.J., 1986, Geology of the Hamlet-North Fork of the Nehalem River area, southern Clatsop and northernmost Tillamook Counties, northwest Oregon: M.S. Thesis, Oregon State University, Corvallis, Oregon, 489 p.

Reed, D.L., Silver, E.A., Wright, A.A., and Prasetyo, H., 1983, Forearc disruption, segmentation, and terrane amalgamation in the eastern Sunda Arc, Indonesia: Eos, v. 64, p. 829.

Reidel, S.P., 1984, The Saddle Mountains: The evolution of an anticline in the Yakima fold belt: American Journal of Science, v. 284, p. 942-978.

Reidel, S.P., Scott, G.R., Bazard, D.R., Cross, R.W., and Dick, B., 1984, Post-12 million year clockwise rotation in the central Columbia Plateau, Washington: Tectonics, v. 3, p. 251-273.

Reilinger, R., and Adams, J., 1982, Geodetic evidence for active landward tilting of the Oregon and Washington Coastal Ranges: Geophysical Research Letters, v. 9, p. 401-403.

Riddihough, R.P., 1984, Recent movements of the Juan de Fuca plate system: Journal of Geophysical Research, v. 89, p. 6980-6994.

Rinehart, W., Bowen, R.G., and Chiburis, E.F., 1964, Airport gravity base station network in Oregon: The Ore Bin, v. 26, p. 37-56.

Roberts, A.E., 1953, A petrographic study of the intrusive at Marys Peak, Benton County, Oregon: Northwest Science, v. 27, p. 43-60.

Roberts, M.C., 1984, The late Cenozoic history of an alluvial fill: The southern Willamette Valley, Oregon, *in* Mahaney, W.C., ed., Correlation of Quaternary Chronologies, Geo-Books, Norwitch, England, p. 491-504.

Roberts, M.C., and Whitehead, D.R., 1984, The Palynology of a nonmarine Neogene deposit in the Willamette Valley, Oregon: Review of Palaeobotany and Palynology, v. 41, p. 1-12.

Schlicker, H.G., 1962, The occurrence of Spencer sandstones in the Yamhill Quadrangle, Oregon: The Ore Bin, v. 24, p. 173-184.

Sheriff, S.D., 1984, Paleomagnetic evidence for spatially distributed post-Miocene rotation of western Washington and Oregon: Tectonics, v. 3, p. 397-408.

Silver, E.A., Reed, D.L., and McCaffry, R., 1983, Back arc thrusting in the eastern Sunda arc, Indonesia: A consequence of arc-continent collision: Journal of Geophysical Research, v. 88, p. 7429-7448.

Silver, E.A., and Reed, D.L., 1988, Backthrusting in accretionary wedges: Journal of Geophysical Research, v. 93, p. 3116-3126.

Simpson, R.W., and Cox, A., 1977, Paleomagnetic evidence of the rotation of the Oregon Coast Range: Geology, v. 5, p. 585-589.

Smithson, S.B., Brewer, J., Kaufman, S., and Oliver, J., 1978, Nature of the Wind River Thrust, Wyoming, from COCORP deep reflection data and from gravity data: Geology, v. 6, p. 648-652.

Snavely, P.D., Jr., 1973, Miocene tholeiitic basalts of coastal Oregon and Washington, and their relations to coeval basalts of the Columbia Plateau: Geological Society of America Bulletin, v. 84, p. 387-424.

Snavely, P.D., Jr., 1987, Tertiary geologic framework, neotectonics, and petroleum potential of the Oregon-Washington continental margin, *in* Scholl, D.W., Grantz, A., and Vedder, J.G., eds., Geology and resource potential of the continental margin of western North America and adjacent ocean basins-Beaufort sea to Baja California, Circum-Pacific Council for Energy and Mineral Resources, Houston, p. 305-335.

Snavely, P.D., Jr., and Wagner, H.C., 1961, Differentiated gabbroic sills and associated alkalic rocks in the central part of the Oregon Coast Range, Oregon: U.S. Geological Survey Professional Paper 424-D, p. 156-161.

Snavely, P.D., Jr., and Wagner, H.C., 1963, Tertiary geologic history of western Oregon and Washington: Washington Division of Mines and Geology, Report of investigations, no. 22, 25 p.

Snavely, P.D. Jr., and MacLeod, N.S., 1974, Yachats Basalt, an upper Eocene differentiated volcanic sequence in the Oregon Coast Range: U.S. Geological Survey Journal of Research, v. 2, p. 395-403.

Snavely, P.D. Jr., and Wagner, H.C., 1982, Geologic cross section across the continental margin of southwestern Washington: U.S. Geological Survey Open-File Report 82-459, 10 p.

Snavely, P.D., Jr., and Wells, R.E., 1984, Tertiary volcanic and intrusive rocks on the Oregon and Washington continental shelf: U.S. Geological Survey Open-File Report 84-282, 17 p.

Snavely, P.D. Jr., Wagner, H.C., and MacLeod, N.S. 1964, Rhythmic bedded eugeosynclinal deposits of the Tyee Formation, Oregon Coast Range: Geological Survey of Kansas Bulletin 169, p. 461-480.

Snavely, P.D. Jr., MacLeod, N.S., and Wagner, H.C., 1968, Tholeiitic and alkalic basalts of the Eocene Siletz River Volcanics, Oregon Coast Range: American Journal of Science, v. 266, p. 454-481.

Snavely, P.D., Jr., MacLeod, N.S., and Rau, W.W, 1969, Geologic sketch of the Newport area, Oregon, pt.1, Ore Bin, v. 31, p. 25-48, pt. 2, Ore Bin, v. 31, p. 49-71.

Snavely, P.D. Jr., MacLeod, N.S., and Rau, W.W., 1970, Summary of the Tillamook area, northern Oregon Coast Range: U.S. Geological Survey Professional Paper 650-A, p. A-47.

Snavely, P.D., Jr., MacLeod, N.S., Wagner, H.C., and Rau, W.W., 1976a. Geologic map of the Waldport and Tidewater quadrangles, Lincoln, Lane, and Benton Counties, Oregon. U.S. Geological Survey Miscelaneous Investigations Series Map I-866. scale 1:62,500.

Snavely P.D., Jr., 1976b. Geologic map of the Yaquina and Toledo quadrangles, Lincoln County, Oregon. U.S. Geological Survey Miscelaneous Investigations Series Map I-867. scale 1:62,500

Snavely P.D., Jr., 1976c. Geologic map of the Cape Foulweather and Euchre Mountain quadrangles, Lincoln County, Oregon. U.S. Geological Survey Miscelaneous Investigations Series Map I-868. scale 1:62,500

Snavely, P.D., Jr., MacLeod, N.S., Wagner, H.C., and Lander, D.L., 1980, Geology of the west-central part of the Oregon Coast Range: in Geologic field trips in western Oregon and southwestern Washington, Oregon Department of Geology and Mineral Industries Bulletin 101, p. 39-76.

Spence, W., 1989, Stress origins and earthquake potential in Cascadia: Journal of Geophysical Research, v. 94, p. 3076-3088.

Stewart, R.M., 1957, Stratigraphic implications of some Cenozoic foraminifera from western Oregon, Ore Bin, v., 19, p. 11-15.

Suppe, J., 1985, Priciples of structural geology, Prentice-Hall, Englewood Cliffs, New Jersey, 537 p.

Suppe, J., 1988, Short course on structural analysis & cross section balancing for prospect development: unpublished report, 124 p.

Sylvester, A.G., 1988, Strike-slip faults: Geological Society of America Bulletin, v. 100, p. 1666-1703.

Tabor, R.W., and Cady, W.M., 1978, The Structure of the Olympic Mountains, Washington-Analysis of a subduction zone: U.S. Geological Survey Professional Paper 1033, 38 p.

Talwani, M., Worzel, J.L., and Landisman, M., 1959, Rapid gravity computations for two dimensional bodies with application to the Mendocino submarine fracture zones: Journal of Geophysical Research, v. 64, p. 49-59.

Tarling, D.H., 1971, Principles and applications of palaeomagnetism, Chapman and Hall, London, 164 p.

Tchalenko, J.S., and Ambraseys, N.N., 1970, Structural analysis of the Dasht-e Bayaz (Iran) earthquake fractures: Geological society of America Bulletin, v. 81, p. 41-60.

Telford, W.M., Geldart, L.P., Sheriff, R.E., and Keys, D.A., 1976, Applied Geophysics, Cambridge University Press, Cambridge, England, p. 7-104.

Terres, R.R., and Sylvester, A.G., 1981, Kinematic analysis of rotated fractures and blocks in simple shear: Bulletin of the Seismological Society of America, v. 71, p. 1593-1605.

Thiruvathukal, J.V., Berg, J.W., and Heinrichs, D.F., 1970, Regional gravity of Oregon: Geological Society of America Bulletin, v. 81, p. 725-738.

Thoms, R.E., Van Atta, R.O., and Taylor, D.G., 1983, Stratigraphy and paleontology of selected sections in the Paleogene rocks, western Tualatin Valley borderlands, northwest Oregon: unpublished report.

Tsuboi, C., 1983, Gravity, George Allen and Unwin LTD, London, 254 p.

United States Department of Commerce, 1942, United States earthquakes: 1942: Coast and Geodetic Survey.

Verplank, E.P., and Duncan R.A., 1987, Temporal variations in volume of volcanism in the western Cascades, Oregon, and the effect of slowing convergence rate: Tectonics, v. 6, p. 197-209.

Vincent, P., Richards, M.A., and Weldon R.J., 1990, Vertical interseismic deformation of the Oregon Cascadia margin: Submitted to Journal of Geophysical Research.

Vokes, H.E., Norbisrath, H., and Snavely., P.D., Jr., 1949, Geology of the Newport-Waldport area, Lincoln County, Oregon: U.S. Geological Survey Oil and Gas Investigations Preliminary Map 88. scale 1: 62,500.

Vokes, H.E., Snavely., P.D., Jr., and Myers, D.A., 1951, Geology of the southern and southwestern border areas, Willamette Valley, Oregon: U.S. Geological Survey Oil and gas Investigations Map Om-110. scale 1: 62,500.

Vokes, H.E., Myers, D.A., and Hoover, L., 1954, Geology of the west-central border area of the Willamette Valley, Oregon: U.S. Geological Survey Oil and gas Investigations Map Om-150. scale 1: 62,500.

Walker, G.W., and Duncan, R.A., 1989, Geologic map of the Salem 1° x 2° sheet, Oregon: U.S. Geological Survey Survey Miscellaneous Investigations Map I-1893, scale 1:250,000.

Wells, F.G., and Peck, D.L., 1961, Geologic map of Oregon west of the 121st meridian: U.S. Geological Survey Miscellaneous Geologic Investigations Map I-325. scale 1:500,000.

Wells, R.E., and Coe, R.S., 1985, Paleomagnetism and geology of Eocene volcanic rocks ofsouthwest Washington, implications for mechanisms of tectonic rotation: Journal of Geophysical Research, v. 90, p. 1925-1947.

Wells, R.E., and Heller, P.L., 1988, The relative contribution of accretion, shear, and extension to Cenozoic tectonic rotation in the Pacific Northwest: Geological Society of America Bulletin, v. 100, p. 325-389.

Wells, R.E., Niem, A.R., MacLeod, N.S., Snavely, P.D., Jr., and Niem, W.A., 1983, Preliminary Geologic map of the west half of the Vancouver (Wa-Or) 1° x 2° quadrangle, Oregon, U.S. Geological Survey Open File Report 83-591.

Wells, R.E., Engebretson, D.C., Snavely, P.D., Jr., and Coe, R.S., 1984, Cenozoic plate motions and the volcano-tectonic evolution of western Oregon and Washington: Tectonics, v. 3, p. 275-294.

Werner, K.S., 1990, Direction of maximum horizontal compression in northwestern Oregon determined by borehole breakouts. Structure and tectonics of the northern Willamette Valley, Oregon. M.S. thesis, Oregon State University, Corvallis, Oregon. In prep.

Werner, K.S., Graven E.P., Berkman T.A., and Parker, M.J., 1990, Direction of maximum horizontal compression in northwestern Oregon determined by borehole breakouts : Tectonics, in press.

Westbrook, G.K., 1982, The Barbados ridge complex: Tectonics of a mature forearc system, *in* Trench Forearc Geology, Geological Society of London Special Publication 10, p. 275-290.

Wilcox, R.E., Harding, T.P., and Seely, D.R., 1973, Basic wrench tectonics: American Association of Petroleum Geologists Bulletin, v. 57, p. 74-60.

Wise, D.U., 1963, An outrageous hypothesis for the tectonic pattern of North American Cordillera: Geological Society of America Bulletin, v. 74, p. 357-362.

Yeats, R.S., Graven, E.P., Werner, K.S., and Goldfinger, C., 1990, Tectonics of the Willamette Valley, Oregon. In prep.

Yelin, T.S., and Patton, H.J., 1989, Seismotectonics of the Portland, Oregon region: Eos, v. 70, p. 1330.

Zoback, M.L., and Zoback, M.D., 1980, State of stress in the conterminous United States: Journal of Geophysical Research, v. 85, p. 6113-6156.

Zoback, M.L., and Zoback, M.D., 1990, Tectonic stress field of the continental United States, *in* Pakiser, L., and Mooney, W., eds., Geophysical framework of the continental United States: Geological Society of America memoir 172, p, 523-540.